INFORMATION TO USERS

This material was produced from a microfilm copy of the original document. While the most advanced technological means to photograph and reproduce this document have been used, the quality is heavily dependent upon the quality of the original submitted.

The following explanation of techniques is provided to help you understand markings or patterns which may appear on this reproduction.

1. The sign or "target" for pages apparently lacking from the document photographed is "Missing Page(s)". If it was possible to obtain the missing page(s) or section, they are spliced into the film along with adjacent pages. This may have necessitated cutting thru an image and duplicating adjacent pages to insure you complete continuity.

2. When an image on the film is obliterated with a large round black mark, it is an indication that the photographer suspected that the copy may have moved during exposure and thus cause a blurred image. You will find a good image of the page in the adjacent frame.

3. When a map, drawing or chart, etc., was part of the material being photographed the photographer followed a definite method in "sectioning" the material. It is customary to begin photoing at the upper left hand corner of a large sheet and to continue photoing from left to right in equal sections with a small overlap. If necessary, sectioning is continued again — beginning below the first row and continuing on until complete.

4. The majority of users indicate that the textual content is of greatest value, however, a somewhat higher quality reproduction could be made from "photographs" if essential to the understanding of the dissertation. Silver prints of "photographs" may be ordered at additional charge by writing the Order Department, giving the catalog number, title, author and specific pages you wish reproduced.

5. PLEASE NOTE: Some pages may have indistinct print. Filmed as received.

Xerox University Microfilms
300 North Zeeb Road
Ann Arbor, Michigan 48106

75-9868

BRITTAIN, Harry G., 1949-
ELECTRONIC STRUCTURE AND BONDING IN SOME 3d TRANSITION METAL COMPLEXES OF ACETYLACETONE.

The City University of New York, Ph.D., 1975
Chemistry, physical

Xerox University Microfilms, Ann Arbor, Michigan 48106

Electronic Structure And Bonding In Some 3d Transition Metal Complexes Of Acetylacetone

by

Harry G. Brittain

A dissertation submitted to the Graduate Faculty in Chemistry in partial fulfillment of the requirements for the degree of Doctor of Philosophy, The City University of New York.

1974

This manuscript has been read and accepted for the Graduate Faculty in Chemistry in satisfaction of the dissertation requirement for the degree of Doctor of Philosophy.

Nov. 21, 1974
date

Raymond T. Disch
Chairman of Examining Committee

November 26, 1974
date

Leonard H. Schwartz
Executive Officer

Bernard J. Bullen

Angelo Santoro
Supervisory Committee

The City University of New York

Abstract

ELECTRONIC STRUCTURE AND BONDING IN
SOME 3d TRANSITION METAL COMPLEXES
OF ACETYLACETONE

by

Harry G. Brittain

Adviser: Professor Raymond L. Disch

The nature of the electronic structure and bonding in some 3d transition metal chelates of 2,4-pentanedione (acetylacetone) has been investigated using a wide variety of techniques. These have involved ultraviolet photoelectron spectroscopy, measurement of the Kerr and Cotton-Mouton effects, and the new spectroscopic technique of magnetic linear dichroism. In addition, a question regarding the definition of the molecular Kerr constant has been answered.

The first section of this dissertation deals with the He(I) photoelectron spectra of the acetylacetonate

and hexafluoroacetylacetonate complexes of Sc(III), Cr(III), Mn(III), Fe(III), Co(III), Ni(II), Cu(II), and Zn(II). To aid in the interpretation of these spectra, the photoelectron spectra of the Al(III) and Mg(II) chelates were also obtained. CNDO/2 calculations were run on model chelates of diformylmethane ($Al(dfm)_3$ and $Mg(dfm)_2$), in order to obtain further information for the assignments. INDO molecular orbital calculations on the ligand and the photoelectron spectra strongly suggest that the enol form of the β-diketones adopts a symmetric bridged conformation in the gas phase. No well-defined vibrational structure could be observed. It was determined that the electronic structures of the hydrogenated and fluorinated chelates must be very similar, since the spectra of analagous chelates resemble each other strongly, except for an approximately 2 ev stabilization of all molecular orbitals of the fluorinated complexes.

The second part treats the controversy which exists regarding the form of the definition of the molecular Kerr constant of a liquid. The original formula (proposed in 1934) was recently challenged. A series of Kerr measurements was carried out and the existing literature on the temperature dependence of the Kerr effect of various non-polar liquids was examined in order to find out which formulation would best explain the experimental results.

It was found that the original definition is most suitable in interpreting the data.

Using the conclusions of the second part, measurements of the Kerr and Cotton-Mouton effects were carried out on solutions of $Be(acac)_2$ and $Al(acac)_3$ in CCl_4. Anisotropies of the optical polarizability and magnetic susceptibility were obtained from these measurements and the extent of a possible ring current in the chelate rings was estimated. It is concluded that the chelate rings are not aromatic.

The final section of the dissertation deals with the new spectroscopic technique of magnetic linear dichroism (MLD). Magnetic circular dichroism (MCD) has been widely used to study spectral features of molecules, and an investigation of the MLD effect was undertaken to determine its merit as a spectroscopic tool. By obtaining the MLD spectra of $Co(acac)_3$, $Cr(acac)_3$, and $Fe(acac)_3$, it was demonstrated that the MLD method is superior to that of MCD. Many new spectral features were uncovered in the MLD spectra that had not been observed before in either the absorption or MCD spectrum. A theory of MLD is developed; three possible lineshapes may be observed under various conditions. It was concluded that the MLD technique has a wide range of application and will be very useful in future studies of electronic structure.

Acknowledgements

I would like to express my deepest appreciation and gratitude to Professor Raymond L. Disch for his guidance during the course of this work. It is not possible to fully describe the support Professor Disch provided, but it shall suffice to mention that his office was always open to me and I knew that any question was certain to be answered. His insistence that all research had to be only of the highest quality is an attitude that I shall adhere to for the rest of my career.

I also wish to thank the staff of Queens College for answering countless questions and for the loan of journals and textbooks whenever a request was made. Special thanks are due to Professor Robert Engel for assistance in determination of the magnetic susceptibilities of the acetylacetonate complexes.

It is impossible to thank my parents enough for allowing me to choose my own area of specialization and for supporting me through many years of schooling. Finally, no words can begin to describe the help and assistance my wife, Betty, has provided during these years of graduate study. Her support to me must be regarded as important as any other.

Table of Contents

Tables

Diagrams

Section I

The He(I) Photoelectron Spectra of Some 3d Transition Metal Acetylacetonate Complexes

contents

A. Introduction

Photoelectron spectroscopy has been used to obtain information regarding the electronic structure of virtually every class of chemical compound.[1] One is able to ionize the deepest core electrons by irradiation of the sample with soft x-rays. This technique has been applied to both solids and gases.[2,3] Typically, it is found that the observed bands may be readily assigned to atomic-type orbitals, such as that of the 1s or 2s levels. These bands are slightly shifted on passing through a series of homologous compounds; this phenemenon is referred to as the "chemical shift."

Of greater interest to chemists, however, are the valence orbitals which are more directly related to the bonding character of the compound in question. These are of course observed with x-ray spectroscopy, but the greater linewidths of the x-rays (which are on the order of one electron volt) result in poor resolution of these bands. Nearly degenerate bands are usually merged, and vibrational fine structure is lost. As a result, the

---

1) D. W. Turner, A. D. Baker, C. Baker, and C. R. Brundle, "Molecular Photoelectron Spectroscopy", Wiley, London (1970).

2) K. Siegbahn et al, "ESCA - Atomic, Molecular, and Solid State Structure Studied by Means of Electron Spectroscopy", Almquist and Wiksells, Uppsula (1967).

3) K. Siegbahn et al, "ESCA Applied To Free Molecules", North-Holland, Amsterdam (1969).

valence electron region is usually studied by bombarding the samples in the gas phase with ultraviolet photons, which have a much smaller linewidth (on the order of a few millivolts). This method has usually only been applied to gases, but has been applied to solids as well.[4]

In ultraviolet photoelectron spectroscopy, the exciting source is usually the He(I) line at 21.22 ev. Thus, any orbital whose energy is less than 21.22 ev may be detected by this technique. The use of the He(II) line at 40.82 ev is now being used to extend studies of the valence region, but some profound theoretical problems still remain. The most serious difficulty observed so far deals with the He(I) and He(II) intensities of the same band in the same compound. Apparently the cross-section for photoionization varies with the exciting source and does not behave in a predictable manner.[5] We have confined this investigation to He(I) excitation.

Many general reviews have been written concerning ultraviolet photoelectron spectroscopy,[6-10] and the number

---

4) W. T. Bordass and J. W. Linnett, Nature, 222, 157 (1969).

5) A. Schweig and W. Thiel, Mol. Phys. 27, 265 (1974).

6) S. D. Worley, Chem. Rev. 71, 295 (1971).

7) A. D. Baker, C. R. Brundle, and M. Thompson, Chem. Soc. Rev. 1, 355 (1972).

8) D. W. Turner, Ann. Rev. Phys. Chem. 21, 107 (1970).

9) R. E. Ballard, Appl. Spect. Rev. 7, 183 (1973).

10) A. D. Baker, Acc. Chem. Res. 3, 17 (1970).

of texts on the same topic is increasing.[1,11,12] However, most of these works deal mostly with organic or heteroatom-organic compounds. The number of papers published which treat inorganic or organometallic compounds cannot exceed one-quarter of the total output.[13] This paucity is easily traced to a fundamental experimental criterion: the compound under investigation must have sufficent vapor pressure to obtain a good flux of photoelectrons. Most inorganic salts and coordination compounds are not the least bit volatile. Progress has been made in this area by allowing the heating of solid samples to improve their vapor pressure. It is precisely this advancement which made this investigation possible.

The most volatile inorganic compounds are electrically neutral organometallic complexes. One very interesting group of compounds which can be sublimed without decomposition (provided the temperature is held below 200°C) are the metal chelates of β-diketones.[14] These have the general formula and structure given in Figure 1.

---

11) A. D. Baker and D. Betteridge, "Photoelectron Spectroscopy", Pergamon Press, Oxford (1972).

12) D. A. Shirley (ed.), "Electron Spectroscopy", North-Holland, London, (1972).

13) A. Hamnett and A. F. Orchard, "Specialist Periodical Reports: Electronic Structure and Magnetism of Inorganic Compounds", The Chemical Society, 1, 1 (1972); 2, 1 (1973).

14) J. P. Fackler, Prog. Inorg. Chem. 7, 361 (1966).

Figure 1 - Structure of the Acetylacetonate Ring

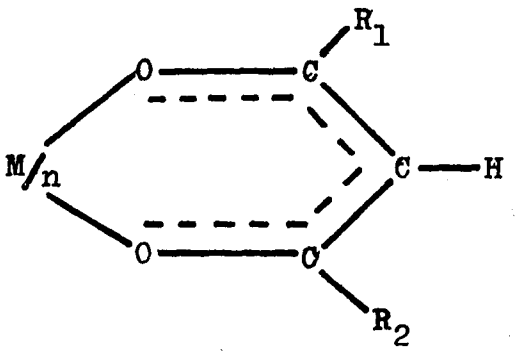

In the diagram, n refers to the formal charge on the central metal atom. The β-diketonate anion has a minus one charge and ligand variations may be studied by varying the groups at the R_1 and R_2 positions. These compounds are of particular interest due to the electron delocalization that is possible within each chelate ring, as symbolized by the dotted lines in the figure. Whether the rings can be considered aromatic or not is a question still open to debate,[15] but it was felt that measurement and assignment of the photoelectron spectra of these complexes might aid in the further understanding of the nature of the bonding and structure.

The first photoelectron spectra to be published all dealt with metal chelates of 1,1,1,5,5,5-hexafluoro-2,4-pentanedione, which is commonly referred to as hexafluoroacetylacetone. This chelate has $R_1 = R_2 = CF_3$ in Figure

15) M. Kuhr and H, Musso, Angew. Chem. Int. Ed. 8, 147 (1969).

1, and shall henceforth be abbreviated as "hfac" for simplicity. The first note[16] which appeared presented the spectra of $Al(hfac)_3$, $Cr(hfac)_3$, and $Co(hfac)_3$. These fluorinated chelates were chosen because of their unusally high volatility[14] and the results were used to support a claim that Electron Impact Spectroscopy had failed to detect first ionization potentials in these compounds. Comparsion was made to an earlier work[17] in which the electron impact results were obtained but the results of this current investigation show the conclusions of both of these papers to be incorrect. The impact spectra did find the first ionization potentials, but the authors did not interpret the trends correctly.

The second note also dealt with hfac spectra, and attempted to refute claims that Koopmans' Theorem was violated in the spectra of these compounds.[18] Briefly, Koopmans' Theorem[19] is an approximation which equates the negative of the orbital energy (as obtained from a self-consistant-field molecular orbital calculation in the Hartree-Fock limit) with the ionization potential observed

---

16) D. R. Lloyd, Int. J. Mass. Spec. Ion Phys. 4, 500 (1970).

17) S. M. Shildcrout, R. G. Pearson, and F. E. Stafford, J. Am. Chem. Soc. 90, 4006 (1968).

18) D. R. Lloyd, Chem. Comm. 868 (1970).

19) T. Koopmans, Physica 1, 104 (1933).

in the photoelectron spectrum. The most celebrated and well-documented violation of this rule was found in the spectrum of molecular nitrogen;[1] there is an inversion of the highest lying $3\sigma_g$ and $1\pi_u$ levels on ionization. This note unfortunately did not present very sophisticated molecular orbital calculations, so its conclusions are also open to possible criticism. It also attempted to apply Koopmans' Theorem to open-shell molecules, such as $Cr(hfac)_3$ or $Fe(hfac)_3$, when it was already known that Koopmans' Theorem must fail for such molecules.[20] A final note by a different group pointed out an error in assignment of the spectrum of $Fe(hfac)_3$;[21] what apparently was a band due to excitation by an additional He(I) band at 23.09 ev had been assigned to a d-orbital ionization. It was at this point that the current investigation was initiated.

After the completion of the photoelectron study of twenty-four β-diketone chelates, and its subsequent presentation,[22] a large work on the photoelectron spectra of many of the same chelates appeared.[23] Our investigation included

---

20) W. G. Richards, Int. J. Mass, Spec. Ion Phys. 2, 419 (1969).

21) S. Evans, A. Hamnett, and A. F. Orchard, Chem. Comm. 1282 (1970).

22) H. G. Brittain and R. L. Disch, paper #206 presented to the Northeast Regional Meeting of the Americal Chemical Society on Oct. 17, 1973.

23) S. Evans, A. Hamnett, A. F. Orchard, and D. R. Lloyd, Far. Diss. Chem. Soc. 54, 227 (1973).

several compounds not included by the other group, and our spectra also seem to be of slightly better quality. In a few places where the discussions overlap, we have new refinements on the spectral interpretations which aid in the understanding of the nature of the bonding in the metal β-diketonate complexes.

B. Experimental Details

Two general types of β-diketone chelates were studied during the course of this investigation. We were interested in the afore-mentioned hexafluoroacetylacetonates, but our primary interest lay in determining the electronic structure of the chelates with R = CH_3 in Figure 1. These are, of course, the acetylacetonates (abbreviated as "acac"), which have been studied extensively since their discovery.[14] The comparison of fluorinated and non-fluorinated compounds has been a feature of photoelectron studies and is used to aid in band assignment.[24] It was originally hoped that comparison of the fluorinated chelates and non-fluorinated chelates would yield similar information.

The acetylacetonates of V(III), Al(III), Zn(II), Co(III), Cu(II), Cr(III), and Fe(III) were obtained from Chemicals Procurement Laboratories. Each complex was recrystallized from a 1:3 benzene-hexane mixture at least once prior to introduction in the spectrometer. $V(acac)_3$ had to be purified immediately before use, or else decomposition was found to occur. The products of this decomposition were not determined (nor are they known), but acetic anhydride was thought to be one of them since the complex quickly smells of the anhydride upon standing. The hexafluoroacetylacetonates of Al(III), Fe(III), Mn(III), Cr(III),

---

24) C. R. Brundle, M. B. Robin, N. A. Kuebler, and H. Basch, J. Am. Chem. Soc. 94, 1451, 1466 (1972).

Cu(II), Ni(II), Zn(II), Mg(II), and Co(II) were obtained from Peninsular Chemical Company. These compounds were sublimed before use. All were found to contain some associated water (as evidenced in the photoelectron spectra themselves) but dehydration was possible within the spectrometer. The sole exception to this practice was found in the case of $Ni(hfac)_2$, in which the compound and its water of hydration seemed to be equally volatile. As a result, I could not obtain a $Ni(hfac)_2$ spectrum free from that of the associated water.

Acetylacetone was obtained from the J. T. Baker Chemical Company and hexafluoroacetylacetone was obtained from Pfaltz and Bauer. Both compounds were distilled under vacuum before use. The fluorinated ligand must be kept free from water or else hydrolysis to yield 1,1,1,5,5,5-hexafluoro-2,2,4,4-tetrahydroxypentane takes place.[25,26]

Standard procedures were followed in the preparation of all other β-diketone chelates. These have been outlined by Marchi[27] and may be divided into three general categories of syntheses: action of a β-diketone on a metal, action of a β-diketone on a compound of a metal,

---

25) B. G. Schultz and E. M. Larsen, J. Am. Chem. Soc. 71, 3250 (1949).

26) R. L. Belford, A. E. Martell, and M. Calvin, J. Inorg. Nucl. Chem. 2, 11 (1956).

27) L. E. Marchi, Inorg. Syn. 2, 10 (1946).

or action of a salt of the β-diketone on a salt of a metal. The first method was not used in the course of this work since it is the most time-consuming of all. The second method was only used in the preparation of $V(hfac)_3$, since it was also lengthy and did not give good yields. All other complexes were prepared by the third method, in which the β-diketone was first converted to either the sodium, potassium, or ammonium salt and then added to a solution containing the salt of the metal whose complex was desired. Most reactions were carried out in a solvent that the reactants were soluble in, but that the product was not. Water was used as the solvent for the acetylacetonate preparations, since both the metal salt and enolized β-diketone are soluble but the resulting complexes are not (this solvent is unsuitable for hexafluoroacetylacetonate preparations since ligand hydrolysis would take place).

$Mn(acac)_3$ was prepared according to the method of Charles.[28] $MnCl_2$ was first converted to the acetate complex and oxidized to the trivalent state with $KMnO_4$ while still in solution. Acetylacetone was converted to the sodium salt with sodium acetate and then added to the manganese solution. Since the solvent used was water, the product precipated immediately as black crystals. $Ni(acac)_2$ was

---

28) R. G. Charles, Inorg. Syn. 7, 183 (1963).

prepared in the fashion described by Bullen et al,[29] in which an ammoniacal solution of acetylacetone was added to an aqueous solution of $NiCl_2$. Once again, the complex immediately precipitated in good yield. When hydrated, the $Ni(acac)_2$ appears light blue, but after heating at 100°C in an oven, it loses the water of hydration and takes on a greenish tint. $Sc(acac)_3$ was made according to Morgan[30] and $Mg(acac)_2$ was prepared following the procedure of Hatch.[31] Both of these preparations followed the same general trend as for $Ni(acac)_2$: conversion of the ligand to the ammonium salt, followed by addition to an aqueous solution of the metal chloride.

No literature preparation could be found for $Sc(hfac)_3$, so it was prepared in a manner analagous to that given by Morris et al.[32] The procedure had been outlined for the preparation of $Al(hfac)_3$, but the close reactivity of Al(III) and Sc(III) allowed the technique to be extended to the Sc(III) chelate. All reactants were dissolved in absolute ethanol, and the product precipitated by the addition of a ten-fold excess of hexane. $V(hfac)_3$ was prepared by the action of hexafluoroacetylacetone on

---

29) G. J. Bullen, R. Mason, and P. Pauling, Inorg. Chem. 4, 456 (1965).

30) G. T. Morgan and H. W. Moss, J. Chem. Soc. 189 (1914).

31) L. F. Hatch and G. Sutherland, J. Org. Chem. 13, 249 (1948).

32) W. L. Morris, R. W. Machier, and R. E. Sievers, Inorg. Chem. 9, 28 (1967).

VCl_3, followed by extraction of the product into benzene. The solvent was then stripped off and the product obtained. All preparations involving the hexafluoro-ligand must be carried out in very dry solvents to prevent hydrolysis of the ligand. The use of a drybox was eliminated by distillation of solvents and careful drying over molecular sieves.

The purity of all diamagnetic compounds was checked by NMR. For the acetylacetonates, the two methyl groups on each ring (R_1 and R_2 in figure 1) give one signal in the NMR spectrum (about 2 ppm from the tetramethylsilane reference) and the ring proton one line (about 5.5 ppm).[33,34] No impurities could be detected in concentrated solutions of the chelates in carbon tetrachloride. The shifts observed agreed well with the literature data.

The photoelectron spectra were measured on a Perkin-Elmer model PS-16 spectrometer. Resolution was estimated to be about 40 mev, using the spin-orbit peaks of the rare gases as the resolution test.[1] The low-energy regions of the spectra were calibrated with the 9.54 ev and 10.16 ev lines of methyl iodide, and the high-energy portions calibrated with the 15.76 ev and 15.94 ev lines of argon. The calibrant and sample were introduced into the target

---

33) R. H. Holm and F. A. Cotton, J. Am. Chem. Soc. 80, 5658 (1958).

34) D. R. Eaton, J. Am. Chem. Soc. 87, 3097 (1965).

chamber either concurrantly or separately; no difference in vertical ionization potential was observed between the two methods.

The PS-16 spectrometer was modified to allow the vaporization of less volatile samples. The heat developed by the helium lamp is used to sublime the samples into the target chamber. The acetylacetonates required an average temperature of 80°C to achieve the necessary vapor pressure, and the hexafluoroacetylacetonates were heated to 30°C. Both these temperatures were well below the temperatures necessary to thermally decompose the substances.

Instrument behavior and response varied markedly during the period when the compounds were being run. Later, it was found that the electron multiplier was being attacked by the chelates. For instance, after obtaining the spectrum of hexafluoroacetylacetone it was found that all the stainless steel fittings had become coated with a red layer of $Fe(hfac)_3$. This spectrometer destruction appears to be an experimental hazard as more corrosive complexes and compounds are studied, but perhaps an experimental design will be proposed which will miminize the effects on the detection system.

C. Photoelectron Spectra and Assignments of The Free Ligands

Orchard et al[23] have reported the photoelectron spectra of acetylacetone ($R_1 = R_2 = CH_3$ in Figure 1), hexafluoroacetylacetone ($R_1 = R_2 = CF_3$), trifluoroacetylacetone ($R_1 = CH_3$ and $R_2 = CF_3$), and dipivaloylmethane ($R_1 = R_2 = C(CH_3)_3$), but they did not attempt an assignment of the two partially resolved bands at low ionization potential. The spectra of acetylacetone and hexafluoroacetylacetone have been obtained in the current study in order to make these necessary assignments. Our spectra generally show better resolution and the trends to be elaborated on shortly are better demonstrated in our results than in the previous ones. It is reasonable to assume that a π-type molecular orbital and a non-bonding molecular orbital (localized primarily on the oxygen atoms) would be among the highest occupied bonding molecular orbitals, but it is not immediately apparent which would lie the highest.

Based on evidence obtained from the gas phase infrared spectra of various β-diketones,[35] it has been shown that the free ligands exist entirely in the enol form while in the gas phase. This result has been tacitly assumed by generations of organic chemists who thought that the stability of the enol form over the keto form was a consequence of intramolecular hydrogen bonding. However, in aqueous solutions of

---

35) A. H. Lowrey, C. George, P. D'Antonio, and J. Karle, J. Am Chem. Soc. 93, 6399 (1971).

sodium acetylacetonate, infrared spectral evidence[36] has shown that the free acetylacetonate anion prefers an open-chain structure, with the oxygen atoms lying trans to each other. Since the predicted intramolecular hydrogen bonding requires a cis oxygen configuration, it is readily seen that some question exists in regard to the actual structure of the gas phase enol form. We believe that the experimental photoelectron spectrum is able to answer this question.

To aid in the interpretation of the photoelectron spectra, INDO[37] calculations were run on both the open-chain enol and the bridged enol forms of both acetylacetone and hexafluoro-acetylacetone. The geometries for the bridged conformer were taken from the data of Lingafelter and Braun,[38] and standard bond lengths and angles[39] were chosen for the open-chain conformer. All the data are summarized in Table I, along with the results of the computations. Our optimized geometries agree excellently with the recent calculations of Gordon and Koob,[40] who considered only closed-ring conformers.

---

36) W. O. George, and F. V. Robinson, J. Chem. Soc., A, 1950 (1968).

37) J. A. Pople, D. L. Beveridge, and P. A. Dobosh, J. Chem. Phys. 47, 2026 (1967).

38) E. C. Lingafelter and R. L. Braun, J. Am. Chem. Soc. 88, 2951 (1966).

39) "Tables Of Interatomic Distances And Configuration In Molecules and Ions", The Chemical Society, London, 1958.

40) M. S. Gordon and R. D. Koob, J. Am. Chem. Soc. 95, 5863 (1973).

Table I

Data and results from the INDO calculations

	Open-Chain		Bridged-Ring	
	Hacac	Hhfac	Hacac	Hhfac
1. Geometries				
C ═ C	1.34 A	1.34 A	1.39 A	1.39 A
C — C	1.54 A	1.54 A	1.39 A	1.39 A
C ═ O	1.36 A	1.36 A	1.27 A	1.27 A
C — O	1.33 A	1.33 A	1.27 A	1.27 A
C — H	1.07 A	1.07 A	1.07 A	1.07 A
C — H(F)	1.09 A	1.33 A	1.09 A	1.33 A
∡ HOC	110°	110°	117°	117°
∡ OCC	124°	124°	125°	125°
∡ CCC	124°	124°	124°	124°
2. Results of the INDO calculations*				
ϕ_1(ev)	-12.458(a")	-12.815	-11.089(b_2)	-13.492
ϕ_2(ev)	-13.016(a')	-13.907	-11.951(b_1)	-13.678
ϕ_3(ev)	-15.889(a')	-16.000	-15.687(a_1)	-17.091
ϕ_4(ev)	-16.567(a")	-16.080	-17.160(a_2)	-17.697
ϕ_5(ev)	-16.696(a')	-17.656	-17.929(b_2)	-18.048
total energy (A.U.)	-58.469	-109.871	-58.564	-115.024
dipole moment	5.306 D	5.186 D	2.774 D	1.777 D

*note: In the group C_s, all π representations transform as a", and in the group C_{2v}, the π representations transform as b_1 and a_2.

It was found that the bridged enol conformer of acetylacetone was 2.58 ev (0.095 A.U.) more stable than the open-chain conformer, and that the bridged hexafluoroacetylacetone was 140.217 ev (5.153 A.U.) more stable than its corresponding open-chain configuration. On this basis alone, one could conclude that the gas phase enol molecules would adopt a bridged configuration, but additional corroborational evidence may be obtained from a consideration of the highest-occupied molecular orbitals, which have been tabulated in Table I.

It may be seen that the bridged conformer (which required approximately 90 separate calculations to carry out the necessary geometry optimization) predicts that the highest occupied molecular orbital would be approximately non-bonding, localized primarily on the oxygen atoms, and that the next highest occupied orbital would be a π-level. These two orbitals are separated by 0.86 ev in the calculations. Replacement of the $-CH_3$ groups by $-CF_3$ groups does not change the ordering of the molecular orbitals, but does narrow the separation between the two highest orbitals to 0.19 ev. This decrease is also demonstrated by the photoelectron spectra of the two molecules, as shown in Figure 2. The photoelectron vertical ionization potentials are summarized in Table II.

Table II

	Hacac	Hhfac
1^{st} band	9.11 ev	10.97 ev
2^{nd} band	9.69 ev	11.37 ev

Figure 2

Photoelectron Spectra of Acetylacetone and Hexafluoroacetylacetone

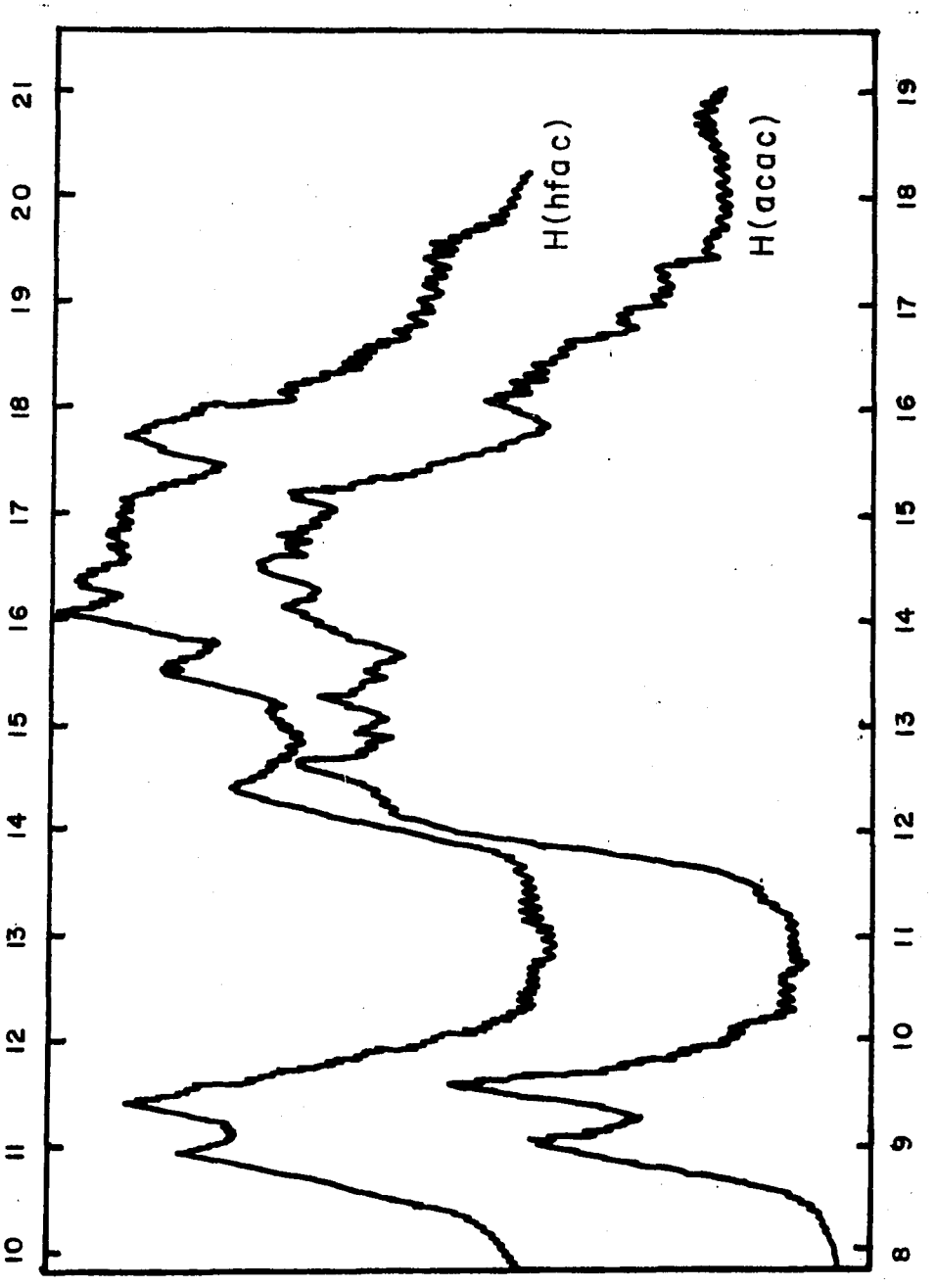

The results in Table II show that the energy difference between the first two bands decreases from 0.58 ev in acetylacetone to 0.40 ev in hexafluoroacetylacetone. This trend is not evident in the calculations on the open-chain conformer. Here, the highest occupied molecular orbital is the π-type orbital, and the next highest orbital corresponds to an oxygen non-bonding level. In this conformer, the levels now split apart (going from 0.56 ev in the open-chain acetylacetone to 1.092 ev in the fluorinated ligand), which is in direct conflict with experiment. Perhaps the most revealing feature of the calculations is the failure of the calculation on the open-chain molecule to predict the ca. 2 ev stabilization of all molecular orbitals on fluorination, as evident in Table II. However, the calculations on the bridged enol forms clearly reproduce this experimental observation.

On the basis of the foregoing arguments, one may conclude that gaseous β-diketones adopt a bridged structure when in the enol form. The open-chain model is not adequate to explain the experimental data. The dipole moment calculated for the open-chain acetylacetone was found to be 5.306 Debye and this disagrees badly with the observed moment of 2.81 Debye.[41] However, calculation on the bridged enol form of acetylacetone predicts a dipole moment of 2.772 Debye, in excellent accord with the value observed in solution. Of course, the solution

---

41) K.L. Wolf, Z. Physik. 31, 227 (1930).

measurement represents the dipole moment of a mixture of 70% enol and 30% keto acetylacetone[14], but since the keto form is probably likely to have a higher dipole moment than the enol, the agreement of the calculated moment and the observed moment is better than the actual numbers indicate.

Calculations were also done on the anions of both the closed and open forms of acetylacetone. It was found that the closed-ring anion was still more stable than the open-chain anion, the energy difference being 1.95 ev. Thus, one may conclude that the preference of the acetylacetonate anion for the trans configuration in aqueous solvents[36] must be a consequence of solvent effects.

In summary, the peak of lowest ionization potential in both acetylacetone and hexafluoroacetylacetone is assigned to ionization from the non-bonding orbital localized on the oxygen atoms ($X\ ^1A_1 \longrightarrow \tilde{X}\ ^2B_2$ in C_{2v} symmetry with the molecule placed in the YZ plane). The next ionization is assigned to the highest π-type molecular orbital ($X\ ^1A_1 \longrightarrow \tilde{A}\ ^2B_1$). Assignment of further bands in the spectra is not warranted due to overlapping in both the INDO results and in the photoelectron results, but structure in the vicinity of 16-18 ev in the spectrum of hexafluoroacetylacetone is similar to that found in fluoroform, CHF_3.[1] It is possible that one is ionizing fluorine lone pairs in this region, but no definite conclusions may be drawn.

D. Photoelectron Spectra Of The Mg(II) And Al(III) Chelates

Before any interpretation of the photoelectron spectra of the transition metal β-ketoenolate complexes can be made, some model for their electronic structure must be developed. Theoretically, one would like to first examine the electronic makeup of the chelates without the complicating influences of their d-electrons and then to feed in the d-electrons and observe the resulting changes. Since this is obviously an impossible task, some closely related compounds must be examined and their electronic structure used to explain the photoelectron spectra of the transition metal chelates. To achieve this end, we have chosen $Mg(acac)_2$ as a model for the bis-chelates and $Al(acac)_3$ for the tris-chelates. These compounds are of extra interest since it is possible to perform CNDO/2[42] calculations on them.

Although one could run a calculation on the full acetylacetonate complex, considerable computational time may be saved by replacing the methyl groups on each ring by hydrogens. Previous work on the free protonated ligands showed that this approximation changed the values of the orbital energies somewhat, but did not affect the ordering of the molecular orbitals. Thus, the actual protonated ligand to be considered is diformylmethane (1,3-propanedial), and this is equivalent

---

42) J. A. Pople and G. A. Segal, J. Chem. Phys. 44, 3289 (1966).

to setting $R_1 = R_2 = H$ in Figure 1. The chelates of this ligand (which shall be abbreviated as $Mg(dfm)_2$ and $Al(dfm)_3$) are largely hypothetical, with only the Cr(III) compound having actually been synthesized.[43] The geometries for the calculations were taken from the data of Lingafelter and Braun,[38] and are summarized in Table III.

Table III

M — O	1.959 A
C — O	1.274 A
C — C	1.390 A
C — H	1.080 A
∠ OCC	125.3°
∠ CCC	124.0°
∠ HCO	117.5°
∠ OMO	90.7°

Due to the excessive time required for these calculations (40 minutes for $Mg(dfm)_2$ and 140 minutes for $Al(dfm)_3$) no geometry optimizations were attempted.

Only one configuration of the diformylmethanido rings was possible for $Al(dfm)_3$, and this arrangement places the molecule in the D_3 point group. However, two conformations

43) J. P. Collman, E. T. Kittleman, W. S. Hunt, and N. A. Moore, Inorg. Syn. 8, 141 (1966).

were possible in the case of $Mg(dfm)_2$. One could either situate the ligand rings coplanar (putting the molecule in the D_{2h} point group), or arrange the rings perpendicular to each other (making the point group D_{2d}). For these calculations, a constant metal-oxygen bond distance was assumed and one chelate ring rotated by 90° while keeping the other fixed in the XY plane (the molecule was placed in the XY plane for the calculation on the D_{2h} form). Computations on both conformers were run at the CNDO/2 level, and it was found that the D_{2d} configuration was 0.466 ev (10.3 Kcal) more stable than the D_{2h}. The actual gas-phase conformation is not known, but the calculations indicate that the molecule would adopt the D_{2d} structure. A few of the highest occupied molecular orbitals of each chelate are tabulated in Table IV.

Upon examination of the actual makeup of these orbitals, it was found that the levels could be classified according to their bonding character in a way which appeared independent of the metal chelate involved, or of the symmetry of the molecule. Orbitals of similar character have been labeled types A through D in Table IV. The levels marked A were largely metal-oxygen π-bonding, with a little ring π-bonding mixed in. The B levels appeared to be non-bonding p-orbitals localized on the oxygen atoms. If one

Table IV

Molecular Orbitals For the Mg(II) and Al(III) Chelates of Diformylmethane

Type	$Al(dfm)_3$	$Mg(dfm)_2(D_{2d})$	$Mg(dfm)_2(D_{2h})$
A (π)	-11.851 (a_2) -12.456 (e)	-12.398 (e)	-12.292 (b_{2g}) -12.345 (b_{1u})
B (n_-)	-12.777 (a_2) -12.804 (e)	-12.737 (e)	-12.681 (b_{2u}) -12.692 (b_{1g})
C (n_+)	-14.894 (e) -15.499 (a_1)	-15.037 (b_2) -15.171 (a_1)	-14.925 (b_{3u}) -15.112 (a_g)
D	-17.083 (e)-π -17.215 (a_1)	-17.018 (a_2)-π -17.431 (b_2)	-16.790 (b_{3u}) -16.883 (a_u)-π
	-17.617 (e) -18.931 (e) -18.942 (a_2) -19.347 (a_1)-π -20.200 (a_2)	-17.551 (a_1) -18.507 (b_1)-π -19.006 (e) -20.661 (e) -22.845 (e)	-17.890 (a_g) -18.419 (b_{3g})-π -18.718 (b_{1u}) -19.063 (b_{2u}) -20.379 (b_{1g})

could consider these type B levels as an out-of-phase combination of oxygen orbitals, then the type C levels appear to be the in-phase combination of the same orbitals. Thus, the B levels shall be denoted as n_- and the C levels as n_+, following the notation of Orchard et al.[23] Finally, the levels marked D are seen to be a combination of the second-highest π-level and some ligand σ-bonding.

Direct comparsion to the experimental photoelectron spectra shown in Figures 3 and 4 is now possible. Although the spectrum of $Al(hfac)_3$ has been previously reported,[16,23] none of the other spectra have been published. The vertical ionization potentials are collected in Table V.

Table V

	acac	hfac
a) Mg(II) chelates		
1st band	8.42 ev	10.28 ev
2nd band	9.44 ev	11.18 ev
3rd band	10.48 ev	12.31 ev
4th band	11.85 ev	13.62 ev
b) Al(III) chelates		
1st band	8.07 ev	10.21 ev
2nd band	9.15 ev	11.27 ev
3rd band	10.31 ev	12.59 ev

Figure 3

Photoelectron spectra of $Mg(acac)_2$ and $Mg(hfac)_2$

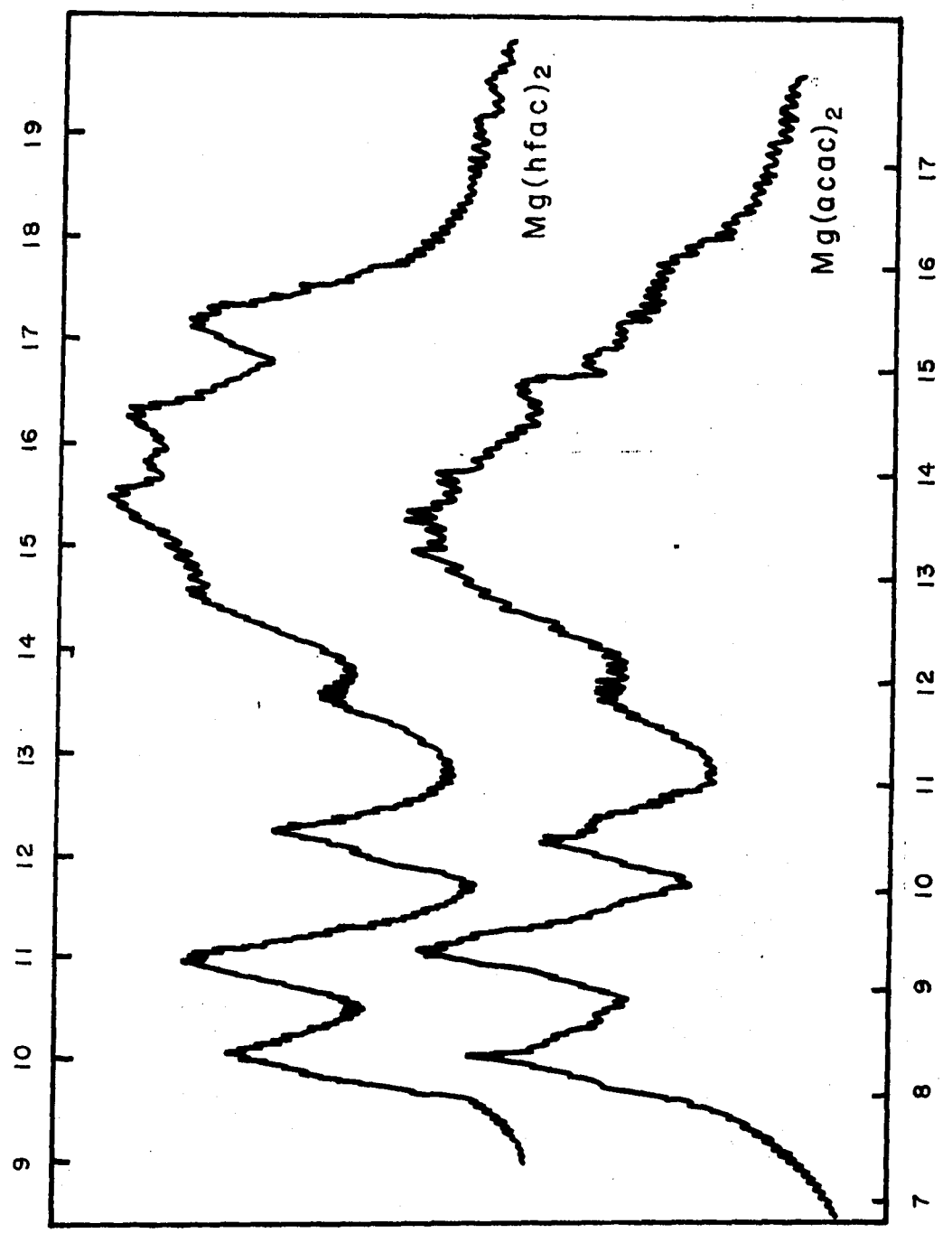

Figure 4

Photoelectron spectra of $Al(acac)_3$ and $Al(hfac)_3$

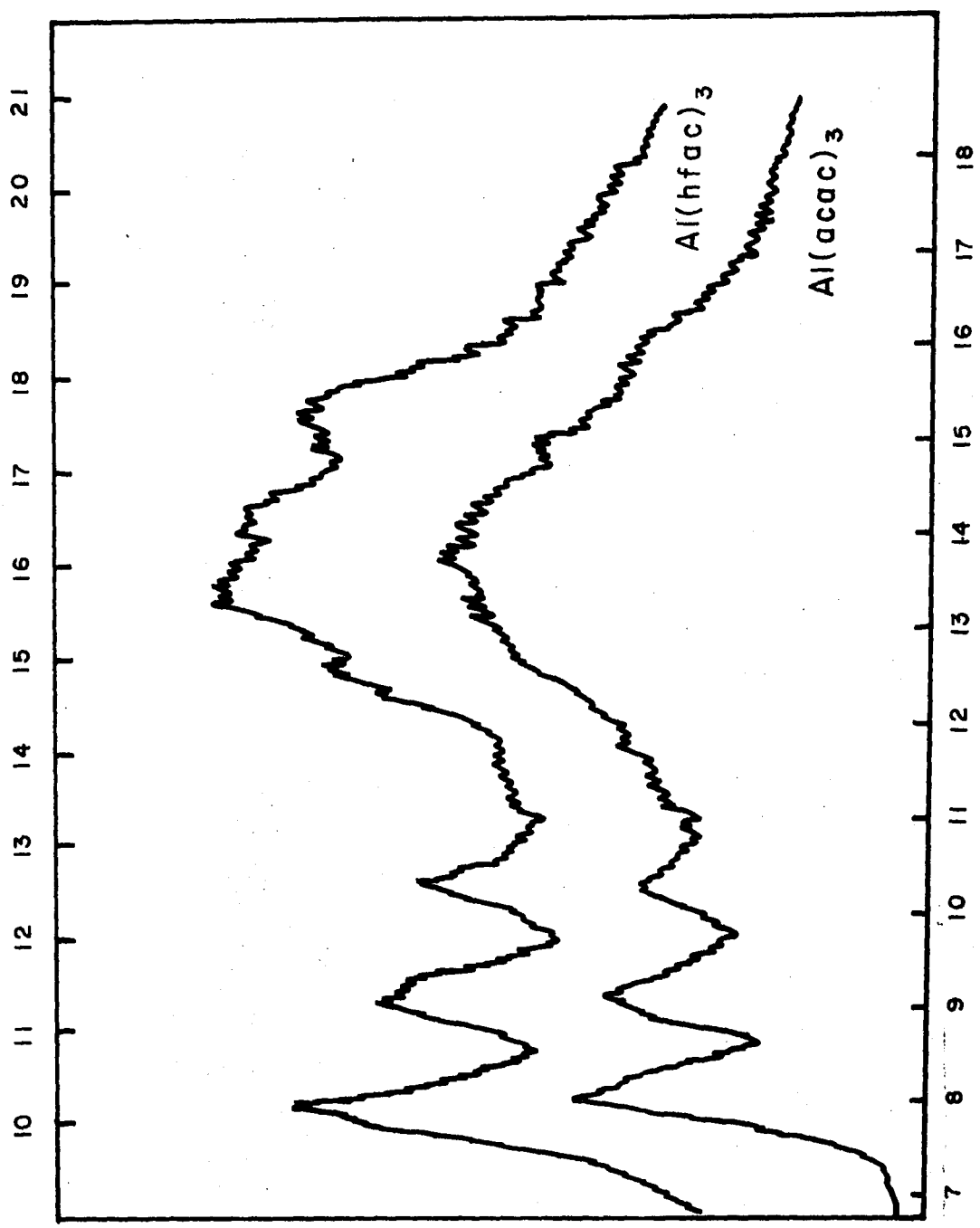

Comparsion of the photoelectron spectra and the CNDO results reveal some very interesting features. Examination of Figures 3 and 4 show that the spectra of the Mg(II) and Al(III) chelates are extremely similar. In fact, the only difference between the two figures is the appearance of a fourth band in the spectra of the Mg(II) compounds that is obscured by other ionizations in the Al(III) spectra. It may be concluded that the electronic structure of each set of chelates is very similar. This situation was also seen in the CNDO results, where the uppermost orbitals could be grouped according to bonding character and where no large differences were found upon replacement of the metal ion.

At this point, we are now ready to make some assignments of the photoelectron bands in Figures 3 and 4. The first band observed in either the Al(III) or Mg(II) spectra is assigned to ionization from the highest occupied π-orbital, which was labelled type A in Table IV. The CNDO results indicate a near degeneracy of the a_2 and e components of these levels in $Al(dfm)_3$ which indicates that no splitting of this π-band ought to be observed in the photoelectron spectra. The fact that all bands have roughly the same area is seen as confirmation of an unsplit π-level, since the split components would have led to a 2:1 intensity ratio. This situation is not possible in the Mg(II) chelates (assuming the D_{2d} symmetry), since the π-level is twofold

degenerate, and could only be split by a Jahn-Teller interaction.

The second band observed is assigned to ionization from the oxygen non-bonding levels, classified as type B in Table IV. By the same arguments used for the type A levels, one concludes that there is again no resolution of the components of these lone pairs. Then, the third band is assigned to ionization out of the type C (the n_+ levels) orbitals, and no splitting is observed for this band as well. No further well-resolved peaks were observed in the Al(III) spectra, but a fourth band was seen in the Mg(II) compounds. The overlapping in both the CNDO results and photoelectron spectra does not allow a firm identifaction of this band, but it is probably due to ionization from the type D levels. One would expect the second-highest π-orbital to be found in this region, and it is possible that the fourth band is due to this orbital.

Some illuminating trends may now be noticed if one compares the spectra of the protonated ligands and those of their metal chelates. It was determined in the previous section that the oxygen non-bonding ionization was found at 9.11 ev and that the π-orbital ionization occured at 9.69 ev in acetylacetone. Since one would not expect the energy of a lone-pair to change a great deal on complexation if it remains non-bonding, one would expect to find a band

in the spectra of the chelates near 9.1 ev. We have already seen that the second band in the spectrum of $Al(acac)_3$ is found at 9.15 ev, and that the second band in the $Mg(acac)_2$ spectrum was found at 9.44 ev. However, these levels were already assigned to the oxygen nonbonding levels on the basis of the CNDO calculations. The fact that both methods of assignment lead to the same conclusion is seen as confirmation of the assignments themselves.

A very puzzling observation is the shift of the highest occupied π-orbital toward lower ionization potential upon complexation. One would normally expect stabilization of orbitals if they are allowed to become more delocalized, but apparently this is not the case in these β-diketone complexes. This destabilization is not dependent on the assignments for the protonated ligands, since there would still be a one electron-volt or greater discrepancy regardless of the assignments made for the first two bands of the ligands. We have run INDO calculations on the anions of acetylacetone and diformylmethane (using the geometry of the metal complexes), and find that for these ligands the π-level lies at higher energy than the oxygen nonbonding. Of course, the anion energy levels lie at considerably higher energy than either the protonated ligand or the metal complexes. Apparently, the movement of a proton into the bridging position stabilizes the π-levels somewhat more

than the movement of a metal ion into the same position. The exact reason for the somewhat unexpected result is not clear, but must be the result of some subtle interelectronic repulsion. It is possible that the metal draws more σ-charge to itself (which would account for the stability of metal complexes over that of the protonated ligands) and that this donation of charge is made up by a π-donation of charge by the metal to the oxygen atoms. We know that the total charge on the oxygens must remain approximately constant on going from the protonated ligands to the metal complexes, since the oxygen nonbonding orbital does not shift a great deal in energy. Only a very detailed calculation (perhaps an ab initio method) might shed some light on this matter, but this approach would be very costly in computer time judging by the size of the molecules involved.

E. Photoelectron Spectra of the Transition Metal Chelates

Now that assignments have been made for the model compounds of the previous section, extension of these ideas to the chelates of the first transition series can now be made. CNDO calculations are not yet available for molecules with atomic number greater than that of chlorine, so all assignments must be based on intuitive reasoning and trends in the spectra themselves. It is possible that errors may be introduced while following this course of action, but no other method of assignment is available. We have used the electronic structure of the Al(III) and Mg(II) chelates (as developed in the previous section) as a basis for the transition metal chelates, and have attempted to account for any new features in the photoelectron spectra as pertubations caused by the addition of d-electrons to the metals. The spectra of each acetylacetonate and hexafluoroacetylacetonate chelate will now be discussed separately (moving along the periodic table from left to right), with a final comparsion of the general features found in the spectra of all the chelates being saved for the next section.

1. Sc(III) Chelates

The photoelectron spectra of the Sc(III) chelates are shown in Figure 5, and the vertical ionization potentials are collected in Table VI.

Figure 5

Photoelectron Spectra of $Sc(acac)_3$ and $Sc(hfac)_3$

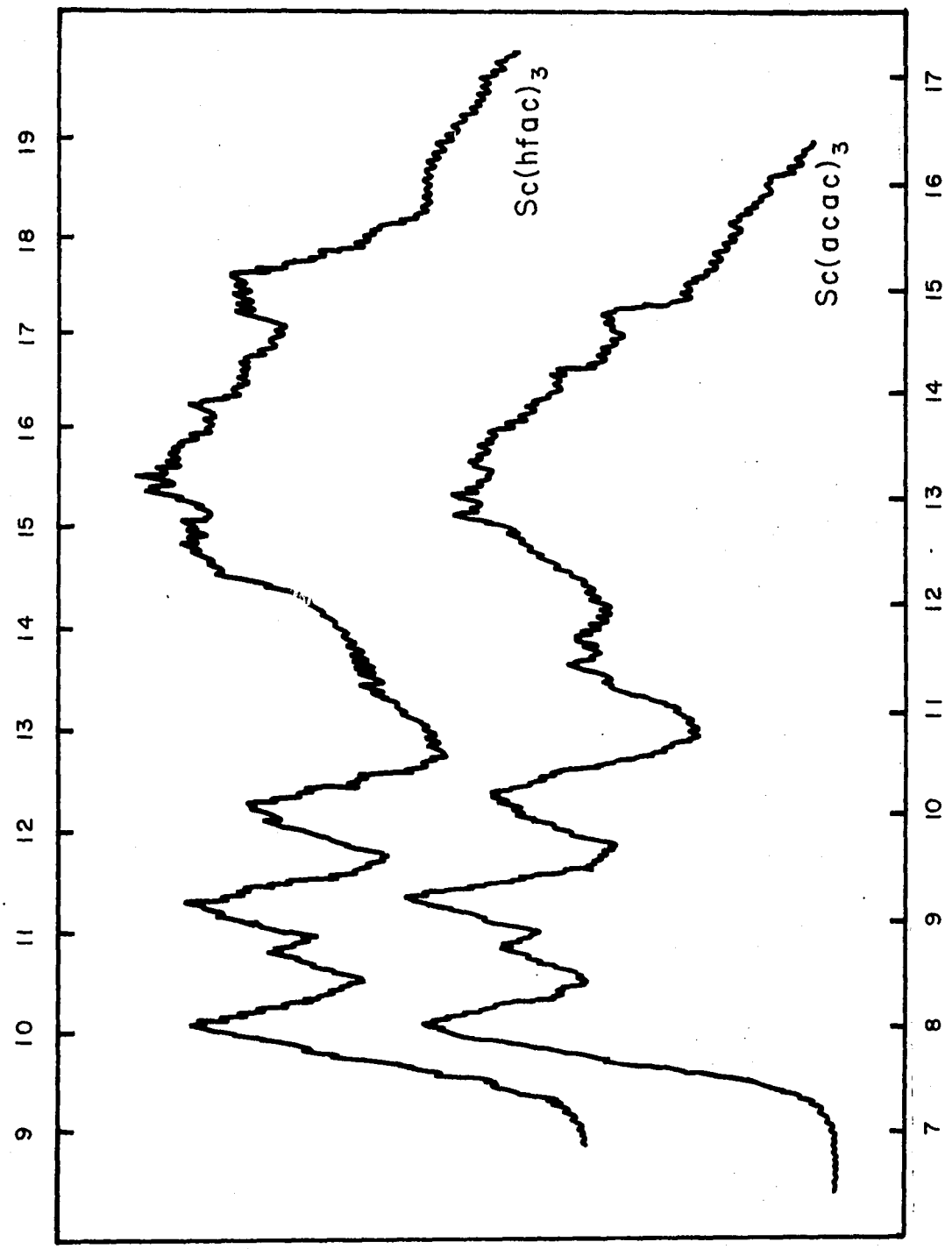

Table VI

	acac	hfac
1st band	8.05 ev	10.01 ev
2nd band	8.77 ev	10.76 ev
3rd band	9.21 ev	11.34 ev
4th band	10.25 ev	12.22 ev
5th band	ca. 11.4 ev	ca. 13.4 ev

Comparsion of Figure 5 and either Figure 3 or 4 reveals a very interesting feature. The band that had been assigned to the n_- ionization in the Al(III) compounds is now seen to have split into two components. The intensity of the components is approximately 2:1, as would be expected from a consideration of the molecular orbitals in Table IV. Since the only difference between Sc(III) and Al(III) is the presence of lower-lying, empty d-orbitals on the scandium atom, it must be concluded that interaction between these orbitals and the n_- levels is responsible for the splitting. If one determines the location of the center of gravity of the n_- levels by weighting the split levels in a 2:1 fashion, one finds that the unsplit peak would have occurred at 9.06 ev for $Sc(acac)_3$. This value is quite close to the ionization potential observed (9.15 ev) for the n_- peak in $Al(acac)_3$. The same situation was also seen in the spectra of $Al(hfac)_3$ and $Sc(hfac)_3$. The ionization potential deduced

for the unsplit n_- levels was 11.15 ev in $Sc(hfac)_3$ and 11.27 ev in $Al(hfac)_3$.

By comparsion to the model compounds, the band at 8.05 ev in $Sc(acac)_3$ has been assigned to ionization from the highest occupied set of π-levels. The band at 8.77 ev is assigned to the a_2 component of the n_- levels, and the band at 9.21 ev to the e component. The next band at 10.25 ev is assigned to the n_+ levels, with no splitting being observed. The final band observed at approximately 11.4 ev cannot really be assigned due to the same problems mentioned in the previous section, but possibly might be due to ionization from the type D levels of Table IV. The close similarity of the $Sc(acac)_3$ and $Sc(hfac)_3$ spectra allows the same assignments to be made for the fluorinated chelate as for the hydrogenated chelate. Thus, the corresponding bands are assumed to have the same origin.

2. Ti(III) and V(III) chelates

The complexes of Ti(III) are very unstable in air, so none of these compounds were prepared. Orchard et al[23] have run the spectrum of $Ti(hfac)_3$, but a discussion of their results will be deferred to the next section. We prepared the $V(acac)_3$ and $V(hfac)_3$ chelates, but were unable to record their photoelectron spectra due to instrument failure. However, Orchard et al[23] had studied the $V(hfac)_3$ chelate, which shall also be discussed in the next section.

3. Cr(III) chelates

The photoelectron spectra of the complexes of Cr(III) are shown in Figure 6, and the observed vertical ionization potentials are collected in Table VII.

Table VII

	acac	hfac
1st band	7.51 ev	9.50 ev
2nd band	8.07 ev	9.93 ev
3rd band	9.02 ev	10.83 ev
4th band	9.56 ev	11.40 ev
5th band	10.53 ev	12.17 ev
6th band	11.43 ev	13.11 ev

The first item of interest is the appearance of a sharp feature on the low ionization potential side of the second band. The low intensity of this band, and its sharpness, suggest that it should be assigned to ionization from the metal d-electrons. Cr(III) formally possesses a d^3 configuration that would be derived from the t_{2g} subset if the molecule were octahedral, and these electrons are considered nonbonding in the absence of π-bonding.[44] The reason for

44) For example, see F. A. Cotton, "Chemical Applications Of Group Theory", second edition, Wiley-Interscience, 1971.

Figure 6

Photoelectron Spectra of $Cr(acac)_3$ and $Cr(hfac)_3$

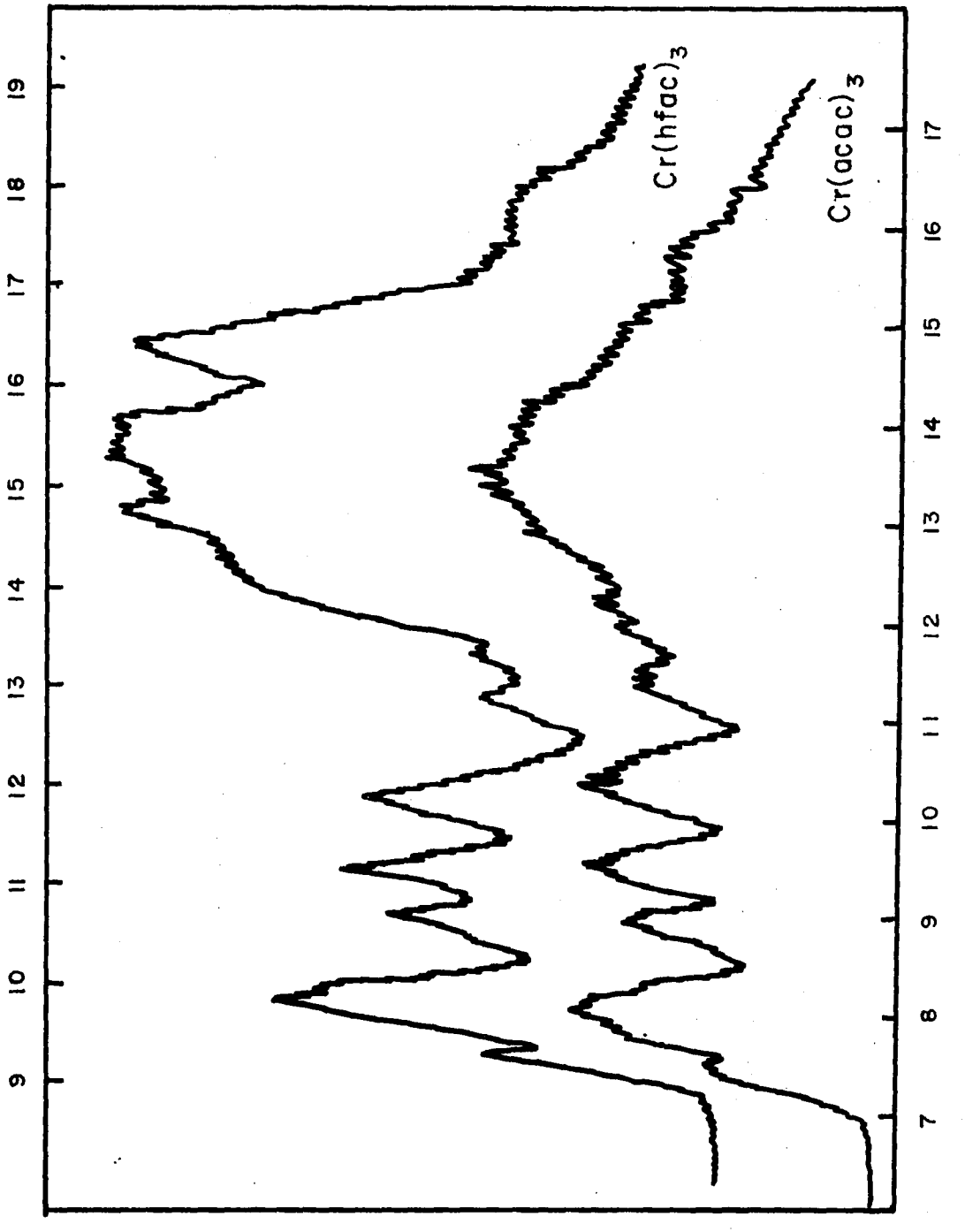

this assignment of d-orbital character comes about from a consideration of group theory; in the absence of π-bonding there are no ligand orbitals available to overlap with the metal t_{2g} subset. Since it is known that nonbonding orbitals lead to exceedingly sharp photoelectron bands,[1] the assignment of this first band to nonbonding d-orbitals contradicts the accepted idea of strong π-bonding in $Cr(acac)_3$.[14]

This conclusion is further supported by the position of the highest π-band. Examination of Table VII shown the presence of a fairly intense band at 8.07 ev in $Cr(acac)_3$ and this peak is assigned to the ligand π-band, since the next two bands are clearly due to the split components of the n_- levels. The fact that this band is found at exactly the same ionization potential in $Cr(acac)_3$ as in $Al(acac)_3$ is further indication that the extent of π-bonding is not as great in the Cr(III) chelates as had been thought.[45] Some interaction between the d-electrons and the ligand π-band is observed, since the photoelectron band appears to be broadened somewhat.

Assignment of the fifth band is the same as in all previous compounds discussed. We have assigned this band to the unsplit components of the n_+ orbitals. Assignment of the sixth band is very uncertain.

---

45) R. D. Hancock, Theor. Chim. Acta 18, 67 (1970).

4. Mn(III) chelates

Two factors serve to complicate the photoelectron spectrum of the Mn(III) complexes. It is known that the structure of these d^4 compounds is distorted by Jahn-Teller effects[46] so that the ^5E ground state is reduced to two orbitally nondegenerate states. Also, since the Mn(III) chelates have electrons in what were the t_{2g} and e_g subsets of an octahedral molecule, several electronic terms arise upon ionization. As a result of these two complications the photoelectron spectra of $Mn(acac)_3$ and $Mn(hfac)_3$ are obscured by overlapping bands. These effects are clearly demonstrated in the spectra of Figure 7. It is observed that hardly any detail may be observed, with only one peak being identified. A band is found at 8.21 ev in $Mn(acac)_3$ and 9.87 ev in $Mn(hfac)_3$ which is assigned to the highest occupied π-level solely on the basis of its location in the experimental spectrum. We recognize that the d-electrons ought to lie somewhere close to this band, but their exact location cannot be stated with certainty. No further assignments are possible since there are no more well-defined peaks.

5. Fe(III) chelates

Having reached the Fe(III) chelates in the periodic

---

46) R. Dingle, J. Mol. Spect. 9, 426 (1962).

Figure 7

Photoelectron Spectra of $Mn(acac)_3$ and $Mn(hfac)_3$

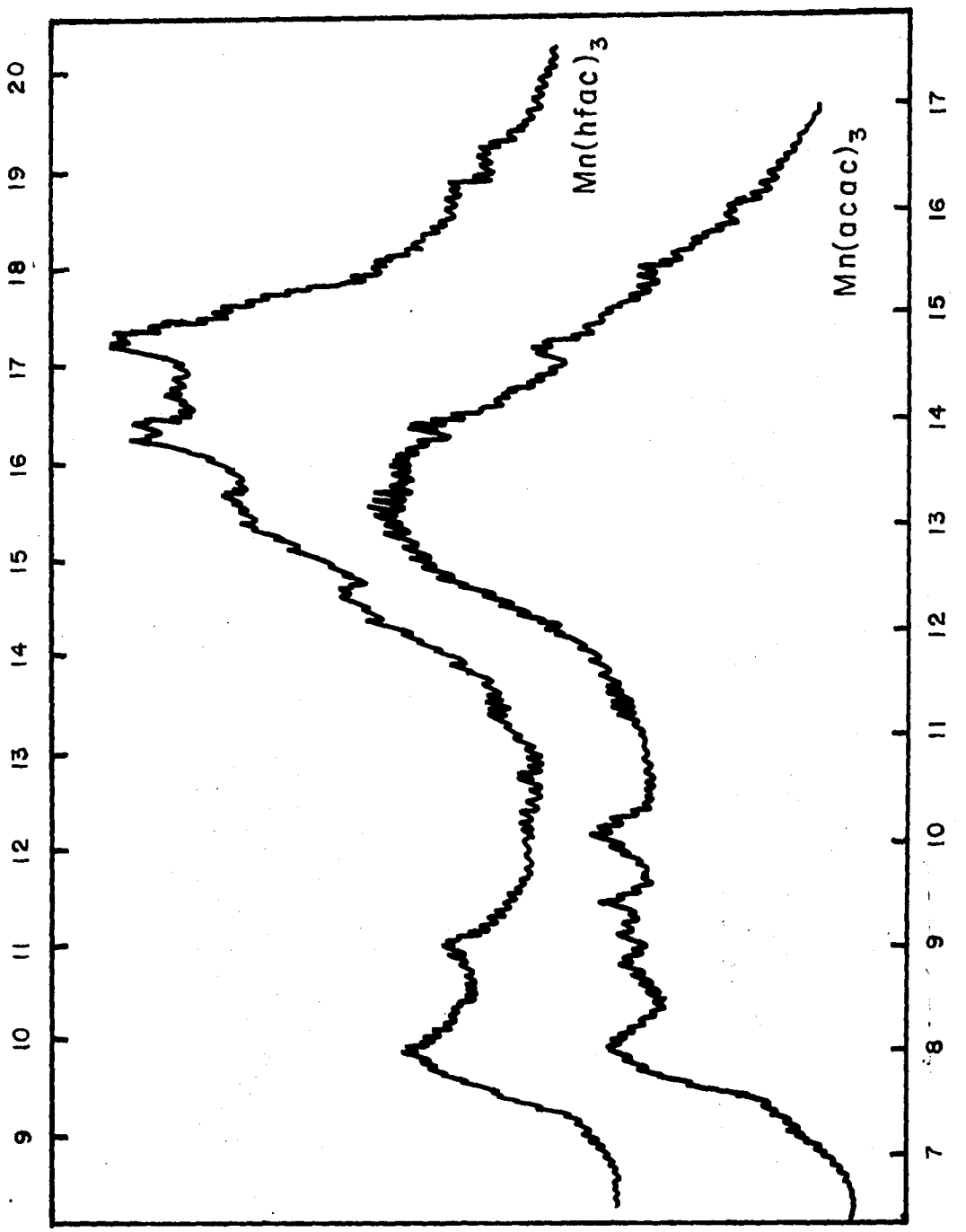

table, we have now achieved a d^5 configuration. This electronic description represents a very stable half-filled shell of d-electrons. It is generally accepted that this situation is not very favorable for large ligand-field interactions in these complexes,[45] so one would not expect a great deal of splitting in the photoelectron spectra. This prediction is confirmed in the experimental spectra shown in Figure 8, and in the vertical ionization potentials listed in Table VIII.

Table VIII

	acac	hfac
1st band	7.98 ev	10.07 ev
2nd band	9.21 ev	11.13 ev
3rd band	10.20 ev	12.11 ev
4th band	11.42 ev	13.29 ev

The resemblance between the photoelectron spectra of the Fe(III) and Al(III) chelates is startling. On first glance, they could almost be interchanged. Closer examination reveals small shifts in ionization potential on going from the Al(III) compounds to the Fe(III) compounds and a higher intensity of the first band in the Fe(III) spectra. The similarities, however, make the interpretation of the spectra very straight-forward. The first band is

Figure 8

Photoelectron Spectra of $Fe(acac)_3$ and $Fe(hfac)_3$

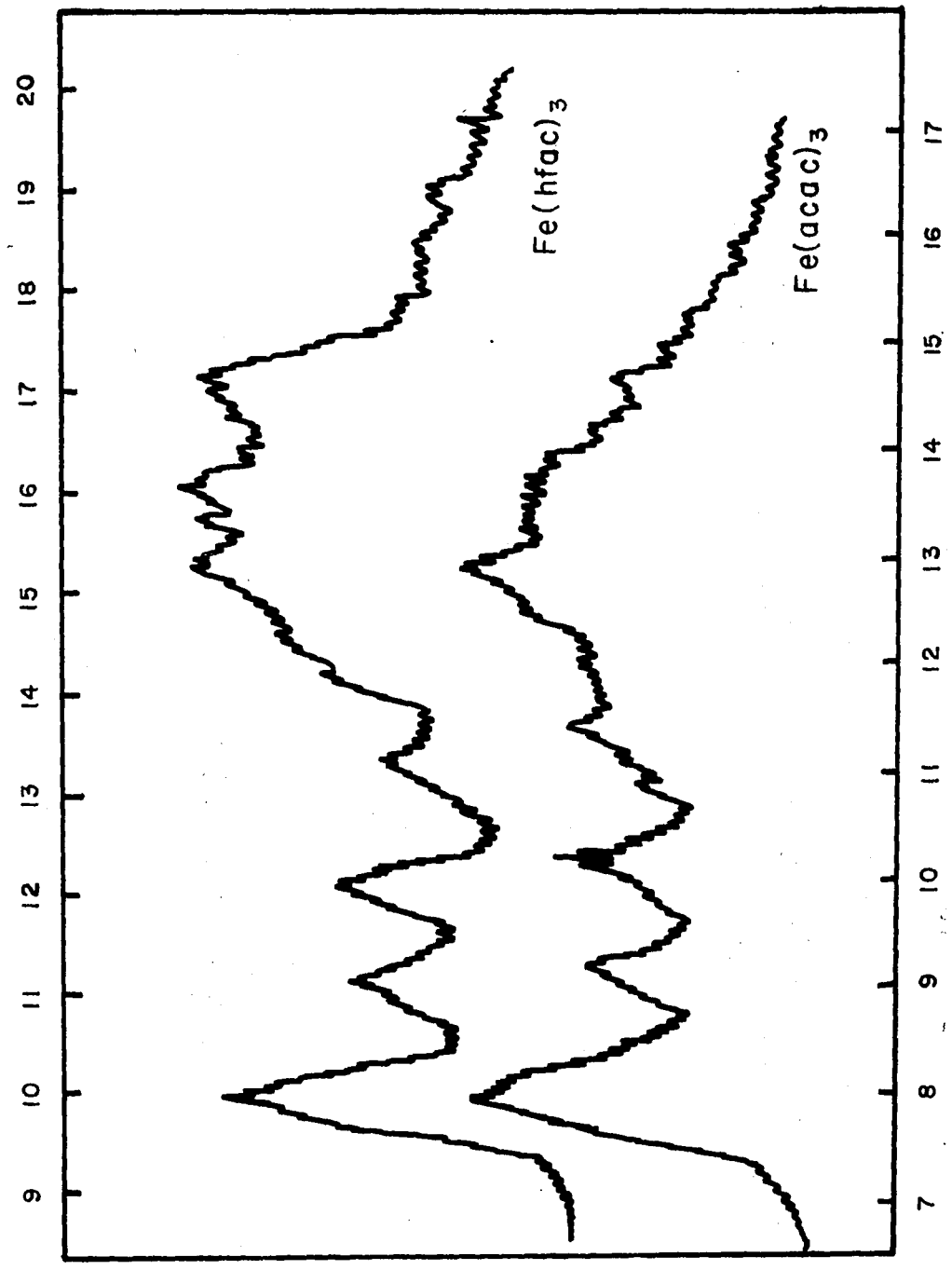

assigned to π-orbital ionization, and the d-electron ionizations are assumed to lie buried under that of the π-levels. It is known that the cross section for d-orbital photoionization is usually much lower than one would expect,[47] although the reasons have not yet been formulated. The extra intensity of this first band must reflect the presence of ionizations other than the π-orbitals at the same energy. The shift of this first band toward lower ionization potential (lower than even that of the Al(III) chelates) is probably a consequence of this overlapping, which was not resolvable by the spectrometer.

The rest of the assignments are exactly the same as in the Al(III) spectra. The second band is assigned to the n_- levels, and the third band to the n_+ orbitals. The origin of the fourth band is still obscure, but might be the class D combination of π- and σ-bonding.

6. Co(III) chelates

The photoelectron spectra of the Co(III) are very rich in detail, as evidenced in Figure 9. It is known that these complexes exhibit the strongest π-bonding of all the β-diketone compounds,[45] and this fact is reflected in the ionization potentials listed in Table IX.

---

47) A. D. Baker, private communication.

Figure 9

Photoelectron Spectra of $Co(acac)_3$ and $Co(hfac)_3$

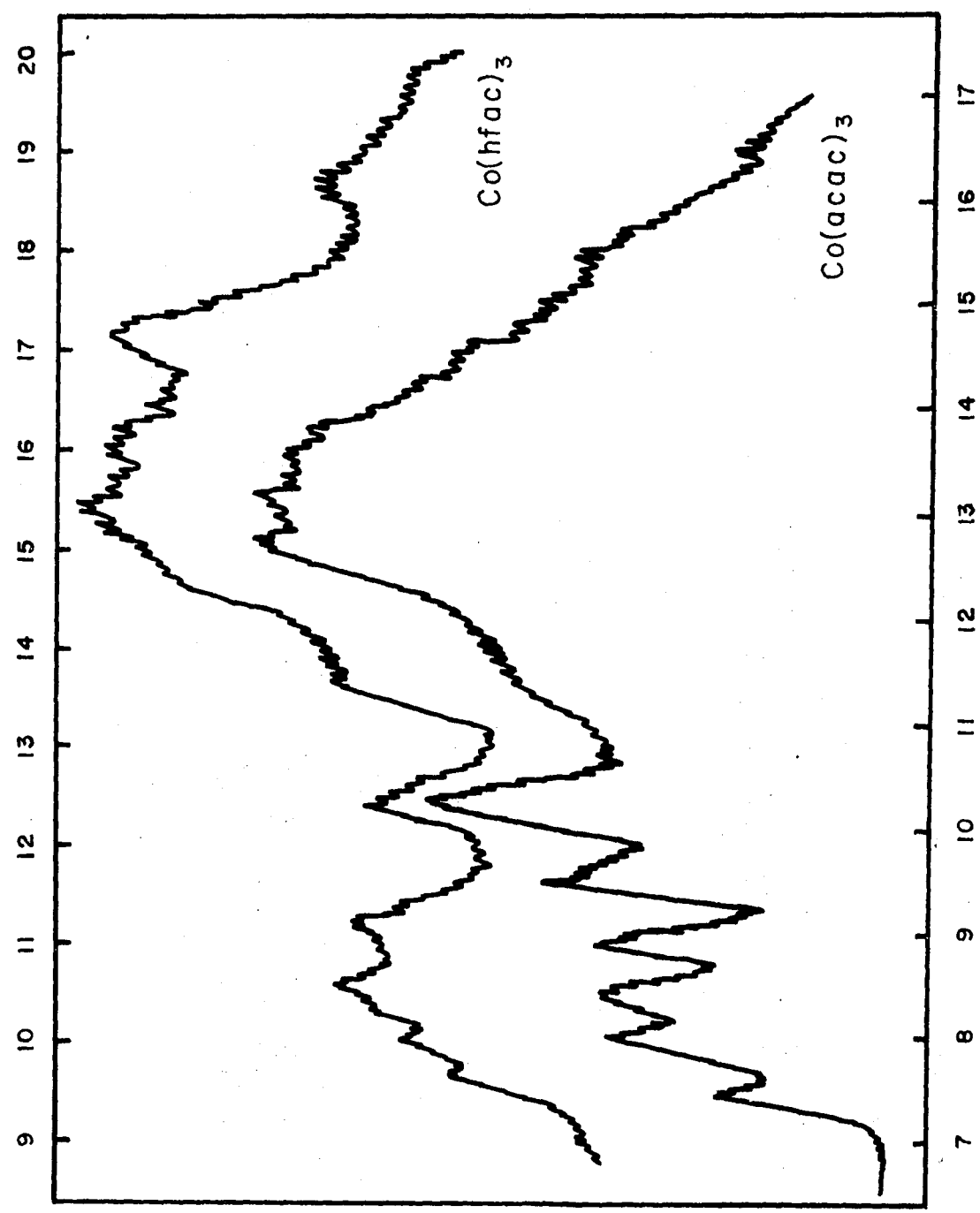

Table IX

	acac	hfac
1st band	7.55 ev	9.70 ev
2nd band	8.09 ev	10.06 ev
3rd band	8.55 ev	10.51 ev
4th band	8.99 ev	10.95 ev
5th band	9.57 ev	11.18 ev
6th band	10.37 ev	12.42 ev
7th band	ca. 11.6 ev	ca. 13.8 ev

Throughout the following discussion, reference will be made to the spectrum of $Co(acac)_3$ and not $Co(hfac)_3$. It is known that $Co(hfac)_3$ is rather unstable[16] and this fact is reflected in the loss of resolution of the photoelectron peaks. Orchard et al[23] did not mention this problem (perhaps they used different sample handling techniques) and did obtain a spectrum for $Co(hfac)_3$, which will be mentioned in the following section. Assignment of the Co(III) spectra parallels that of the Cr(III) spectra, since their electronic structure is so similar. As previously mentioned, the ion Cr(III) possesses a d^3 shell, and it is known that the Co(III) complexes have a low-spin d^6 shell.[14] In the approximation that the metal atoms see an effectively octahedral configuration of oxygen atoms, these metals represent a half-full and completely full t_{2g} subset.

The first band in the photoelectron spectra is assigned to d-orbital ionization. Previously, Orchard et al[23] had assigned this band to a π-orbital ionization, but we do not feel that this interpretation is exactly correct. We assigned the second band to a π-level ionization, and this agrees with Orchard's group. However, Orchard et al assigned the third band to d-orbital ionization whereas we have assigned it to a π-orbital ionization. The reasoning of the previous workers was that the d-electrons were becoming more stable as one crossed the first transition series, but consideration of the Ni(II) spectra will be shown not to be consistant with this trend. In assigning the first band to d-orbital ionization, we have realized that the band is really an antibonding π^*-level that resulted from the interaction of a ligand π-orbital and a d-orbital of proper symmetry. However, we believe that this uppermost orbital would possess largely d-electron character and should thus be formally labelled as a d-orbital ionization rather than as a π-orbital ionization. This belief is supported by our photoelectron spectra in Figure 9 which show that the intensity of the first band is much less than any of the other bands, a feature which is expected of d-electron ionization. In Orchard's spectra, the first band is of equal intensity when compared to the rest of the spectrum, but repeated runs on our instrument were unable

to reproduce the features that the other group had reported.

The rest of the assignments are basically the same as for the Cr(III) chelates. The fourth and fifth bands are assigned to the split components of the n_- orbitals, and the sixth peak to the unsplit n_+ set or orbitals. It is presumed that some d-electrons are being ionized along with the π-orbitals in order to account for the lack of 2:1 ratios observed for the π-level components. Only a detailed calculation might be able to predict where the rest of the d-electrons are being ionized.

7. Ni(II) chelates

The metal acetylacetonates and hexafluoroacetylacetonates of the rest of the transition series were all studied in the divalent state, so we shall henceforth be dealing with bis-complexes instead of tris. However, the previous comparsion of the Al(III) and Mg(II) chelates indicate that the electronic structures of both classes of compounds were the same, so that no discontinuities in band assignment are to be expected. The photoelectron spectra of the Ni(II) chelates are shown in Figure 10, and the corresponding vertical ionization potentials are listed in Table X. A great deal of structure was found in the spectrum of $Ni(acac)_2$ but some features were lost in the spectrum of $Ni(hfac)_2$. As mentioned in the experimental section, the fluorinated

Figure 10

Photoelectron Spectrum of $Ni(acac)_2$ and $Ni(hfac)_2$

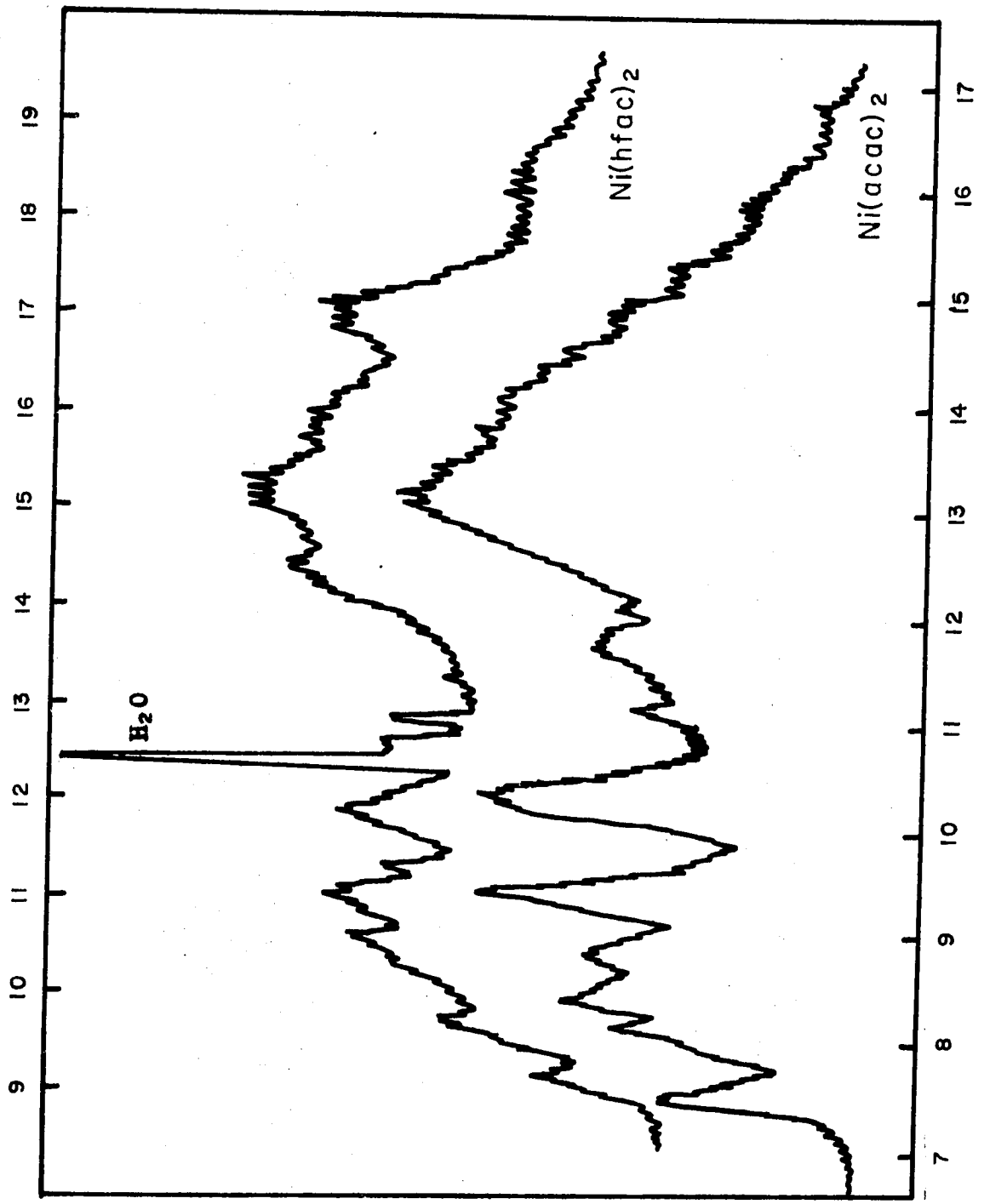

chelate could not be freed of its water of hydration and this problem complicated the spectrum considerably. The water peak was observed at 12.6 ev, close to the value observed by Turner[1] for pure water.

Table X

	acac	hfac
1st band	7.61 ev	9.35 ev
2nd band	8.29 ev	9.84 ev
3rd band	8.52 ev	10.67 ev
4th band	8.83 ev	?
5th band	9.51 ev	11.11 ev
6th band	10.39 ev	12.01 ev
7th band	11.21 ev	?
8th band	11.81 ev	?

Correspondence between the $Ni(acac)_2$ and $Ni(hfac)_2$ spectra was made on the basis of relatitive peak areas.

It may be noted that the spectra of $Ni(acac)_2$ and $Co(acac)_3$ are quite similiar, which would indicate that the same assignments ought to hold for each. The well-resolved band at 7.61 ev in $Ni(acac)_2$ is assigned to d-electron ionization, in good agreement with the values obtained for analagous ionizations in $Co(acac)_3$ and $Cr(acac)_3$. The second band at 8.29 ev is also assigned to a d-orbital ionization because of its sharpness. The intensity of the first band

suggests that more than one d-orbital ionization is contributing to the observed lineshape. The third and fourth bands are assigned as the components of the π-levels, with the b_{1u} level (which has no d-orbital participation) found at 8.52 ev and the b_{2g} level at 8.83 ev.

The fifth band is assigned to ionization from the b_{2u} component of the n_- level. It is believed that the other component of the n_- set coincides with the n_+ ionization observed at 10.39 ev, by virtue of the high intensity of this band. It is observed that two more bands are visible in the $Ni(acac)_2$ spectrum, but assignment of these is not yet possible. Quite possibly, one of them could be due to ionization from the second-highest π-levels (or level), but a firm assignment is out of the question. It is very interesting to note that the photoelectron spectra refute the extended Huckel calculations of Cotton et al,[48] who predicted that a single d-electron ought to be ionized at a much lower potential than the rest. This prediction has not been confirmed despite a careful search of the low-energy region of the spectra (down to 4 ev).

8. Cu(II) chelates

Accidental degeneracies in the electronic structure

---

48) F. A. Cotton, C. B. Harris, and J. J. Wise, Inorg. Chem. 6, 909 (1967).

$Cu(acac)_2$ and $Cu(hfac)_2$ have made their photoelectron spectra deceptively simple. No well-resolved bands due to d-electrons are evident in Figure 11, or in the energies of Table XI.

Table XI

	acac	hfac
1st band	8.20 ev	9.92 ev
2nd band	8.53 ev	10.20 ev
3rd band	9.13 ev	10.88 ev
4th band	9.75 ev	ca. 11.7 ev
5th band	10.23 ev	11.93 ev
6th band	10.44 ev	ca. 12.3 ev
7th band	11.41 ev	ca. 13.6 ev

Since no d-electron peaks were found, it was assumed that the d-electrons must be buried under the other ionizations. We have assigned the first two peaks to the split halves of the π-levels, and the third and fourth bands to the split components of the n_- orbitals. The fifth band is clearly due to ionization from the n_+ levels, but the origin of the shoulder on the high energy side is not clear. It is possible that the n_+ band is beginning to split and has not yet been resolved, or it might be due to ionization from some undetermined orbital. These photoelectron results also refute the extended Huckel calculations performed on $Cu(acac)_2$ by Cotton et al[48] for the same reasons as mentioned

Figure 11

Photoelectron Spectra of $Cu(acac)_2$ and $Cu(hfac)_2$

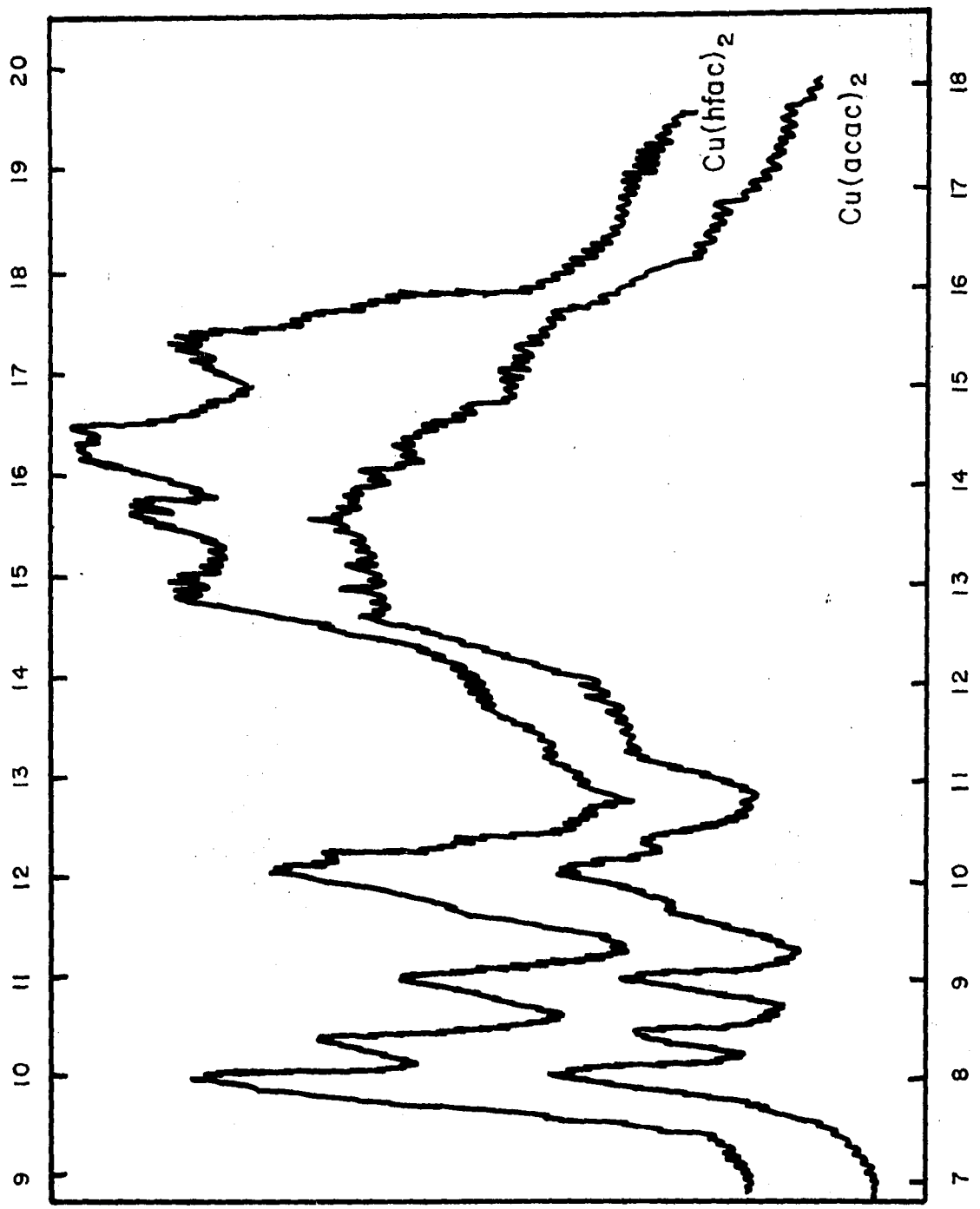

in the previous section. These calculations appear to have made the d-electrons more nonbonding than they really are.

9. Zn(II) chelates

Having reached the complexes of Zn(II), we have now reached the end of the first transition series. Since Zn(II) possesses a full d^{10} configuration, one would not expect to find a great deal of ligand-field splitting. This belief is confirmed in the spectra of Figure 12, along with the ionization potentials of Table XII.

Table XII

	acac	hfac
1^{st} band	8.46 ev	10.25 ev
2^{nd} band	9.22 ev	11.17 ev
3^{rd} band	10.39 ev	12.53 ev
4^{th} band	10.72 ev	12.78 ev
5^{th} band	11.52 ev	13.50 ev

Upon examination of the spectra, one might wonder where the d-electrons have gone. It is assumed that they lie buried under both the first peak (which has been assigned to the π-orbital ionizations) and under the second peak (assigned to the n_- ionizations). It is entirely possible that they have been stabilized even further and have been

Figure 12

Photoelectron Spectra of $Zn(acac)_2$ and $Zn(hfac)_2$

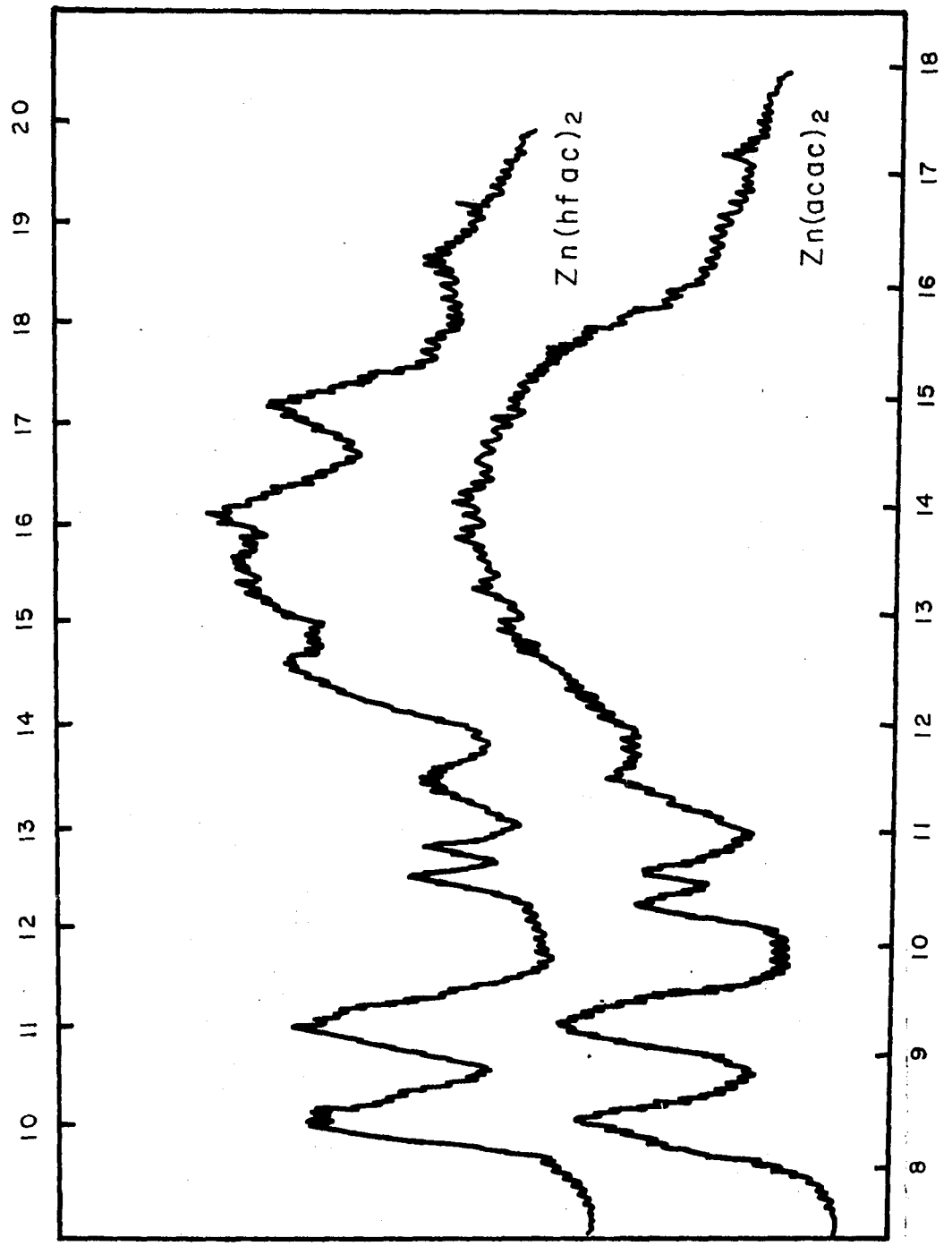

lost under the large "haystack" of peaks that has been a general feature of all the photoelectron spectra. But the most interesting item of all is the splitting of the n_+ levels. Two bands of exactly equal intensity are observed in the region where a single n_+ peak is expected, and are thus assigned formally to the n_+ levels. Exactly why this set of orbitals ought to split is uncertain, but a possible reason is a change in molecular symmetry. It has been established by electron diffraction studies that the Cu(II)[49] and Ni(II)[50] chelates are square planar while in the gas phase, but that the Zn(II) chelates adopt a D_{2d} symmetry[51] in the vapor phase (this conformation places the oxygen atoms in an approximately tetrahedral arrangement). It is possible that the change in geometry produces the splitting, but we cannot be certain at this time.

---

49) S. Shibata and K. Sone, Bull. Chem. Soc. Jap. 29, 856 (1956).

50) S. Shibata, Bull. Chem. Soc. Jap. 30,753 (1957).

51) F. A. Cotton and J. S. Wood, Inorg. Chem. 3, 245 (1964).

F. Discussion of The Photoelectron Spectral Results

In the preceeding sections, the photoelectron spectra of twenty-two acetylacetonate and hexafluoroacetylacetonate complexes have been presented along with assignments of most of the photoelectron peaks. It must be pointed out that the proposed assignments are at best tentative, since without detailed (and reliable) calculations no definite assignments are possible. However, by a judicious combination of CNDO theory and experimental trends, we feel that we have made the best possible assignments of the spectra. Our conclusions have agreed for the most part with those of Orchard et al,[23] wherever the same compounds were run. We have extended this work to include all members of the first transition series and are now in a position to make some observations regarding the bonding in these complexes.

In Table XIII, the ionization potentials of all hexafluoroacetylacetonate chelates of the first transition series have been collected. Data from the work of Orchard et al[23] have been included for completeness; we did not record the photoelectron spectrum of $Ti(hfac)_3$ or $V(hfac)_3$, and their $Co(hfac)_3$ spectrum was superior to ours. An attempt was made to correlate Pauling electronegativities[52] with the

---

52) L. Pauling, "The Nature Of The Chemical Bond", Cornell University Press, Third edition, 1960

Table XIII

Vertical Ionization Potentials of all First Transition Series Hexafluoroacetylacetonate Complexes

Compounds marked with an asterisk refer to data of Orchard et al.[23]

Metal	d		π		n_-		n_+	
Mg	-		10.28		11.18		12.31	
Al	-		10.21		11.27		12.59	
Sc	-		10.01		10.76	11.34	12.22	
Ti*	7.94		10.24		10.87	11.28	12.24	
V*	8.68		10.10		10.96	11.39	12.20	
Cr	9.50		9.93		10.83	11.40	12.17	
Mn	-		9.87		-		-	
Fe	-		10.07		11.13		12.11	
Co*	9.73	10.13		10.73	11.15	11.75	12.56	
Ni	9.35	9.84	-	10.67	11.11	ca. 11.9	12.01	
Cu	-		9.92	10.20	10.88	ca. 11.7	11.93	ca. 12.3
Zn	-		10.25		11.17		12.53	12.78

ionization potentials of a particular type of orbital, but totally negative results were obtained. Since the values of electronegativity chosen were those of neutral atoms, the lack of correlation is not surprising. One can easily observe certain groupings in Table XII that indicate that all chelates are bound in a similar fashion and that they must possess a common electronic structure. We have not yet found explanations for the shifts in ionization potential on passing from chelate to chelate, but when a better description of the electronic structure becomes available (requiring a good ab initio calculation) some further explanation may be attempted.

Some observations may be made regarding the π-bonding in these metal complexes. A large change in the photoelectron spectrum was found in passing from the protonated ligands to the metal chelates, and this would imply a large change in electronic structure. The nature of the assignments we have made and the results of the CNDO calculations bears out this point. However, relatitively little change was observed in examining the various metal compounds, with all the spectra appearing similar except for a few splittings. Thus, one may conclude that all the complexes do indeed possess virtually the same electronic structure, and that any π-bonding effects (such as those in $Co(acac)_3$) are secondary in importance when compared to the electronic reorganization

brought about by the σ-bonding. It would be very interesting to measure the X-ray photoelectron spectra of the chelates in order to learn about the more strongly bonding molecular orbitals, but to this date only some of the bands of $Cr(acac)_3$[53] and $Cr(hfac)_3$[54] have been measured. The weak π-bonding of the Fe(III) chelates has been demonstrated by noting the similarity of their spectra with those of the Al(III) chelates. Evidence based on nuclear magnetic resonance spectroscopy has been presented[55] which indicates that the ligand π-delocalization does not include the bridging metal atom to any observable extent. Our photoelectron spectra show that <u>some</u> interaction of the metal π-levels and the ligand π-levels is taking place, but that its extent of interaction is not very large (at least in the orbitals accessible to He(I) ionization).

---

53) M. V. Zeller and R. G. Hayes, Chem. Phys. Lett. <u>10</u>, 610 (1971).

54) D. T. Clark and D. B. Adams, Chem. Phys. Lett. <u>10</u>, 121, (1971).

55) B. Bock, K. Flatau, H. Junge, M. Kuhr, and H. Musso, Angew. Chem. Int. Ed. <u>10</u>, 225 (1971).

Section II

The Interpretation of the Kerr Effect in Liquids

contents

A. Introduction

Since the discovery of electrically-induced birefringence by John Kerr in 1875,[57] many studies of molecular structure have been carried out utilizing this effect. For instance, Le Fevre and coworkers[58,59] have studied the conformations of many compounds in solution by comparing experimental Kerr constants with those predicted from possible molecular conformations. A statistical mechanical theory was developed by Buckingham and Pople.[60] The generally accepted expression for the molecular Kerr constant of a liquid was originally proposed by Otterbein,[61] and has the form:

$$mK = \frac{6n\,V_m}{(n^2+2)^2(\epsilon+2)^2} \lim_{E\to 0}\left(\frac{n_{\parallel}-n_{\perp}}{E^2}\right) \qquad (1)$$

where $(n_{\parallel} - n_{\perp})$ is the anisotropy induced in the refractive index by the electric field, n is the refractive index of the isotropic medium at the wavelength used, V_m is the molar volume, ϵ is the static dielectric constant, and E is the

---

57) J. Kerr, Phil. Mag. 50, 337, 446 (1875).

58) C. G. Le Fevre and R. J. W. Le Fevre, "The Kerr Effect", in Physical Methods of Chemistry, IIIC, ed. Weissburger, Wiley, New York, 1972.

59) R. J. W. Le Fevre, "Molecular Refractivity and Polarizability", in Advances In Physical Organic Chemistry, V, ed. Gold, Academic Press, New York, 1965.

60) A. D. Buckingham and J. A. Pople, Proc. Phys. Soc. A68, 905, 910 (1955).

61) G. Otterbein, Physik. Z. 35, 249 (1934).

electric field strength. More recently, Vuks[62] has proposed an alternative formulation:

$$mK = \frac{2n\,V_m}{3(n^2+2)(\epsilon+2)} \lim_{E \to 0} \left(\frac{n_{\parallel} - n_{\perp}}{E^2} \right) \quad (2)$$

Vuks justified his version by theoretical and experimental arguments. He pointed out in a previous paper[63] that the classical Lorentz-Lorenz formula was derived for isotropic substances, and that its extension to anisotropic substances:

$$\frac{n_{\parallel}^2 - 1}{n_{\parallel}^2 + 2} = \frac{4}{3} N_o \langle \pi_{\parallel} \rangle \quad (3a)$$

$$\frac{n_{\perp}^2 - 1}{n_{\perp}^2 + 2} = \frac{4}{3} N_o \langle \pi_{\perp} \rangle \quad (3b)$$

had no experimental or theoretical support. He then argued that in an anisotropic crystal, consideration of the internal electric fields would yield instead:

$$\frac{n_{\parallel}^2 - 1}{n^2 + 2} = \frac{4}{3} N_o \langle \pi_{\parallel} \rangle \quad (4a)$$

$$\frac{n_{\perp}^2 - 1}{n^2 + 2} = \frac{4}{3} N_o \langle \pi_{\perp} \rangle \quad (4b)$$

---

62) M. F. Vuks, Opt. i. Spektroskopiya 21, 697 (1966); Opt. Spect. (eng. trans.) 21, 383 (1966).

63) M. F. Vuks, Opt. i. Spektroskopiya, 20, 644 (1966); Opt. Spect. (eng. trans.) 20, 361 (1966).

It should be noted that in equations (3) and (4), the quantity $\langle \pi_i \rangle$ refers to the averaged component of the polarizability either parallel or perpendicular to the applied field. Vuks derived his version of the Kerr formula from his formulation of the Lorentz-Lorenz equation for anisotropic substances. He compared polarizability anisotropies of various liquids and gases (as calculated by each theory) and found that his formula led to better agreement of gas and liquid phase polarizabilities, while the Otterbein formula led to discrepencies between the values.

However, it is not clear whether the gas and liquid phase polarizabilities ought to be the same, since there are perturbing molecular interactions present in the liquid which are absent in the vapor phase. For instance, one would certainly not expect the polarizability of a liquid which shows strong intermolecular hydrogen bonding (such as water) to be the same in the gas phase, where only isolated molecules are expected. Thus, comparsion of liquid-phase and vapor-phase polarizability anisotropies may not be a valid test of which theory better explains the experimental facts. Equations (1) and (2) lead to different values for the anisotropy, with the Vuks formalism yielding values which are typically twice that of the Otterbein formula.

The only meaningful and self-consistent method to test

the two theories is to vary the refractive index and dielectric constant systematically and then measure the resulting birefringences of the solutions. There are two ways to approach this: either one can examine a series of mixtures of two solvents which possess widely differing values of refractive index and dielectric constant, or one can vary the temperature of a single solvent over as wide a range as possible. Both approaches have been considered in this investigation.

B. Theory

Buckingham and Pople[60] have shown for dense media consisting of axially-symmetric, non-polar molecules, that the molecular Kerr constant is given by:

$$mK = \frac{4\pi N_o}{405}\left[\gamma_{\alpha\alpha\beta\beta} + 3\,\frac{(a_{\alpha\beta}\alpha_{\alpha\beta} - 3\,\bar{a}\,\bar{\alpha})}{2kT}\right] \qquad (5)$$

where $\gamma_{\alpha\alpha\beta\beta}$ is the hyperpolarizability tensor, $a_{\alpha\beta}$ is the optical polarizability, $\alpha_{\alpha\beta}$ is the static polarizability. Equation (5) holds only if short-range intermolcular forces are absent; a form will be presented shortly which will allow for intermolecular correlation. In equation (5), a cartesian tensor notation has been used in which a repeated greek letter indicates summation. For spherical molecules, equation (5) reduces to:

$$mK = \frac{4\pi N_o\,\gamma}{81} \qquad (6)$$

If we now consider a mixture containing one spherically-symmetric component (such as CCl_4) and one axially-symmetric, non-polar component (such as CS_2), then equation (5) yields:

$$mK = \frac{4\pi\rho}{405}\left[X_1\gamma_1 + X_2\left(\gamma_2 + \frac{(a_{\parallel} - a_{\perp})(\alpha_{\parallel} - \alpha_{\perp})}{kT}\right)_2\right] \qquad (7)$$

where ρ is the total number of molecules per unit volume,

and X_1 is the mole fraction of the spherical component. Equation (7) can now be equated separately to equations (1) and (2), and the resulting relations solved for the birefringences. One obtains:

$$\left(\frac{\Delta n}{E^2}\right)_o = \frac{2\pi\rho(n^2+2)^2(\epsilon+2)^2}{1215\,n}\left[X_1\gamma_1 + X_2\left(\gamma + \frac{\Delta a\,\Delta\alpha}{kT}\right)_2\right] \quad (8)$$

$$\left(\frac{\Delta n}{E^2}\right)_v = \frac{2\pi\rho(n^2+2)(\epsilon+2)}{135\,n}\left[X_1\gamma_1 + X_2\left(\gamma + \frac{\Delta a\,\Delta\alpha}{kT}\right)_2\right] \quad (9)$$

It should be noted that the values used for the polarizability anisotropy and hyperpolarizability will be different for each formulation. It is possible to find numerical values for these quantities by measuring the Kerr constants of the pure components, setting either X_1 or X_2 equal to zero in equations (8) and (9) (depending on the component in question), and then solving for the values of the molecular parameters.

A test of the relative validity of equations (8) and (9) would consist of Kerr effect measurements on a series of mixtures that display a wide variation in both refractive index and dielectric constant. The values for the polarizability anisotropy and hyperpolarizability (as obtained from the measurements on pure components) would be substituted in equations (8) and (9) for each mole fraction, and then the calculated value of $(\Delta n/E^2)$ compared with that from experiment. The theory which allows the use of a single

set of molecular parameters through the entire concentration range would be judged the most consistent.

One possible objection that can be raised to this method is the neglect of short-range intermolecular forces. Molecules which are spherically-symmetric can not exhibit strong orienting intermolecular forces, but axially-symmetric molecules conceivably might. We can add a term to (7) to allow for this effect;[64] after doing so we obtain:

$$mK = \frac{4\pi\rho}{405}\left[X_1\gamma_1 + X_2\left(\gamma + \frac{\Delta a \Delta\alpha}{kT}\right)_2\left(1 + \langle P_2(\cos\theta)\rangle\right)\right] \quad (10)$$

where $\langle P_2(\cos\theta)\rangle$ is the correlation term, and has the form:

$$\langle P_2(\cos\theta)\rangle = \tfrac{1}{2}\iint (3\cos^2\theta - 1)\, n_2(\vec{r},\omega)\, d\vec{r}\, d\omega \quad (11)$$

In equation (11), $n_2(\vec{r},\omega)\, d\vec{r}\, d\omega$ is the probability of there being a molecule in the volume element $d\vec{r}$ and in the orientational element $d\omega$ relative to the fixed molecule. If there are no short-range molecular correlations, then $\langle P_2(\cos\theta)\rangle$ vanishes, since the unweighted average of $\cos^2\theta$ is 1/3. In that case, equation (10) would reduce to equation (7). The effect of this correlation could be described as a change in the value of the polarizability anisotropy that is used in the calculation of the birefringence. This term is not

---

64) A. D. Buckingham and R. E. Raab, J. Chem. Soc. 2341 (1957).

expected to be very large,[64] so if one formulation requires a large value of $\langle P_2(\cos\theta)\rangle$, then this would be viewed as a **deficency** in that theory.

The second method of testing the two theories is to determine the Kerr effect of a liquid as a function of temperature. We can rearrange equation (5) slightly to yield:

$$\frac{405\ mK}{4\pi N_o} = \gamma + \frac{\Delta a\ \Delta\alpha}{kT} \qquad (12)$$

and thus generate the equation of a straight line. By plotting the left-hand-side of equation (12) versus the reciprocal of the absolute temperature, we can obtain the hyperpolarizability by extrapolation to zero temperature. Presumably, one theory will yield acceptable values for the hyperpolarizability and polarizability anisotropy, while the other will not. Thus, further verifaction of one of the theories is possible.

C. Experimental Details

Spectral grade CCl_4 and CS_2 (MCB Associates) were used to make up a series of mixtures. The refractive index of each mole fraction was measured on an Abbe-3L refractometer which was thermostated at 25°C, and a dispersion relation was used to convert the observed readings taken at 589 nm to the desired values at 633 nm. All dielectric constant measurements were made on a precision capacitance measuring device (model 1610 manufactured by the General Radio Company), from which the dielectric constant was obtained by:

$$\epsilon = \frac{C_{soln}}{C_{air}} \qquad (13)$$

The density of each solution was obtained by the use of a pycnometer. All data obtained were checked against the International Critical Tables[65] whenever a correspondence could be found.

The Kerr constants were measured on a sensitive laser polarimeter,[66] which operated at 633 nm. The Kerr cell used in the measurements had gold-plated, phosphor-bronze electrodes which were 100 cm long, and were separated by 0.7 cm. The electrodes were mounted inside a cylindrical

---

65) Int. Crit. Tables, 3, 23, 28, 33, 143; 6, 76, 82, 83, 101, 105; 7, 12, 14, 34, 72, 78.

66) Built by the late John Matuska, in partial fulfillment of his requirements for the Ph.D. degree.

teflon sleeve, which was 120 cm long and 5 cm in diameter. The cell windows were made of zero-stress optical glass (1 mm thick and 10 mm across), to which an anti-reflection coating of MgF_2 had been applied to the outside surfaces. All the Kerr measurements were made at room temperature, since the Kerr cell itself was not thermostatted. However, the temperature of all measurements was determined to be $25^{\circ} \pm 1^{\circ}$ C by measuring the cell temperature with a thermocouple in contact with the electrodes.

The major cause of experimental error did not lie in the polarimeter (which has measured 10^{-6} degrees of rotation in the past using a 10 mW He-Ne laser as the light source), but in the laser used for these measurements. A 1 mW, Spectra-Physics He-Ne laser (model 132) was used in this study. This laser was prone to instability at times, and its low power level led to a poorer signal-to-noise ratio than in previous work.[66] The resulting error introduced by this laser led to an error in the Kerr constants of about 2%. The Kerr constants of the pure components were compared to the values of Le Fevre et al,[67] but since their data were taken at 589 nm, no direct comparsion could be made. Our values were slightly lower than those of Le Fevre et al, but this is to be expected, since the Kerr constant decreases with increasing wavelength in the absence of any

---

67) R. S. Armstrong, M. Aroney, C. G. Le Fevre, R. J. W. Le Fevre, and M. R. Smith, J. Chem. Soc. 1474 (1958).

strong visible or infrared absorptions.

The only other source of experimental error lay in the lack of precise temperature control of the Kerr cell. However, the effect of a $\pm$ 1° C temperature variation was estimated to lead to a 1% error in the Kerr constant, so it was concluded that the observed Kerr constants are accurate to within 3%.

D. Discussion

1. CCl_4 - CS_2 Mixtures

To test the relative validity of equations (8) and (9), the Kerr constants of a series of CCl_4 - CS_2 mixtures were measured. The only other literature data on these mixtures are those of Le Fevre et al,[67] who measured the Kerr effect in solutions that each had CS_2 and CCl_4 mole fractions of 0.1, respectively. Since they did not examine any intermediate mole fractions, and since their data were taken at 589 nm, these results were not included in the present work. The results of my Kerr effect determinations are gathered in Table XV, along with all pertinent experimental information. Before any birefringence predictions can be made, however, values for the polarizability anisotropy and hyperpolarizability must be determined for each component. These were calculated from my data on the pure components (for each formalism) using equations (5) and (6), and these results are tabulated in Table XIV.

Table XIV

	Otterbein	Vuks
mK (CCl_4) x 10^{12}	1.227	2.373
mK (CS_2) x 10^{11}	2.879	6.037
γ (CCl_4) x 10^{35}	1.313	2.540
$\left[\gamma + \frac{\Delta\alpha\,\Delta\alpha}{kT}\right]$ (CS_2) x 10^{33}	1.357	3.231

Table XV

Experimental data for the CCl_4 - CS_2 Mixtures

X_{CS_2}	n	ϵ	d	$B \cdot 10^7$
0.0000	1.4555	2.227	1.5846	0.0693
0.1121	1.4640	2.240	1.5595	0.180
0.1949	1.4722	2.255	1.5400	0.328
0.3081	1.4856	2.283	1.5105	0.534
0.4000	1.4983	2.311	1.4840	0.740
0.5020	1.5144	2.348	1.4520	0.967
0.6936	1.5500	2.434	1.3844	1.594
0.7982	1.5725	2.490	1.3434	1.981
0.9031	1.5971	2.553	1.2994	2.509
1.0000	1.6234	2.625	1.2559	3.103

All the quantities in Table XIV are expressed in terms of CGS units. A computer program was written which would take the values for the polarizability anisotropies and hyperpolarizabilities of Table XIV along with the experimental data of Table XV and then predict the birefringence value that each theory required. To compare with experiment, the specific Kerr constant, B, was actually calculated. This is defined as:

$$B = \frac{(n_{\parallel} - n_{\perp})}{\lambda E^2} \qquad (14)$$

so that the birefringence predicted by equations (8) and (9) is related to B by:

$$\left(\frac{\Delta n}{E^2}\right) = B \lambda \qquad (15)$$

These computed results are summarized in Table XVI.

It is seen in Table XVI that both theories predict the solution birefringences adequately near the extremes in mole fraction. This behavior is expected, since the specific Kerr constant of equation (14) is required to be the same for each theory in the limiting case of a pure component. However, the Vuks formalism fails badly in the intermediate mole fraction region. The Otterbein formula is able to predict the Kerr constants (within experimental error)

Table XVI

Predicted Kerr constants for CS_2 - CCl_4 mixtures

X_{CS_2}	Otterbein $B \cdot 10^7$	% error	Vuks $B \cdot 10^7$	% error
0.1121	0.183	1.7	0.189	5.0
0.1949	0.321	2.1	0.355	8.4
0.3081	0.534	0.0	0.633	18.5
0.4000	0.732	1.1	0.855	15.5
0.5020	0.985	1.9	1.129	16.8
0.5902	1.237	2.6	1.391	16.5
0.6936	1.584	0.6	1.738	9.0
0.7982	2.006	1.3	2.139	8.0
0.9031	2.520	0.4	2.606	3.9

within the entire range of concentrations possible. The failure of the Vuks theory implies that one would not be able to employ a consistent set of polarizabilities through the entire concentration range if this theory were to be accepted. Since one would not expect these molecular parameters to vary with concentration, it is clear that the Vuks formula is not internally consistent.

An alternative explanation is possible, however. If the effects of intermolecular correlation as defined in equation (11) are not insignificant, then by equation (10) one might expect the value of the polarizability anisotropy to vary somewhat with concentration, although the expected variation ought not to be very great. To study this possibility, the preceeding data were re-examined and values for $\langle P_2(\cos\theta)\rangle$ were calculated for each theory. These are summarized in Table XVII. Two assumptions were made. The first was that the contribution of the hyperpolarizability of CS_2 to the Kerr constant could be neglected, and the second was that the value of $\langle P_2(\cos\theta)\rangle$ could be taken as zero at the lowest mole fraction of CS_2 studied. This last assumption was made since little association of CS_2 molecules would be expected in a solution that had a CCl_4 mole fraction of 0.9.

Examination of Table XVII shows that while the Otterbein

Table XVII

Values of $\langle P_2(\cos\theta)\rangle$ predicted by each theory for the CS_2 - CCl_4 mixtures at 25° C

X_{CS_2}	Vuks $\langle P_2(\cos\theta)\rangle$	Otterbein $\langle P_2(\cos\theta)\rangle$
0.1121*	0.0000	0.0000
0.1949	0.0354	0.0102
0.3081	0.0374	0.0120
0.4000	0.0548	0.0100
0.5020	0.0545	0.0105
0.5902	0.0564	0.0102
0.6936	0.1296	0.0117
0.7982	0.1407	0.0130
0.9031	0.1860	0.0112
1.0000	0.2318	0.0157

* assumed that $\langle P_2(\cos\theta)\rangle$ = 0 for this mole fraction

formula predicts negligble values of $\langle P_2(\cos\theta)\rangle$, the Vuks formula requires much larger ones. In fact, the Vuks theory seems to require considerable correlation even at the lowest CS_2 concentration. Calculated values for $\langle P_2(\cos\theta)\rangle$ are two orders of magnitude less than the ones observed.[64] One would expect the value of this correlation to go to zero at infinite dilution, but this does not seem to be happening in the Vuks theory. While there is some evidence for self-association in pure liquid CS_2,[68] appreciable association is not expected for low mole fractions in non-interacting solvents. Since the justifcation of the Vuks formula by this correlation argument requires the use of unreasonably large corrections, this approach cannot be used to justify the use of equation (2) over equation (1).

2. Variable-Temperature Studies of the Kerr Effect

Since the results just summarized cast doubt on the Vuks explanation of the Kerr effect, it seemed worthwhile to find out whether any additional evidence could be obtained. In particular, an explanation for the agreement of Vuks polarizability anisotropies with values obtained from gas-phase Kerr measurements was desirable. As mentioned earlier, a second method to vary the refractive index and

---

68) R. Ulbrich, Z. Naturforsh, 146, 978 (1964).

dielectric constant of a medium is to vary the temperature of a pure solvent and to measure the resulting change in Kerr constant. This has been done by Zuehlke and Ingersoll[69] for carbon disulfide, and by Le Fevre and Le Fevre[70] for benzene, p-xylene, mesitylene (1,3,5-trimethylbenzene), and tetrachloroethylene. Since both groups tabulated values for the refractive index, dielectric constant, and density along with the observed Kerr constants, no further experimental work was necessary.

The procedure followed was to take the observed Kerr constants along with the experimental data provided by the other groups, and to calculate a value for the polarizablity anisotropy. This was done by setting $X_1 = 0$ and $X_2 = 1$ in equations (8) and (9), and then applying equation (15). These relations were then solved for the polarizability anisotropy, and the resulting equations are:

$$\frac{1215\, B \lambda n}{2\pi\rho(n^2 + 2)^2(\epsilon + 2)^2} = \left[\gamma + \frac{\Delta a \Delta \alpha}{kT}\right] \qquad (16)$$

$$\frac{135\, B \lambda n}{2\pi\rho(n^2 + 2)(\epsilon + 2)} = \left[\gamma + \frac{\Delta a \Delta \alpha}{kT}\right] \qquad (17)$$

---

69) A. A. Zuehlke and L. R. Ingersoll, J. Opt. Soc. Am. 27, 314 (1937).

70) C. G. Le Fevre and R. J. W. Le Fevre, J. Chem. Soc. 2670 (1959).

All work in these studies was done at a wavelength of 589 nm. It is easily seen that equations (16) and (17) are in the form of straight-line equations, with:

$$\text{slope} = \frac{\Delta a \, \Delta \alpha}{k} \tag{18}$$

$$\text{intercept} = \gamma \tag{19}$$

If one plots the left-hand-sides of equations (16) and (17) versus the reciprocal of the absolute temperature, the hyperpolarizability and polarizability anisotropy are easily obtained. Calculations of this sort were carried out using a least-squares method of curve fitting. In the case of p-xylene and tetrachloroethylene, the right-hand-side of equations (16) and (17) is not as simple (since they are not symmetric tops), but the hyperpolarizability is still obtained on extrapolation to zero temperature. The computed results are summarized in Table XVIII. It was observed that the slope error averaged about 5% for both theories, and that the intercept error averaged about 20%.

The most noteworthy feature of these extrapolations is the unreasonable values for the hyperpolarizability that are computed using the Vuks formalism. In all cases, it was seen that the Vuks method predicted hyperpolarizability values which were at least an order of magnititude greater than those of the Otterbein method, and usually of opposite

Table XVIII

Results of the Effect of temperature on the Kerr constants of several pure liquids

The data for CS_2 were obtained from Zuehlke and Ingersoll,[69] and all other data was obtained from Le Fevre and Le Fevre.[70]

	Otterbein formula	Vuks formula
a) Benzene		
$\gamma \cdot 10^{35}$	0.969	-18.88
$\Delta a \cdot 10^{24}$	-3.621	-5.778
$\bar{a} \cdot 10^{24}$	10.465	10.465
$a_{\parallel} \cdot 10^{24}$	8.051	6.613
$a_{\perp} \cdot 10^{24}$	11.672	12.391
b) Mesitylene		
$\gamma \cdot 10^{35}$	1.274	-12.24
$\Delta a \cdot 10^{24}$	-5.570	-8.828
$\bar{a} \cdot 10^{24}$	16.325	16.325
$a_{\parallel} \cdot 10^{24}$	12.612	10.440
$a_{\perp} \cdot 10^{24}$	18.182	19.268
c) Carbon Disulfide		
$\gamma \cdot 10^{35}$	7.981	-41.41
$\Delta a \cdot 10^{24}$	5.916	10.993
$\bar{a} \cdot 10^{24}$	8.480	8.480
$a_{\parallel} \cdot 10^{24}$	10.452	12.144
$a_{\perp} \cdot 10^{24}$	4.536	1.151
d) P-Xylene		
$\gamma \cdot 10^{35}$	0.719	-10.05
slope $\cdot 10^{30}$	0.229	0.488
e) Tetrachloroethylene		
$\gamma \cdot 10^{35}$	1.354	-35.58
slope $\cdot 10^{30}$	0.205	0.514

sign. Buckingham et al[71] have examined the temperature dependence of gaseous benzene and carbon disulfide, and the results of their work are presented in Table XIX. These values are of interest since both the Otterbein and Vuks theories predict the same expression for the molecular Kerr constant in the vapor phase (where $n^2 = \epsilon = 1$).

Table XIX

	C_6H_6	CS_2
$\Delta a \cdot 10^{24}$	-5.6 ± 0.1	10.7 ± 0.2
$\gamma \cdot 10^{35}$	0.8 ± 0.4	7.1 ± 0.6

Not much is known about the behavior of the hyperpolarizability in the liquid phase, but is seems unlikely that it would change sign and increase by an order of magnitude on passing from the gas phase to the liquid. The Otterbein theory predicts much more reasonable values for the hyperpolarizability, as may be seen by comparing Tables XVIII and XIX. The fact that the Vuks theory leads to such unreasonable values for the hyperpolarizability may be viewed as additional evidence against it.

These large, negative values of the hyperpolariz-

71) M. P. Bogaard, A. D. Buckingham, and G. L. D. Ritchie, Mol. Phys. 18, 575 (1970).

ability that are obtained by the Vuks theory are the reason that Vuks was able to reconcile gaseous and liquid phase polarizability anisotropies. However, even Vuks[62] admitted that his theory only gave agreement for some compounds and failed for others. It is clear now that the Vuks theory actually overestimates the polarizability anisotropy and then balances this exaggeration by introducing an artifically large and negative hyperpolarizability. For example, Vuks found that his theory worked quite well for mexitylene, and he was able to predict the observed Kerr constant quite well. He calculated a value for the polarizability anisotropy at a single temperature by neglecting the contribution of the hyperpolarizability (which is not negligable if his theory is accepted), and found a value of -7.61×10^{-24} esu. Examination of the results in Table XVIII, which were calculated by the more correct method of determining slope and intercept, show that the correct value of the polarizability anisotropy (as predicted by the Vuks theory) was actually -8.828×10^{-24} esu. It was the effect of the exaggerated hyperpolarizability that brought the apparent polarizability down to the gas phase value.

We have concluded that the success of the Vuks theory in finding solution polarizability anisotropies equal to the gas phase values was actually based on chance cancellations. The only experimental support of the Vuks theory arose from

the agreement of these polarizability values, but this was not shown to be a general phenemenon. Vuks[62] obtained reasonable agreement for mesitylene, napthalene, carbon dioxide, and cyclohexane, but obtained poorer results for benzene, p-xylene, p-dichlorobenzene, carbon disulfide, and p-dioxane. Comparsion of Tables XVIII and XIX shows agreement of the polarizability anisotropies actually required excessively large values for the hyperpolarizability. This fact is viewed as another deficency in the Vuks theory.

E. Summary

This work has cast considerable doubt on the Vuks explanation for the Kerr effect, and thus his agrument for the Lorentz local field must be viewed with caution. Vuks assumed a form for the local electric fields, and obtained a different statement of the Kerr constant formula from these arguments. The Otterbein formulation has been shown to be superior in explaining the temperature dependence of the Kerr effect, and is the only theory which is able to employ a consistent set of polarizability anisotropies and hyperpolarizabilities in a series of mixtures of two components. The Vuks method appears to overestimate both the polarizability anisotropy and the hyperpolarizability. Cancellation of these excesses is obtained by forcing the hyperpolarizability to be opposite in sign to the polarizability anisotropy.

In his paper, Vuks[62] also applied his version of the Lorentz local field to the study of polar molecules, and obtained the same sort of agreement for some compounds. However, neither the field assumed by Vuks nor the field assumed by Otterbein is sufficent for the theory of polar molecules, so any agreement of the Vuks theory for polar molecules must also be regarded with extreme caution. The doubt cast on the Vuks theory for the Kerr effect also

discredits the work of Boyle,[72] which attempted to justify the same sort of correction to the theory for the Cotton-Mouton effect (the magnetic analogue of the Kerr effect). If the local field assumed by Vuks is incorrect, then the Boyle formula must also be incorrect, since he used the Vuks field to derive his formula.

At the present time, it is still not understood why the polarizability anisotropy of liquids ought to be about half that of the gas phase molecules. It is well known[73] that polarizability anisotropies cannot be obtained from Rayleigh scattering experiments on liquids, whereas they are readily calculated from vapor phase work. It has been pointed out that the available theories for scattering cannot yet be applied to interpretation of liquid phase data, except in a very qualitative fashion. Until further theory is developed, no explanation will be available to explain the difference in polarizability anisotropy.

---

72) L. L. Boyle, Chem. Phys. Lett. 1, 404 (1967).

73) I. L. Fabelinskii, "Molecular Scattering Of Light", Plenum Press, New York, 1968.

Section III

Magnetic Anisotropy Of Metal Acetylacetonates

contents

A. Introduction

Since the first preparation of a metal complex of acetylacetone in the ninteenth century, there has been considerable interest in the physical properties of these compounds. The principal controversy has dealt with the question of whether there exists aromatic character in the chelate rings. Calvin and Wilson[74] were the first to propose a benzenoid resonance in the metal complexes of acetylacetone:

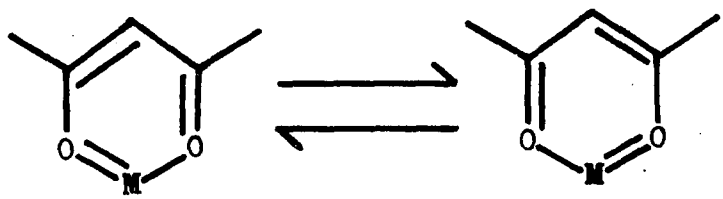

This idea was later supported by the observations of Collman and coworkers[75] that the ring hydrogen para to the metal could be replaced by a variety of groups, using electrophilic attack. These reactions were all reminiscant of the electrophilic substitutions that organic chemists have used on aromatic compounds, so Collman inferred that the metal complexes possessed aromatic character as well.

Supporting evidence for the aromaticity was sought elsewhere. It had been known[76,77] that the diamagnetic

---

74) M. Calvin and K. W. Wilson, J. Am. Chem. Soc. 67, 2003 (1945).

75) J. P. Collman, Inorg. Syn. 7, 134 (1963); J. P. Collman and W. L. Young, Inorg. Syn. 7, 205 (1963).

76) J. A. Pople, J. Chem. Phys. 24, 1111 (1956).

77) C. E. Johnson and F. A. Bovey, J. Chem. Phys. 29, 1012 (1958).

anisotropy of an aromatic ring was able to affect the position of a proton resonance in a NMR spectrum. Protons in the plane of an aromatic ring are shifted to lower magnetic fields and protons above or below the interior of the ring are shifted to higher fields. This magnetic anisotropy is currently accepted as the simplest criterion of aromatic character.[55] Many examples of the use of this technique have filled the literature, such as for cyclophanes[78] and for annulenes,[79] so that the concept is well established.

The first attempts at applying the NMR spectra of diamagnetic acetylacetonates to an evaluation of aromatic character were interpreted quite differently.[14] Some authors argued that the spectra confirmed the original supposition of Calvin,[80,81] but the bulk of the investigators believed that the NMR results did not indicate aromatic character in the metal complexes.[82,83,84]

---

78) D. J. Wilson, V. Boeketheide, and R. W. Griffin, J. Am. Chem. Soc. 82, 6302 (1960).

79) I. C. Calder, Y. Gaoni, P. J. Garratt, and F. Sondheimer, J. Am. Chem. Soc. 90, 4954 (1968).

80) J. P. Collman, R. L. Marshall, and W. L. Young, Chem. Ind. (London), 1380 (1962).

81) R. E. Hester, Chem. Ind. (London), 1397 (1963).

82) A. Trestianu, H. Niculescu-Majewska, I. Bally, A. Barabas, and A. T. Balaban, Tetrahedron, 23, 2499 (1968).

83) R. H. Holm and F. A. Cotton, J. Am. Chem. Soc. 80, 5658 (1958).

84) J. A. S. Smith and E. J. Wilkins, J. Chem. Soc. A, 1749 (1966).

The only clear-cut method of determinining the extent of aromatic character in the acetylacetonate complexes is to measure their magnetic anisotropy directly. It is to be noted that while it is comparatively easy to measure paramagnetic anisotropy, it is considerably more difficult to measure the necessary diamagnetic anisotropy.[85] Interestingly enough, an extensive literature search has shown that it had not occurred to any previous workers that magnetic anisotropies could be used to establish the presence or absence of aromatic character in these compounds. The purpose of this investigation, therefore, was to determine the diamagnetic anisotropy of as many acetylacetonate complexes as possible and to relate these values to those of known aromatic compounds.

There are basically three methods for measuring the anisotropy in magnetic susceptibility of a molecule. These involve magnetic susceptibility measurements on single crystals (86), the microwave Zeeman effect (87), and the Cotton-Mouton effect (88). It is almost impossible to detect

---

85) B. N. Figgis and J. Lewis, "The Magnetic Properties Of Transition Metal Complexes", in Progress In Inorganic Chemistry, volume 6, ed. F. A. Cotton, Wiley-Interscience, 1964.

86) S. Mitra, "Magnetic Anisotropy", in Transition Metal Chemistry, volume 7, ed. R. L. Carlin, Marcel Dekker, 1972.

87) W. H. Flygare and R. L. Shoemaker, Symp. Far. Soc. 3, 119 (1969).

88) A. D. Buckingham and J. A. Pople, Proc. Phys. Soc. B69, 1133 (1956).

a microwave spectrum in large molecules, so attention was focused on the first and third methods. The Cotton-Mouton effect has been mentioned briefly in the previous section as the magnetic analogue of the Kerr effect. In short (this will be further developed in the next section), the measurement of magnetically-induced birefringence enables one to determine the product of the magnetic susceptibility anisotropy and the polarizability anisotropy, for an axially-symmetric molecule. The previous work has shown that a measurement of the Kerr effect leads to a determination of the polarizability anisotropy. Thus, a measurement of both the Cotton-Mouton and Kerr effects of the same axially-symmetric molecule enables a direct determination of the magnetic anisotropy.

We have carried out the induced-birefringence measurements and have contrasted the results with published data of single crystal paramagnetic anisotropy. The diamagnetic anisotropy was obtained from variable-temperature studies of the magnetic susceptibility of single crystals of paramagnetic acetylacetonates. One would then want to compare the anisotropies with those of aromatic compounds in an attempt to deduce the extent of delocalization in the chelates.

B. Theory

As mentioned in the preceeding section, determination of the anisotropy in the magnetic susceptibility requires a measurement of both the Cotton-Mouton and Kerr effects. The theory of the Kerr effect has been fully developed in Section II of this work; since the results of that section showed that the Otterbein formulation of the Kerr effect is preferable, it will be employed throughout the course of the current investigation. It only remains to set out the theory of the Cotton-Mouton effect.

Buckingham and Pople[88] have developed a statistical mechanical theory for the Cotton-Mouton effect of non-absorbing molecules, which was extended to paramagnetic molecules by Stiles.[89] However, since all our Cotton-Mouton measurements were made on diamagnetic molecules, the theory of Buckingham and Pople was used. A formula for the molecular Cotton-Mouton constant of a liquid may be defined in a fashion analgous to the Otterbein definition for the molecular Kerr constant:

$$mC = \frac{2 n V_m}{3 (n^2 + 2)^2} \lim_{H \to 0} \left(\frac{n_{\parallel} - n_{\perp}}{H^2} \right) \qquad (20)$$

89) P. J. Stiles, Mol. Phys. 15, 405 (1968).

where H is the strength of the magnetic field, and the rest of the symbols have been defined previously. Buckingham and Pople[88] showed for dense fluids of axially-symmetric molecules that the molecular Cotton-Mouton constant equals:

$$mC = \frac{4\pi N}{135}\left[\eta_{\alpha\beta:\alpha\beta} - \frac{1}{3}\eta_{\alpha\alpha:\beta\beta} + \frac{(\alpha_{\parallel} - \alpha_{\perp})(\gamma_{\parallel} - \gamma_{\perp})}{3\ kT}\right] \qquad (21)$$

where $\eta_{\alpha\beta:\alpha\beta} - \frac{1}{3}\eta_{\alpha\alpha:\beta\beta}$ is a tensor allowing for the dependence of electric polarizability on the magnetic field, α is the optical polarizability, and γ is the magnetic susceptibility. For spherical molecules, equation (21) reduces to:

$$mC = \frac{4\pi N}{135}\left(\eta'' - \eta^{\perp}\right) \qquad (22)$$

where $(\eta'' - \eta^{\perp})$ represents the values of the tensor components parallel and perpendicular to the field. To simplify the equations, the following contraction will be used:

$$\Delta\eta = \eta_{\alpha\beta:\alpha\beta} - \frac{1}{3}\eta_{\alpha\alpha:\beta\beta} \qquad (23)$$

If we now consider an axially-symmetric solute (such as a metal acetylacetonate) dissolved in a solvent composed of spherically-symmetric molecules (such as CCl_4), equation (21) yields:

$$mC = \frac{4\pi\rho}{135}\left[X_1\Delta\eta_1 + X_2\left(\Delta\eta + \frac{(\alpha_{\parallel} - \alpha_{\perp})(\gamma_{\parallel} - \gamma_{\perp})}{3\ kT}\right)_2\right] \qquad (24)$$

It is convenient at this point to define a specific Cotton-Mouton constant, and it is this quantity that is actually measured in the laboratory:

$$C = \frac{(n_{\parallel} - n_{\perp})}{\lambda H^2} \tag{25}$$

If one substitutes equation (25) into equation (20), then one obtains:

$$mC = \frac{2 n V_m \lambda C}{3 (n^2 + 2)^2} \tag{26}$$

Now equations (26) and (24) may be equated and the resulting relation solved for the solute's product of polarizability anisotropy and magnetic susceptibility anisotropy:

$$\left[\Delta\eta + \frac{(\alpha_{\parallel} - \alpha_{\perp})(\gamma_{\parallel} - \gamma_{\perp})}{3\ kT}\right]_2 = \frac{1}{X_2}\left[\frac{n \lambda C}{\pi \rho (n^2 + 2)^2} - X_1 \Delta\eta_1\right] \tag{27}$$

The polarizability anisotropy may be obtained by applying equation (16) of the previous section to a measurement of the Kerr effect. Then a measurement of the Cotton-Mouton effect enables the direct calculation of the anisotropy in the magnetic susceptibility. It is this **anisotropy** which one hopes will either confirm or disprove the presence of aromaticity in the acetylacetonate complexes.

C. Experimental Details

The Cotton-Mouton birefringence measurements were made on the same laser polarimeter described in a previous section, except that the 1 mW He-Ne laser was replaced by a 5 mW model to improve the signal-to-noise ratio. The Cotton-Mouton cell was made of a cylindrical glass tube (65 cm long) which was surrounded by a water jacket for precise temperature control. With the thermostating bath available, the temperature of all measurements was 25 $\pm$ 0.1 ^{o}C. The cell windows were made of the same zero stress-optical glass previously used in the Kerr effect measurements. An electromagnet which could develop up to 18 kilogauss was used to induce the birefringences. Unfortunately, its field contained a small longitudinal component which would induce a sizable Faraday rotation in the sample. This rotation would be measured as an induced birefringence by the polarimeter, but the result would have no meaning. To eliminate this undesired effect, number 24 magnet wire was wound about the entire length of the Cotton-Mouton cell and sufficent current was passed through the turns to suppress the Faraday rotation entirely.

Kerr effect determinations were made in the same manner as previously described, and the same cell was used. However, since this cell was not thermostated, the effects

had to be measured at room temperature. Densities, refractive indices, and dielectric constants were all taken at the same temperature as the Kerr measurements to remove any problems in the computation of polarizability anisotropies.

Preparation and purification of the acetylacetonate complexes has been described in the experimental section dealing with the Photoelectron Spectroscopy of these chelates. However, solution of these compounds in spectral grade CCl_4 (MCB Associates) raised a major problem. Although a visual examination of the solutions indicated complete dissolution, passage of a laser beam through the solution revealed considerable scattering due to undissolved particles. It was necessary to filter all solutions through activated charcoal to remove these particles and their spurious effects. Prior to the filtration, the solutions were mixed with a liberal quantity of charcoal, and the mixtures stirred for approximately half an hour. Mole fractions were obtained by a combination of spectrophotometric determinations and density measurements. Greater precision than previously was obtained by the use of the more powerful laser, so the concentration error was found to be the limiting quantity in the accuracy of the results. It was estimated that the observed Cotton-Mouton constants are accurate to within 2%.

D. Experimental Diamagnetic Anisotropies Of Some Metal Acetylacetonates

1. Magnetic Anisotropies of Various Aromatic Ring Combinations

Before an estimate of the degree of aromaticity in the metal complexes of acetylacetone can be made, it is first necessary to estimate the magnetic susceptibility anisotropy that these complexes would have if their rings were fully aromatic. We shall take the benzene ring as the prototype of an aromatic ring and calculate the expected anisotropies that would result if benzene rings were combined in a fashion duplicating the geometry of an acetylacetonate complex. Comparsion of the predicted and experimental values should be able to indicate whether these complexes are really aromatic.

Buckingham and coworkers[90] have measured both the Kerr and Cotton-Mouton effects of gaseous benzene, and have thus been able to obtain the magnetic anisotropy, finding a value of:

$$\chi_{\parallel} - \chi_{\perp} = -8.9 \times 10^{-29} \text{ emu} \qquad (28)$$

However, the mean susceptibility of benzene is also known,[91] and its value is:

$$\overline{\chi} = -9.1 \times 10^{-29} \text{ emu} \qquad (29)$$

---

90) M. P. Bogaard, A. D. Buckingham, M. G. Corfield, D. A. Dunmur, and A. H. White, Chem. Phys. Lett. 12, 558 (1972).

91) Landolt-Bornstein, Zahlenwerte and Funktionen, Band II, part 10, Springer, Berlin, 1967.

Using these two pieces of information, Buckingham et al were able to calculate:

$$\chi_{\parallel} = -15.0 \times 10^{-29} \text{ emu} \quad (30)$$

$$\chi_{\perp} = -6.1 \times 10^{-29} \text{ emu} \quad (31)$$

It is to be noted that the direction of $\chi_{\parallel}$ was taken to be parallel to the principal symmetry axis of the ring (a C_6 axis), or perpendicular to the plane of the ring. For our calculations, we define local ring susceptibilities parallel and perpendicular to the ring itself, and these values shall be denoted as $S_{\parallel}$ and $S_{\perp}$, respectively. These have the values:

$$S_{\parallel} = -6.1 \times 10^{-29} \text{ emu} \quad (32)$$

$$S_{\perp} = -15.0 \times 10^{-29} \text{ emu} \quad (33)$$

so that:

$$S_{\parallel} - S_{\perp} = +8.9 \times 10^{-29} \text{ emu} \quad (34)$$

We shall now combine rings having the anisotropy value of equation (34) into conformations which are identical to those of various acetylacetonate complexes, and to compute the resulting anisotropy. In comparing these values to those of the complexes, we are assuming that the two principal susceptibilities in the plane of the acetylacetonate ring are the same. We are also ignoring the effect of the bridging metals on the anisotropy of the complex as well as any differences between six hydrogens on the benzene rings when compared to two methyl groups and one hydrogen on an

acetylacetonate ring. The anisotropy to be calculated will result only from the bringing together of either two or three benzene rings in a manner which duplicates the arrangement of acetylacetonate rings in a complex.

a. D_{2d} symmetry

If one places two benzene rings on a common axis, forcing their ring planes to lie at right angles, the resulting combination belongs to the D_{2d} point group. An example of this type of conformation is provided by $Be(acac)_2$.[14] The common axis (which is a S_4 axis) passes through both rings and their junction, so that the susceptibility along this principal symmetry axis shall be denoted as $\chi_{\parallel}$. In this point group, the other two axes are equivalent, so that the two susceptibilities that lie along these axes shall each be labelled as $\chi_{\perp}$. For this type of arrangement, the relation between the ring susceptibilities (which were called $S_{\parallel}$ and $S_{\perp}$ using the same definitions as before) and the molecular susceptibilities is quite simple, since the directions of the ring susceptibilities coincide with the directions of the molecular susceptibilities.

Since the S_4 axis passes through the planes of both rings, the susceptibility along this parallel direction is simply given by:

$$\chi_{\parallel} = 2\, S_{\parallel} \qquad (35)$$

One of the two axes perpendicular to the S_4 axis passes parallel to the plane of one ring, but perpendicular to the plane of the other ring. It is seen that this susceptibility is:

$$\chi_{\perp} = S_{\parallel} + S_{\perp} \tag{36}$$

We are now in a position to calculate the anisotropy expected from these arguments:

$$\begin{aligned} \Delta\chi &= \chi_{\parallel} - \chi_{\perp} \\ &= + (S_{\parallel} - S_{\perp}) \end{aligned} \tag{37}$$

If one substitutes the value of equation (34) into equation (37), then one would obtain an approximate value for the magnetic anisotropy of an aromatic D_{2d} chelate of:

$$\Delta\chi = + 8.9 \times 10^{-29} \text{ emu} \tag{38}$$

b. D_{2h} symmetry

To achieve this conformation, we again take two benzene rings and place them on a common axis, but we now situate both rings in the same plane. This configuration is equivalent to taking the D_{2d} configuration and rotating one of the rings by 90° while holding the other ring fixed in space. In the D_{2h} point group, the three symmetry axes are not equivalent, but we shall make the reasonable approximation that the two axes parallel to the ring plane are approximately equivalent, so that we may equate the principal suscept-

ibilities along these axes. The principal symmetry axis shall be taken as the C_2 axis perpendicular to the plane containing both rings, and shall be denoted as the parallel direction. Since this axis passes perpendicular to both rings, the susceptibility along this direction is easily obtained as:

$$\chi_{\parallel} = 2\, S_{\perp} \tag{39}$$

For the axes perpendicular to the principal axis, the susceptibility is:

$$\chi_{\perp} = 2\, S_{\parallel} \tag{40}$$

So that the anisotropy is given by:

$$\begin{aligned} \Delta\chi &= \chi_{\parallel} - \chi_{\perp} \\ &= -2\,(S_{\parallel} - S_{\perp}) \end{aligned} \tag{41}$$

The value of equation (34) may now be substituted into equation (41) to obtain the anisotropy that one would expect from a D_{2h} chelate, provided the two axes in the plane of the rings are taken to be equivalent:

$$\Delta\chi = -\,17.8 \times 10^{-29} \text{ emu} \tag{42}$$

This rough value is the one expected for a planar chelate, such as $Ca(acac)_2$, if there is aromatic character.

c. D_3 symmetry

To achieve this symmetry, one must imagine an octahedron whose six apices have been occupied by three rings, each of

which occupies two positions. The principal symmetry axis is a C_3 axis which passes through a pair of parallel faces of the octahedron, and the rings are situated so that their planes lie at 45° with respect to this axis. In the point group D_3, the other two principal axes are completely equivalent. Due to the nature of this conformation, the ring susceptibilities are not easily related to the molecular susceptibilities, but it is possible to calculate what the approximate relations are. In the following derivation, the cartesian tensor notation introduced in Section II of this work shall be used.

Consider the magnetic susceptibility tensor of a molecule written in diagonal form:

$$\chi_{\alpha\beta} = \chi_{zz}\hat{k}\hat{k} + \chi_{xx}\hat{i}\hat{i} + \chi_{yy}\hat{j}\hat{j} \qquad (43)$$

where $\hat{i}$, $\hat{j}$, and $\hat{k}$ are unit vectors lying along the molecular x, y, and z axes and with the direction of $\hat{k}$ being perpendicular to the plane of the ring. We can then define an analagous tensor for the ring susceptibilities:

$$S_{\alpha\beta} = S_{zz}\hat{k}\hat{k} + S_{xx}\hat{i}\hat{i} + S_{yy}\hat{j}\hat{j} \qquad (44)$$

Equations (43) and (44) are related by:

$$\chi_{\alpha\beta} = S_{\alpha\beta}{}^{a} + S_{\alpha\beta}{}^{b} + S_{\alpha\beta}{}^{c} \qquad (45)$$

In equation (45), the superscripts a, b, and c refer to each of the three rings. The identity operator is defined as:

$$\delta_{\alpha\beta} = \hat{i}\hat{i} + \hat{j}\hat{j} + \hat{k}\hat{k} \tag{46}$$

If we now assume axial symmetry, then $S_{xx} = S_{yy} = S_{\parallel}$, and $S_{zz} = S_{\perp}$, so that we can rewrite equation (44) as:

$$S_{\alpha\beta} = S_{\perp}\hat{k}\hat{k} + S_{\parallel}\hat{i}\hat{i} + S_{\parallel}\hat{j}\hat{j} \tag{47}$$

We can multiply the identity operator by $S_{\parallel}$, and solve the resulting relation to obtain:

$$S_{\parallel}\hat{i}\hat{i} + S_{\parallel}\hat{j}\hat{j} = S_{\parallel}\delta_{\alpha\beta} - S_{\parallel}\hat{k}\hat{k} \tag{48}$$

We now substitute equation (48) into equation (47) and obtain a general equation for the susceptibility tensor:

$$S_{\alpha\beta} = (S_{\perp} - S_{\parallel})\,\hat{k}\hat{k} + S_{\parallel}\delta_{\alpha\beta} \tag{49}$$

At this point, we shall use the tensor $S_{\alpha\beta}$ in terms of the unit vectors e_{α}, which correspond to the unique axes of the ring. Equation (49) is then written:

$$S_{\alpha\beta} = (S_{\perp} - S_{\parallel})\,e_{\alpha}e_{\beta} + S_{\parallel}\delta_{\alpha\beta} \tag{50}$$

To find the susceptibility of a D_3 molecule, we shall find it easier to determine its magnetic moment, since the moment and the susceptibility are related by:

$$m_{\alpha} = \chi_{\alpha\beta} H_{\beta} \tag{51}$$

What has to be done is to dot the $S_{\alpha\beta}$ tensor of equation (50) into a cartesian vector specifying the direction of the

desired susceptibility, and then to extract the $\chi_{\alpha\beta}$ tensor by comparsion of the resulting equations with equation (51).

We shall first compute a value for $\chi_{\parallel}$. This is equivalent to letting $\beta = z$ in equation (51). By the properties of cartesian tensors:

$$\delta_{\alpha\beta} k_\beta = k_\alpha \tag{52}$$

and since the chelate rings lie at 45° with respect to the C_3 axis, we find:

$$e_\beta k_\beta = 1/\sqrt{2} \tag{53}$$

From the results of equations (52) and (53), we can now carry out the necessary dot product and obtain an expression for the magnetic moment of one ring:

$$m_\alpha = \left[\frac{1}{\sqrt{2}}(S_\perp - S_\parallel)\, e_\alpha + S_\parallel k_\alpha\right] H \tag{54}$$

With equation (54), we have the magnetic moment of one ring, but now we must find the resultant moment along the C_3 axis of all three rings taken together. However, in equation (45) we found that the susceptibility of the molecule was obtained by adding the susceptibility of the three individual rings. Since the moments are related to the susceptibilities by equation (51), we may write:

$$m_\parallel = m_\alpha^a + m_\alpha^b + m_\alpha^c \tag{55}$$

We can also relate the ring unit vectors to the molecular unit vectors, since each ring is situated at 45° to the symmetry axis. This leads to:

$$e_{\alpha}^{a} + e_{\alpha}^{b} + e_{\alpha}^{c} = 3/\sqrt{2}\ k_{\alpha} \tag{56}$$

It is now possible to sum equation (55) using the moments described by equation (54), and the relation among the unit vectors given in equation (56). We then obtain:

$$m_{\parallel} = \left[\frac{3}{2}(S_{\perp} - S_{\parallel}) + 3\,S_{\parallel}\right] H \tag{57}$$

Equation (51) leads to:

$$m_{\parallel} = \gamma_{\parallel} H \tag{58}$$

So that we find for the susceptibility parallel to the principal symmetry axis:

$$\gamma_{\parallel} = \frac{3}{2}\,(S_{\parallel} + S_{\perp}) \tag{59}$$

We shall now compute the susceptibility along either one of the axes perpendicular to the principal C_3 symmetry axis. A convenient axis to choose is a C_2 axis which passes parallel to the plane of one ring and at 45° to the planes of the other two rings. The dot product of equation (50) with the proper cartesian vector for the ring which is bisected by the C_2 axis vanishes:

$$e_{\alpha}\, i_{\alpha} = 0 \tag{60}$$

Equation (60) leads to:

$$m_{\alpha}^{a} = \left[S_{\parallel} i_{\alpha}\right] H \tag{61}$$

where we have used the relation:

$$H_{\alpha} = H i_{\alpha} \tag{62}$$

The result of the same dot product does not vanish for the other two rings, and is given by:

$$m_{\alpha}^{b} = m_{\alpha}^{c} = \left[\frac{1}{\sqrt{2}}(S_{\perp} - S_{\parallel})\, e_{\alpha} + S_{\parallel} i_{\alpha}\right] H \tag{63}$$

If we carry out the summation described by equation (55) on equations (62) and (63), we obtain:

$$m_{\perp} = \left[3 S_{\parallel} i_{\alpha} + \frac{1}{\sqrt{2}}(S_{\perp} - S_{\parallel})(e_{\alpha}^{b} + e_{\alpha}^{c})\right] H \tag{64}$$

But since two of the rings lie at 45° to the C_2 axis:

$$e_{\alpha}^{b} + e_{\alpha}^{c} = \frac{2}{\sqrt{2}}\, i_{\alpha} \tag{65}$$

we find that equation (64) becomes:

$$m_{\perp} = \left[3 S_{\parallel} + (S_{\perp} - S_{\parallel})\right] H \tag{66}$$

We are now able to obtain the susceptibility perpendicular to the principal symmetry axis, because if:

$$m_{\perp} = \chi_{\perp} H \tag{67}$$

then:

$$\chi_{\perp} = 2 S_{\parallel} + S_{\perp} \tag{68}$$

The anisotropy in the magnetic susceptibility of a D_3 molecule may now be obtained by subtracting equation (68) from equation (59):

$$\Delta\chi = \chi_{\parallel} - \chi_{\perp}$$
$$= -\frac{1}{2}(S_{\parallel} - S_{\perp}) \tag{69}$$

Finally, if we substitute the value for the ring anisotropy given in equation (34), then we find a rough value for the magnetic anisotropy of an aromatic D_3 molecule:

$$\Delta\chi = -4.5 \times 10^{-29} \text{ emu} \tag{70}$$

These simple arguments indicate that even in the absence of large ring currents, the signs of the anisotropies of the D_2h and D_3 chelates ought to be negative, but that of a D_2d chelate ought to be positive. Whether the complexes are aromatic will be indicated by comparing the anisotropy values computed for aromatic rings with the experimental anisotropies.

2. Kerr and Cotton-Mouton Effect Measurements on $Be(acac)_2$ and $Al(acac)_3$

To determine the magnetic anisotropy of some diamagnetic acetylacetonates which are not expected to possess large ring currents, Kerr and Cotton-Mouton effect measurements were made on solutions of $Be(acac)_2$ and $Al(acac)_3$ in CCl_4. Since these chelates were not expected to be aromatic, they were considered ideal model compounds for the chelates which might possibly be aromatic. A large disparity between the values of the diamagnetic anisotropy of the model compounds and a transition metal compound could be viewed as evidence supporting the benzenoid resonance concept of Calvin. If the anisotropy approached that of the aromatic model compounds, then the data would conclusively indicate aromatic character.

The results of the induced-birefringence measurements are shown in Table XX, along with all pertinent experimental data. However, since the only previously attempted measurement of the Cotton-Mouton effect of the solvent CCl_4 failed to detect any birefringence at all,[92] it was first necessary to measure accurately the Cotton-Mouton constant of CCl_4. Kerr effect measurements were made on CCl_4 in the previous section, and the results of the magnetic

---

92) R. J. W. LeFevre, D. S. N. Murthy, and G. L. D. Ritchie, Aust. J. Chem. 24, 1177 (1971).

Table XX

Experimental Data for the Kerr and Cotton-Mouton Measurements on $Be(acac)_2$ and $Al(acac)_3$

X_{solute}	n	d	ϵ	C x 10^{15}	B x 10^{8}
a) $Be(acac)_2$					
0.0026*	1.4545	1.58229	—	+7.93	—
0.0051*	1.4551	1.58033	—	+12.2	—
0.0030**	1.4546	1.58146	2.330	—	+1.841
0.0044**	1.4549	1.58088	2.376	—	+2.410
b) $Al(acac)_3$					
0.0018*	1.4545	1.58101	—	+5.41	—
0.0034*	1.4550	1.57823	—	+7.97	—
0.0009*	1.4542	1.58741	2.240	—	+1.080
0.0037**	1.4551	1.54662	2.267	—	+2.191

* data taken at 25° C

** data taken at 30° C

measurements on CCl_4 are listed in Table XXI.

Table XXI

C	=	$+ 3.39 \times 10^{-15}$	emu
mC	=	$+ 1.19 \times 10^{-18}$	emu
$\Delta\eta$	=	$+ 4.25 \times 10^{-42}$	emu

Once the contribution of the solvent to the induced birefringence was known, it became possible to apply equations (16) and (27) to compute the polarizability anisotropies and magnetic susceptibility anisotropies of Table XXII.

The precision in the computed values of Table XXII is seen to be excellent. The fact that the computed molecular parameters are independent of concentration to within experimental error is seen as confirmation that one is observing effects due to the solute alone. Previously, before all undissolved particles were eliminated, spurious birefringences could be obtained which led to extreme variations in calculated anisotropies. The careful preparation of all solutions (as discussed in the experimental section) has apparently removed these effects.

It is usual practice in the evaluation of polarizability anisotropies from Kerr effect data to assume that

Table XXII

Molecular Paramaters Calculated for $Be(acac)_2$ and $Al(acac)_3$ from the Kerr and Cotton-Mouton Effect Measurements

X_{solute}	$\left[\Delta\eta + \frac{\Delta\alpha\Delta\chi}{3kT}\right] \times 10^{39}$	$\left[\gamma + \frac{\Delta a \Delta\alpha}{3kT}\right] \times 10^{32}$
a) $Be(acac)_2$		
0.0026*	+ 10.3	——
0.0051*	+ 10.5	——
0.0030**	——	+ 3.37
0.0044**	——	+ 3.37
b) $Al(acac)_3$		
0.0018*	+ 7.06	——
0.0034*	+ 7.01	——
0.0009*	——	+ 3.96
0.0037**	——	+ 3.89

* data taken at 25° C

** data taken at 30° C

the optical polarizability anisotropy equals the static polarizability anisotropy.[93] However, if a molecule exhibits a large "atomic polarization" (which represents a distortion of the nuclear framework and arises from absorption in the infrared or microwave region), then a discrepancy will exist between the static and optical polarizability anisotropies.[60] It has been known for some time[94] that the metal acetylacetonates do possess a sizable atomic polarization, and this observation has led various authors[95,96] to conclude that these non-polar molecules possessed a permanent dipole moment. However, we have made use of the fact that the optical polarizability is usually about 90% the static polarizability[97] and assumed the same ratio between the anisotropies as exists between the mean values of the polarizability.

Using the above assumption, values for the polarizability anisotropy were computed for $Be(acac)_2$ and

---

93) R. Gans, Ann. Physik, 65, 97 (1921).

94) A. E. Finn, G. C. Hampson, and L. E. Sutton, J. Chem. Soc. 1254 (1938).

95) R. D. Nelson and C. E. White, J. Phys. Chem. 73, 3439 (1969).

96) S. Dasgupta and C. P. Smyth, J. Am. Chem. Soc. 89, 5532 (1967).

97) L. G. Groves and S. Sugden, J. Chem. Soc. 1779 (1937).

$Al(acac)_3$ from the values of the Kerr effect measurements in Table XXII. In these calculations, the effect of the hyperpolarizability was neglected. These anisotropies were then used to evaluate the magnetic susceptibility anisotropies of the Cotton-Mouton determinations (neglecting the contribution of $\Delta\eta$), and all these computed results are collected in Table XXIII.

Table XXIII

	$Be(acac)_2$	$Al(acac)_3$
$\Delta\alpha \times 10^{23}$	+ 3.96	- 4.25
$\Delta\chi \times 10^{29}$	+ 3.30	- 2.04

It is worth comparing the magnetic susceptibility anisotropy found for the acetylacetonates with that of the aromatic models previously discussed. The signs of the magnetic susceptibility anisotropies and polarizability anisotropies have been assigned on the basis of the expected signs of the model compounds. Since all the observed Cotton-Mouton effects were found to be positive, the sign of the polarizability anisotropy is required to be the same as that of the magnetic susceptibility

anisotropy. It is seen in Table XXIII that the magnetic anisotropy of $Be(acac)_2$ is 37% that of its corresponding model, and that the anisotropy of $Al(acac)_3$ is 46% of its model. These differences would seem to rule out any aromaticity in these complexes, but a final statement on this point will be deferred until the final discussion following this section.

3. Single Crystal Magnetic Anisotropies

Since none of the transition metal acetylacetonates were transparent at the laser wavelength,[98] measurement of the Kerr and Cotton-Mouton effects could not be made. It is known that both the Kerr[99] and Cotton-Mouton[100] effects display anomalous dispersion in absorption bands and evaluation of the desired molecular parameters is not easily performed. As a result, single crystal magnetic susceptibility anisotropies were obtained from the literature.

To find out with what confidence the single crystal anisotropies could be compared to those of Cotton-Mouton measurements, literature data on four aromatic compounds were obtained. Single crystal anisotropies of benzene,[101] napthalene,[101] pyridine,[102] and anthracene[102] were compared with the Cotton-Mouton anisotropies,[103] and all corresponding values agreed to within better than 3%. Thus, we feel

---

98) D. W. Barnum, J. Inorg. Nucl. Chem. 21, 221 (1961).

99) A. D. Buckingham, Proc. Roy. Soc. A267, 271 (1962).

100) T. Y. Chang, J. Chem. Phys. 56, 1752 (1972).

101) Y. A. Dorfman, "Diamagnetism and the Chemical Bond", Elsevier, Holland, 1965.

102) M. A. Lasheen, Phil. Trans. Roy. Soc. A256, 357 (1964).

103) C. L. Cheng, D. S. N. Murthy, and G. L. D. Ritchie, J. Chem. Soc. (Far. Trans. II), 1679 (1972).

confident that the anisotropies as determined by either method of measurement may be compared meaningfully.

The anisotropies of $Fe(acac)_3$ and $Mn(acac)_3$ were plotted against 1/kT and the temperature independent contribution to the anisotropy was obtained as the intercept. The temperature independent term is regarded as the sum of the diamagnetic anisotropy and any Van Vleck paramagnetism.[85] Only the sum of these susceptibilities is independent of the origin of the coordinate system, and thus only the sum of the two has physical meaning. The results of the extrapolations are found in Table XXIV.

Table XXIV

	$\Delta\chi$ (intercept) x 10^{29} (emu)	ref.
$Fe(acac)_3$	- 2.5 ± 1.0	104
$Mn(acac)_3$	- 2.3 ± 1.0	105

No reliable data have been published for the magnetic anisotropy of any other acetylacetonates.

104) M. Gerloch, J. Lewis, and R. C. Slade, J. Chem. Soc. A, 1422 (1969).

105) B. D. Bhattacharyya, Phys. Stat. Sol. 43, 495 (1971).

Comparsion of the values in Tables XXIII and XXIV reveals that there is very little change in anisotropy on passing from $Al(acac)_3$ to the transition metal chelates. The anisotropy of $Fe(acac)_3$ is 56% that of the aromatic D_3 model compound, and the anisotropy of $Mn(acac)_3$ is 51% of the model. Since the anisotropy of $Al(acac)_3$ was found to be 46% that of the aromatic model, it would appear that no change in aromatic character is found on passing from a non-transition metal acetylacetonate to a transition metal compound.

4. Mean Susceptibilities and Polarizabilities of Some Acetylacetonates

In order to obtain the individual components of the magnetic susceptibility and polarizability tensors, it became necessary to measure the mean values of these quantitities. The mean polarizability of the molecules in a pure liquid is easily obtained from a measurement of the refractive index and subsequent application of the Lorentz-Lorenz equation:

$$\frac{n^2 - 1}{n^2 + 2} = \frac{4}{3} \pi \rho \bar{a} \qquad (72)$$

The quantity $\bar{a}$ is the mean value of the optical polarizability and ρ is the number density. Equation (72) may be extended to mixtures:

$$\frac{n^2 - 1}{n^2 + 2} = \frac{4}{3} \pi \rho (X_1 \bar{a}_1 + X_2 \bar{a}_2) \qquad (73)$$

From the data of Table XXI, the mean polarizability of $Al(acac)_3$ and $Be(acac)_2$ is obtained immediately, and the results are found in Table XXV.

Calculation of the mean value for the magnetic

Table XXV

Mean Polarizabilities of $Be(acac)_2$ and $Al(acac)_3$

X_{solute}	$\bar{a} \times 10^{24}$ (cm^3)
a) $Be(acac)_2$	
0.0026	21.46
0.0030	21.78
0.0044	21.42
0.0051	21.67
average	21.58
b) $Al(acac)_3$	
0.0009	38.66
0.0018	38.23
0.0034	38.92
0.0037	38.54
average	38.59

susceptibility of the diamagnetic chelates is more difficult. While the mean susceptibility of a number of paramagnetic acetylacetonates has been reported,[104-108] the magnetic susceptibility of a diamagnetic acetylacetonate has never been published. As mentioned previously, the experimental measurement of diamagnetic susceptibilities by either the Gouy or Faraday method is difficult,[85] and this observation would account for the absence of experimental data. However, it is possible to measure the diamagnetic susceptibility using NMR techniques[109] and it is through this method that the experimental determinations were carried out. The concentric tube method described by Engel et al[110] involves the observation of a reference NMR signal under inhomogeneous field conditions caused by the presence of an inner tube (containing the liquid whose susceptibility is desired) which creates a difference in shielding of the reference. The single resonance of the reference is split into a doublet under these conditions, and the

---

106) P. K. Biswas and P. Sengupta, Phys. Stat. Sol. 40, 339 (1970).

107) A. K. Gregson and S. Mitra, J. Chem. Soc. (Dalton Trans.) 1098 (1973).

108) B. C. Guka, Proc. Roy. Soc. A206, 353 (1951).

109) C. A. Reilly, H. M. McConnell, and R. E. Meisenheimer, Phys. Rev. 98, 264 (1955).

110) R. Engel, D. Halpern, and S. Bienenfeld, Anal. Chem. 45, 367 (1973).

expression relating this splitting to the susceptibility is:

$$\nu = 4\pi\nu_o \left[(K_1 - K_2) \frac{a^2}{r^2} + (K_2 - K_3) \frac{b^2}{r^2} \right] \quad (74)$$

In equation (74), ν is the frequency of the splitting, ν_o is the frequency of the spectrometer, K_1 is the volume susceptibility of the unknown liquid, K_2 is the susceptibility of the glass used to make the NMR tubes, and K_3 is the susceptibility of the reference liquid. The constants a, b, and r describe the geometry of the concentric tubes. The molar susceptibility is related to the volume susceptibility by:

$$\chi = \frac{M K}{d} \quad (75)$$

where M is the molecular weight of the liquid and d is its density. Equation (74) may be solved for the volume susceptibility of the unknown liquid, and equation (75) used to obtain the molar susceptibility of the unknown directly. One then finds:

$$\chi_{12} = \frac{M}{d} \left[\frac{r^2 \nu}{a^2 \, 4\pi\nu_o} - (K_2 - K_3) \frac{b^2}{a^2} + K_2 \right] \quad (76)$$

where $\bar{M}$ is the mean molecular weight of the unknown liquid, and χ_{12} is its susceptibility. The magnetic susceptibility of the solute may be obtained from equation (76), since:

$$\chi_{12} = x_1 \chi_1 + x_2 \chi_2 \qquad (77)$$

Mean diamagnetic susceptibilities have been obtained for $Be(acac)_2$, $Al(acac)_3$, and $Co(acac)_3$ using this method, and the results are collected in Table XXVI. The temperature of the NMR probe was 36° C, so that the densities of each mole fraction had to be determined at that temperature. However, the final calculated susceptibility is independent of temperature.

In the discussion following this section, the mean values of the polarizability and magnetic susceptibility will be used to calculate the components of these tensors. It is these tensor components which will be able to give an estimate of how aromatic these complexes are.

Table XXVI

Mean Molar Susceptibilities of some Acetylacetonates

X_{solute}	d (36° C)	ν (Hz)	$\chi \times 10^6$ (emu)
a) $Be(acac)_2$			
0.040	1.5318	-9.3	- 121
0.061	1.5159	-9.6	- 121
b) $Al(acac)_3$			
0.027	1.5400	-8.9	- 201
0.036	1.5323	-9.4	- 201
c) $Co(acac)_3$			
0.024	1.5428	-10.1	- 210
0.033	1.5354	-12.6	- 210

note: The frequency splitting observed for pure CCl_4 was -7.8 Hz.

E. Discussion

We are now able to draw some conclusions regarding the extent of aromatic character in the acetylacetonate rings. Using the value obtained for the magnetic anisotropy:

$$\Delta\chi = \chi_{\parallel} - \chi_{\perp} \tag{78}$$

and that of the mean susceptibility

$$\bar{\chi} = \frac{\chi_{\parallel} + 2\chi_{\perp}}{3} , \tag{79}$$

it becomes possible to calculate the values of the tensor components, $\chi_{\parallel}$ and $\chi_{\perp}$. They are given by:

$$\chi_{\perp} = \frac{3\bar{\chi} - \Delta\chi}{3} \tag{80}$$

$$\chi_{\parallel} = \frac{3\bar{\chi} + 2\Delta\chi}{3} \tag{81}$$

The components of the polarizability tensor may also be obtained in an analagous fashion.

Once the values for the principal magnetic susceptibilities ($\chi_{\parallel}$ and $\chi_{\perp}$) are known, one is then able to calculate approximate values for the acetylacetonate ring

susceptibilities, using the equations relating the ring and molecular susceptibilities that were derived in a previous section. For a D_{2d} molecule, we find:

$$S_{\parallel} = \frac{\chi_{\parallel}}{2} \tag{82}$$

$$S_{\perp} = \frac{2\chi_{\perp} - \chi_{\parallel}}{2} \tag{83}$$

and for a D_3 molecule, we obtain:

$$S_{\parallel} = \frac{3\chi_{\perp} - 2\chi_{\parallel}}{3} \tag{84}$$

$$S_{\perp} = \frac{4\chi_{\parallel} - 3\chi_{\perp}}{3} \tag{85}$$

Using the equations just developed, values for $a_{\parallel}$, $a_{\perp}$, $\chi_{\parallel}$, $\chi_{\perp}$, $S_{\parallel}$, and $S_{\perp}$ were calculated for $Be(acac)_2$ and $Al(acac)_3$ employing the results of Tables XXIII, XXV, and XVI. These tensor components are collected in Table XXVII.

The near equality of the $S_{\parallel}$ values of $Be(acac)_2$ and $Al(acac)_3$ (and of the $S_{\perp}$ values also) indicates that the simple model we have advanced to relate the ring and molecular susceptibilities is approximately valid. Thus, one may feel confident in using the values of the ring

Table XXVII

Polarizability and Susceptibility Components For $Be(acac)_2$ and $Al(acac)_3$ in cgs units

	$Be(acac)_2$	$Al(acac)_3$
$a_{\parallel} \times 10^{24}$	+ 48.0	+ 10.3
$a_{\perp} \times 10^{24}$	+ 8.4	+ 52.8
$\chi_{\parallel} \times 10^{29}$	- 17.8	- 34.8
$\chi_{\perp} \times 10^{29}$	- 21.1	- 32.7
$S_{\parallel} \times 10^{29}$	- 8.91	- 9.54
$S_{\perp} \times 10^{29}$	- 12.2	- 13.6
$\Delta S \times 10^{29}$	+ 3.3	+ 4.1

susceptibilities to obtain conclusions about the aromatic character of these compounds. The average value of ΔS for the acetylacetonate rings was found to be $+3.7 \times 10^{-29}$ emu, and this value is 42% of the value of $+8.9 \times 10^{-29}$ emu obtained for benzene. This difference is large enough to enable one to conclude that in the acetylacetonate rings of $Be(acac)_2$ and $Al(acac)_3$ there is not enough of a ring current to call these chelates aromatic.

If one accepts the magnetic susceptibility anisotropy of $Al(acac)_3$ as that of a non-aromatic D_3 chelate, then one must immediately conclude from a consideration of the single crystal magnetic anisotropies of Table XXIV, that $Fe(acac)_3$ and $Mn(acac)_3$ are also not aromatic. There appears to be no significant difference between the diamagnetic anisotropies of $Al(acac)_3$ and the transition metal compounds that were studied. By extension, it would appear that none of the first-row transition metal acetylacetonates is aromatic.

However, this argument is not complete. Hancock[45] has pointed out that the degree of metal-to-ligand π-bonding is strongest in the cases of $Cr(acac)_3$ and $Co(acac)_3$, so that if any chelate could possess a ring current, these would. We are not in a position to state unequivocally that there is no ring current in these compounds,

since we are not in possession of the necessary anisotropy data. Certain qualitative arguments are possible, using the data of previous sections. The sharp photoelectron band attributed to the d-electrons of $Cr(acac)_3$ (as found in Section I of this work) does not support the idea of strong metal-to-ligand π-bonding, and neither does the lack of splitting in the highest occupied π-band. If the degree of π-bonding is not as strong as had been thought, then this reduction would be reflected in a suppression of the ring current. However, $Co(acac)_3$ did exhibit a broader d-electron band and splitting was observed in the π-band. The broadness of the d-band is probably due to overlapping ionizations, but it would appear that $Co(acac)_3$ is the most likely possibility for the existence of a ring current.

We can use the measurement of the mean susceptibility of $Co(acac)_3$ to gain additional information regarding the bonding in this compound. The use of Pascal's rules[111] to calculate the mean diamagnetic susceptibility of a molecule are well known. This method starts with the molecular formula of the compound and obtains the susceptibility by use of the formula:

---

111) For example, see Y. G. Dorfman, "Diamagnetism and the Chemical Bond", American Elsevier, New York, 1965.

$$\bar{\chi} = \sum_i n_i \chi_i + \sum_j \lambda_j \qquad (86)$$

where χ_i is the atomic susceptibility of the i^{th} atom, n_i is the number of i-type atoms, and the λ_j are constitutive corrections which allow for the additional susceptibility due to the presence of multiple bonds.

Unfortunately, equation (86) cannot be readily applied to the acetylacetonate complexes because the proper values for the constitutive corrections are not available. One can, however, subtract the experimental mean susceptibilities of $Al(acac)_3$ and $Co(acac)_3$ and compare this difference to the difference in atomic susceptibilities of the Al^{+3} and Co^{+3} ions. This procedure is the same as finding the mean susceptibilities of the two chelates by Pascal's rules, subtracting the two results, and comparing this difference to the experimental difference. If a ring current were present in $Co(acac)_3$ but absent in $Al(acac)_3$ (as has been already shown), then an extra constitutive correction would be necessary for $Co(acac)_3$. The difference in experimental susceptibilities would have to reflect this extra correction, while the difference in atomic susceptibilities would not.

Selwood[112] has tabulated values for the diamagnetic

---

112) P. W. Selwood, "Magnetochemistry", 2nd edition, Wiley-Interscience, New York, 1956.

susceptibilities of a number of metal cations. The atomic susceptibility of Al^{+3} is -2×10^{-6} emu and that of Co^{+3} is -10×10^{-6} emu, so that the difference in atomic susceptibilities is -8×10^{-6} emu. The experimental mean susceptibilities of $Al(acac)_3$ and $Co(acac)_3$ are found in Table XXVI, and the difference between these values is -9×10^{-6} emu. Since these values are identical to within experimental error, it is concluded that there is no extra constitutive correction in $Co(acac)_3$ that may be ascribed to the presence of ring currents. Consequently, we conclude that there is no aromaticity. If $Co(acac)_3$ is not aromatic, then one may conclude that none of the first row transition metal acetylacetonates is aromatic, because according to Hancock,[45] $Co(acac)_3$ possesses the largest degree of π-bonding of all the first row complexes.

The preceding arguments do not imply that there is no metal-to-ligand π-bonding in these complexes. DeArmond and Forster[113] have shown that by substituting various groups on the rings of $Cr(acac)_3$, some variation in the energy of the first $^4A_2 \longrightarrow {}^2E$ transition is possible. It appeared that resonance effects in the chelate rings were able to influence this transition, which corresponds to a d-electron reorganization. The NMR of paramagnetic

---

113) K. DeArmond and L. S. Forster, Spectrochim. Acta, 19, 1403 (1963).

acetylacetonates[34,114] clearly shows that the spin of the central metal atom is delocalized around the entire chelate ring and shifts the resonance of the proton attached para to the metal. With these arguments supporting the presence of metal-to-ligand π-bonding, one may ask why a ring current is absent in these molecules.

The answer is apparent in the CNDO calculations performed on the model chelate $Al(dfm)_3$ in Section I of this work. If one examines the charges on the atoms which make up the chelate rings, one observes that there is a severe alternation of the magnititude and sign of the charges on the atoms. This effect is illustrated in Figure 13, where the charges on the atoms making up one ring of $Al(dfm)_3$ are shown. It is known,[115,116] that in order for a cyclic molecule to possess a ring current, the charges on the ring must be smalll and of the same sign.

We conclude, then, that the alternation of signs of the charges on the atoms and their sizable magnitude have effectively reduced any ring current. The observation of Collman and coworkers[117] that electrophilic substitution

---

114) A. Foreman, J. N. Murrell, and L. E. Orgel, J. Chem. Phys. 31, 1129 (1959).

115) R. J. Abraham, Mol. Phys. 4, 145 (1961).

116) D. P. Craig, M. L. Heffernam, R. Mason, and N. L. Paddock, J. Chem. Soc. 1376 (1961).

117) J. P. Collman and R. H. Barker, Angew. Chem. Int. Ed. 4, 132 (1965).

Figure 13

Illustration of the charges on the atoms of one ring of $Al(dfm)_3$

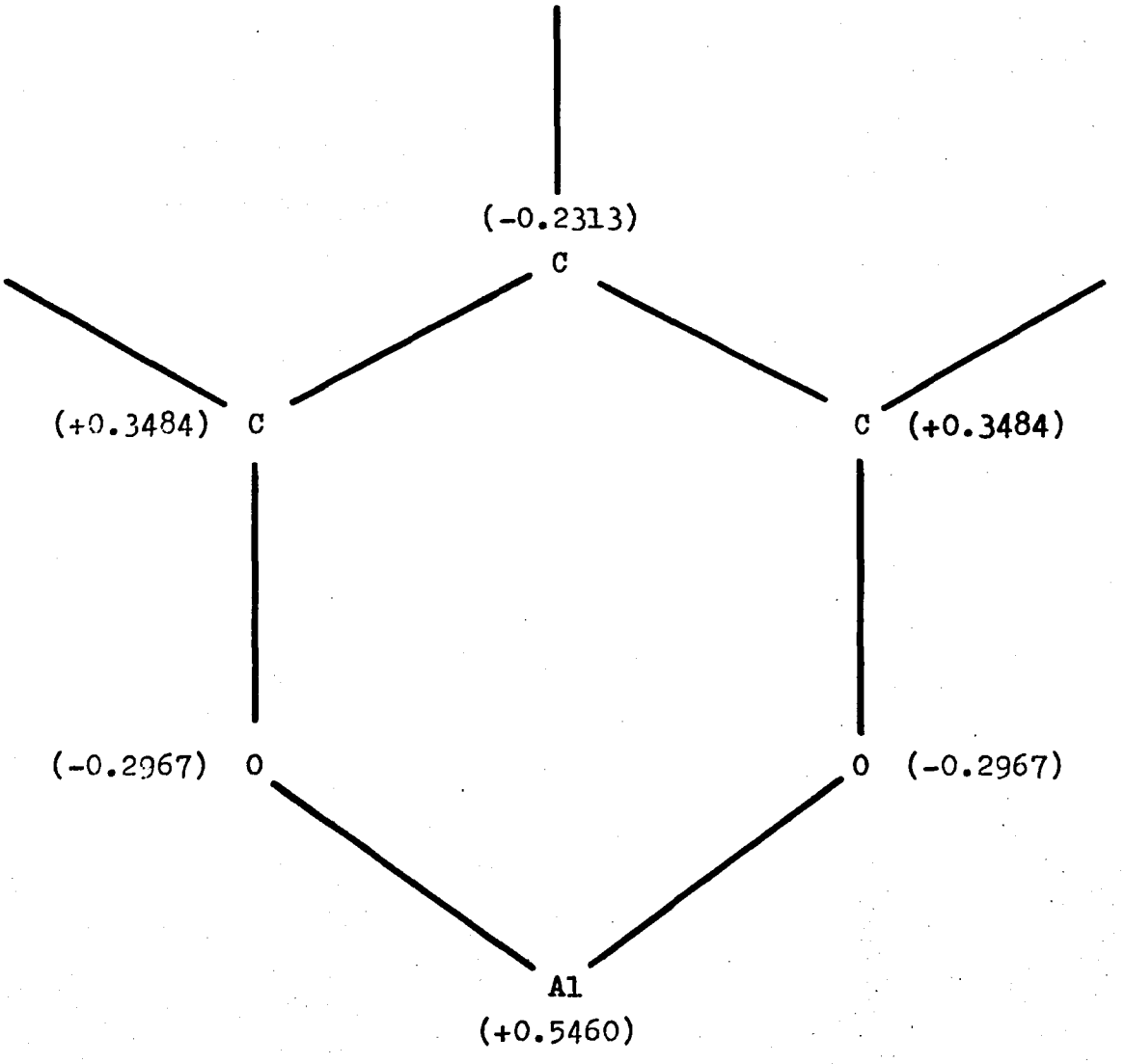

on the acetylacetonate rings is possible indicates a delocalization on the atoms making up the acetylacetonate anion, while the photoelectron spectral results and the magnetic anisotropy data do not indicate that the delocalization is as extensive as had been thought. When all these observations are taken together, they seem to indicate that electron delocalization is confined primarily to the acetylacetonate moiety.

Section IV

Measurement and Interpretation of Magnetic Linear Dichroism

Contents

A. Introduction

Absorption spectroscopy has played a very important role in elucidation of molecular electronic structure. However, when two absorption bands overlap the analysis becomes more difficult, because a more intense absorption might mask a weaker one. Better resolution of spectral features is sometimes possible by cooling the samples to very low temperatures or examination of single crystals by polarized light, but other methods of clarifying spectroscopic assignments are desirable.

One of the most successful of the newer techniques is that of Magnetic Circular Dichroism (abbreviated as MCD). Under the influence of a magnetic field whose direction is parallel to the direction of propagation of the analyzing light beam, all molecules become optically active and hence will exhibit circular dichroism in absorption bands.[118,119] Since is is possible to observe zeroth and first derivative MCD lineshapes of either positive or negative sign, considerably more information is obtainable from a MCD spectrum than from an ordinary absorption spectrum. The theory

---

118) P. N. Schatz, R. B. Shiflett, J. A. Spencer, A. J. McCaffery, S. B. Piepho, J. R. Dickinson, and T. E. Lester, Symp. Far. Soc. 3, 14 (1969).

119) P. N. Schatz, Quart. Rev. 23, 552 (1969).

regarding the MCD parameters is now well developed.[120-123]

Since the circular dichroism is usually more sensitive to wavelength than the absorption, new spectral features are often uncovered in MCD that were merely hinted at in the absorption spectrum. There are many examples in the literature of how MCD spectra have clarified spectroscopic assignments or have uncovered new states, but these are too numerous to be mentioned here.

A similar technique that has received little attention is the method of Magnetic Linear Dichroism (MLD). MLD differs from MCD in that the former measures the difference in absorption of orthogonal planes of linearly polarized light, while the latter measures the difference in absorption of left and right circularly polarized light. Measurement of the MLD effect requires a transverse magnetic field, while MCD is measured using a longitudinal field. It is reasonable to assume that MLD spectra might be able to be used in the same fashion as MCD spectra, but experimental work has dealt almost exclusively with MCD results. The only experimental MLD spectrum reported to date is that of Badox and

---

120) A. D. Buckingham and P. J. Stephens, Ann. Rev. Phys. Chem. 17, 399 (1966).

121) C. H. Henry, S. E. Schnatterly, and C. P. Slichter, Phys. Rev. 137, A 583 (1965).

122) P. J. Stephens, J. Chem. Phys. 52, 3489 (1970).

123) P. J. Stephens, R. L. Mowery, and P. N. Schatz, J. Chem. Phys. 55, 224 (1971).

coworkers.[124-126] These workers examined the $^7F_0 \longrightarrow {}^5D_1$ absorption band of aqueous $EuCl_3$ and presented a very simple account of the theory for the MLD effect they observed. These workers felt that the MLD technique was limited to bands having narrow linewidths and thus most applicable to rigid media at low temperature.

To investigate the MLD effects further, we have assembled an apparatus which is capable of measuring exceedingly small dichroism values and have carried out a series of measurements on solutions at room temperature. We have also derived the necessary theory to interpret the MLD spectra, and this will be developed in the next section.

---

124) A. C. Boccara, J. Ferre, B. Briat, M. Billardon, and J. P. Badoz, J. Chem. Phys. 50, 2716 (1969).

125) J. Badoz, Ann. Phys. 5, 22 (1970).

126) J. Badoz, M. Billardon, A. C. Boccara, and B. Briat, Symp. Far. Soc. 3, 27 (1969).

B. General Theory Of Magnetic Linear Dichroism

1. Non-degenerate Ground States

The extent to which a substance absorbs light is measured by its extinction coefficent, which appears in the familar Beer-Lambert law:[127]

$$I = I_o e^{-\epsilon \ell} \tag{87}$$

where ϵ is the extinction coefficent, ℓ is the path length, I is the intensity of light leaving the cell, and I_o is the intensity of light which entered it. The value of the extinction coefficent for light of polarization λ is given by:[128]

$$\epsilon_\lambda = \frac{8\pi^2 \rho \nu}{h c} \sum_i \overline{|\vec{\lambda} \cdot \langle o|\vec{\mu}|i\rangle|^2} \; S^{oi}(\nu, \nu_{oi}) \tag{88}$$

where ρ is the number density of absorbing molecules, $\vec{\lambda}$ is the unit polarization vector of the incident light, ν is the frequency of the light, $\vec{\mu}$ is the electric dipole operator, and S^{oi} is a function which characterizes the absorption wave form and has the dimensions of time. In equation (88), the state $|o\rangle$ is the ground state and the state $|i\rangle$ is some

---

127) W. Kauzman, "Quantum Chemistry", Academic Press, New York, 1957.

128) G. Herzberg, "Electronic Spectra Of Polyatomic Molecules", Van Nostrand, New York, 1967.

excited state; it is to be noted that the summation runs over all the excited states responsible for the absorption. The bar over the terms indicates that a statistical average must be taken over all molecular orientations. The center frequency, ν_{oi} , of the band is given by:

$$\nu_{oi} = \frac{E_i - E_o}{h} \tag{89}$$

and is measured at the peak of S^{oi}.

We will now rewrite equation (88), evaluating the square modulus and introducing the cartesian tensor notation that has been used in previous sections. Equation (88) now becomes:

$$\epsilon_\lambda = \frac{8\pi^2 \rho \nu}{h\, c} \sum_i \lambda_\alpha \lambda_\beta \overline{\langle o|u_\alpha|i\rangle \langle i|u_\beta|o\rangle}\, S^{oi} \tag{90}$$

It is seen that the integrals in equation (90) define the elements of a second-rank tensor, so we shall denote them as:

$$P^{oi}_{\alpha\beta}(H) = \langle o|u_\alpha|i\rangle \langle i|u_\beta|o\rangle \tag{91}$$

Now equation (90) becomes:

$$\epsilon_\lambda = \frac{8\pi^2 \rho \nu}{h\, c} \sum_i \lambda_\alpha \lambda_\beta \overline{P^{oi}_{\alpha\beta}(H)}\, S^{oi} \tag{92}$$

The quantity $P^{oi}_{\alpha\beta}(H)$ is called the extinction tensor and is expected to be a function of the magnetic field, since the

field is able to modify the wavefunctions. We expand $P^{oi}_{\alpha\beta}(H)$ as a Taylor series about the magnetic field:

$$P^{oi}_{\alpha\beta}(H) = P^{oi}_{\alpha\beta} + \left(\frac{\partial P^{oi}_{\alpha\beta}(H)}{\partial H_\gamma}\right)_{H=0} H_\gamma + \frac{1}{2}\left(\frac{\partial^2 P^{oi}_{\alpha\beta}(H)}{\partial H_\gamma \partial H_\delta}\right)_{H=0} H_\gamma H_\delta + \ldots. \quad (93)$$

$P^{oi}_{\alpha\beta}$ is the value of the extinction tensor in zero magnetic field. The n^{th} derivative in equation (93) is a tensor of rank n + 2. These derivatives may be abbreviated as:

$$P^{oi}_{\alpha\beta;\gamma} = \left(\frac{\partial P^{oi}_{\alpha\beta}(H)}{\partial H_\gamma}\right)_{H=0} \quad (94)$$

$$P^{oi}_{\alpha\beta;\gamma\delta} = \left(\frac{\partial^2 P^{oi}_{\alpha\beta}(H)}{\partial H_\gamma \partial H_\delta}\right)_{H=0} \quad (95)$$

so that equation (93) may be rewritten as:

$$P^{oi}_{\alpha\beta}(H) = P^{oi}_{\alpha\beta} + P^{oi}_{\alpha\beta;\gamma} H_\gamma + \frac{1}{2} P^{oi}_{\alpha\beta;\gamma\delta} H_\gamma H_\delta \quad (96)$$

We shall return to equation (96) shortly, but first we shall consider the effect of the magnetic field on the waveform, S^{oi}. This can be written as $S^{oi}(Y)$, and:

$$Y = \frac{\nu - \nu_{oi}}{\Delta} \quad (97)$$

where Δ is the width of the band. We can expand $S^{oi}(Y)$ about the center frequency of absorption, since the magnetic

field affects this frequency:

$$S^{oi}(Y) = S(X) + \frac{d\,S(X)}{d\,\nu}\,\Delta\left(\frac{\nu^{o}_{oi} - \nu_{oi}}{\Delta}\right) + \frac{d^2\,S(X)}{d\nu^2}\,\frac{\Delta^2}{2!}\left(\frac{\nu^{o}_{oi} - \nu_{oi}}{\Delta}\right)^2 \tag{98}$$

In equation (98), X refers to the quantity Y evaluated at zero magnetic field, and is given by:

$$X = \frac{\nu - \nu^{o}_{oi}}{\Delta} \tag{99}$$

We have assumed that the bandwidth, Δ, is independent of the magnetic field. In equation (98), ν^{o}_{oi} refers to the center frequency in the absence of the magnetic field. To simplify these equations, the derivatives of the waveform shall be abbreviated as:

$$S = S(X) \tag{100}$$

$$S^{I} = \frac{d\,S(X)}{d\,\nu}\,\Delta = \frac{d\,S(X)}{d\,X} \tag{101}$$

$$S^{II} = \frac{d^2\,S(X)}{d\nu^2}\,\frac{\Delta^2}{2!} = \frac{1}{2!}\,\frac{d^2\,S(X)}{d\,X^2} \tag{102}$$

When the notation of equations (100), (101), and (102) is included in equation (98), it is found that:

$$S^{oi} = S + S^{I}\left(\frac{\nu^{o}_{oi} - \nu_{oi}}{\Delta}\right) + S^{II}\left(\frac{\nu^{o}_{oi} - \nu_{oi}}{\Delta}\right)^{2} + \cdots\cdots \qquad (103)$$

Now that a form for S^{oi} has been determined, it is necessary to establish its behavior in the magnetic field. This problem reduces to finding the form of ν_{oi}. We can do this by finding the energy of the i^{th} state in the magnetic field, since the transition frequency is simply related to the energy by:

$$\nu_{oi} = \frac{E_i - E_o}{h} \qquad (104)$$

Expansion of the energy of the i^{th} state about the magnetic field yields:

$$E_i = E_i^o + \left(\frac{\partial E_i}{\partial H_\gamma}\right)_{H=0} H_\gamma + \frac{1}{2}\left(\frac{\partial^2 E_i}{\partial H_\gamma \partial H_\delta}\right)_{H=0} H_\gamma H_\delta + \cdots\cdots \qquad (105)$$

Using the definitions:

$$m_{i\gamma} = -\left(\frac{\partial E_i}{\partial H_\gamma}\right)_{H=0} \qquad (106)$$

$$\chi_{i\gamma\delta} = -\left(\frac{\partial^2 E_i}{\partial H_\gamma \partial H_\delta}\right)_{H=0}, \qquad (107)$$

it is possibly to rewrite equation (105) as:

$$\nu_{oi} = \nu^{o}_{oi} - \frac{(m_{i\gamma} - m_{o\gamma})\, H_\gamma}{h} - \frac{(\chi_{i\gamma\delta} - \chi_{o\gamma\delta})\, H_\gamma H_\delta}{2h} + \cdots\cdots \quad (108)$$

Combination of equations (103) and (108) yields a complete specification of the bandshape:

$$S^{oi} = S + \frac{S^{I}}{h\Delta}\left[(m_{i\gamma} - m_{o\gamma})\, H_\gamma + \tfrac{1}{2}(\chi_{i\gamma\delta} - \chi_{o\gamma\delta})\, H_\gamma H_\delta + \cdots\cdots\right] + \frac{S^{II}}{h^2\Delta^2}\left[(m_{i\gamma} - m_{o\gamma})\, H_\gamma + \tfrac{1}{2}(\chi_{i\gamma\delta} - \chi_{o\gamma\delta})\, H_\gamma H_\delta + \cdots\cdots\right]^2 \quad (109)$$

It is possible to expand the bandshape in a Taylor series about the magnetic field:

$$S^{oi}(X) = S + \left(\frac{\partial S^{oi}}{\partial H_\gamma}\right)_{H=0} H_\gamma + \tfrac{1}{2}\left(\frac{\partial^2 S^{oi}}{\partial H_\gamma \partial H_\delta}\right)_{H=0} H_\gamma H_\delta + \cdots\cdots \quad (110)$$

However, all the derivatives of equation (110) are already known. It is merely necessary to differentiate equation (109) with respect to the magnetic field to obtain:

$$\left(\frac{\partial S^{oi}}{\partial H_\gamma}\right)_{H=0} = S^{I}\,\frac{(m_{i\gamma} - m_{o\gamma})}{h\Delta} \quad (111)$$

$$\left(\frac{\partial^2 S^{oi}}{\partial H_\gamma \partial H_\delta}\right)_{H=0} = S^{I}\,\frac{(\chi_{i\gamma\delta} - \chi_{o\gamma\delta})}{h\Delta} + 2\,S^{II}\,\frac{(m_{i\gamma} - m_{o\gamma})^2}{h^2\Delta^2} \quad (112)$$

In equation (92), the product of the extinction tensor and the bandshape was required. First, we shall expand the product of $P^{oi}_{\alpha\beta}\, S^{oi}$ as a Taylor series:

$$P^{oi}_{\alpha\beta}\, S^{oi} = P^{oi}_{\alpha\beta}\, S^{oi(o)} + \left(\frac{\partial (P^{oi}_{\alpha\beta}\, S^{oi})}{\partial H_\gamma}\right)_{H=0} H_\gamma + \frac{1}{2}\left(\frac{\partial^2 (P^{oi}\, S^{oi})}{\partial H_\gamma\, \partial H_\delta}\right)_{H=0} H_\gamma H_\delta + \ldots\ldots \tag{113}$$

The derivatives of equation (113) may be obtained by multiplying equations (96) and (110), and then differentiating with respect to the magnetic field. One then obtains:

$$\left(\frac{\partial (P^{oi}_{\alpha\beta}\, S^{oi})}{\partial H_\gamma}\right)_{H=0} = S\, P^{oi}_{\alpha\beta;\gamma} + S^{I}\, \frac{(m_{i\gamma} - m_{o\gamma})}{h\Delta}\, P^{oi}_{\alpha\beta} \tag{114}$$

$$\left(\frac{\partial^2 (P^{oi}\, S^{oi})}{\partial H_\gamma\, \partial H_\delta}\right)_{H=0} = S\, P^{oi}_{\alpha\beta;\gamma\delta} + 2\, S^{I}\, \frac{(m_{i\gamma} - m_{o\gamma})}{h\Delta}\, P^{oi}_{\alpha\beta;\gamma} + S^{I}\, \frac{(\gamma_{i\gamma\delta} - \gamma_{o\gamma\delta})}{h\Delta}\, P^{oi}_{\alpha\beta} + S^{II}\, \frac{(m_{i\gamma} - m_{o\gamma})}{h^2\Delta^2}\, P^{oi}_{\alpha\beta} \tag{115}$$

The experimental measurement of magnetic linear dichroism involves determinig the difference between the extinction coefficents parallel and perpendicular to the applied field. This is given by:

$$\epsilon_{\parallel} - \epsilon_{\perp} = \frac{8\pi^2 \rho \nu}{h c}\, (\lambda^{\parallel}_{\alpha}\, \lambda^{\parallel}_{\beta} - \lambda^{\perp}_{\alpha}\, \lambda^{\perp}_{\beta}) \sum_i \overline{P^{oi}_{\alpha\beta}\, S^{oi(\parallel - \perp)}} \tag{116}$$

The term to be averaged in equation (116) may be obtained from equation (113). We shall find it useful to employ this result for a uniform magnetic field:

$$H_\alpha = H \lambda''_\alpha \tag{117}$$

The averaging in equation (116) is to be carried out over all molecular orientations, but this is equivalent to holding the molecule fixed and averaging over all coordinates. If this is done, only terms quadratic in the magnetic field remain. Thus equation (116) becomes:

$$\epsilon_{\parallel} - \epsilon_{\perp} = \frac{4\pi^2 \rho v H^2}{h c} \overline{(\lambda''_\alpha \lambda''_\beta \lambda''_\gamma \lambda''_\delta - \lambda^{\perp}_\alpha \lambda^{\perp}_\beta \lambda''_\gamma \lambda''_\delta)} \cdot \sum_i \left[\left(\frac{\partial^2 (P^{oi}_{\alpha\beta} S^{oi})}{\partial H_\gamma \partial H_\delta} \right)_{H=0} \right] \tag{118}$$

The averaging of unit vectors required in equation (118) has been carried out, for example, by Buckingham and Pople;[60] one obtains as a result:

$$\epsilon_{\parallel} - \epsilon_{\perp} = \frac{4\pi^2 \rho v H^2}{h c} \sum_i \left[\left(\frac{\partial^2 (P^{oi} S^{oi})}{\partial H_\gamma \partial H_\delta} \right)_{H=0} \right] \cdot \frac{1}{30} \left[3(\delta_{\alpha\gamma}\delta_{\beta\delta} + \delta_{\alpha\delta}\delta_{\beta\gamma}) - 2\delta_{\alpha\beta}\delta_{\gamma\delta} \right] \tag{119}$$

If we substitute equation (115) into (119) and contract, we then arrive at:

$$\epsilon_{\parallel}-\epsilon_{\perp}=\frac{2\pi^2\rho\nu H^2}{15\,h\,c}\sum_i\Bigg\{S\left[3\,P^{oi}_{\alpha\beta;\alpha\beta}+3\,P^{oi}_{\alpha\beta;\beta\alpha}-2\,P^{oi}_{\alpha\alpha;\gamma\gamma}\right]$$
$$+\frac{S^I}{h\Delta}\left[3\,P^{oi}_{\alpha\beta}\left(\lambda^i_{\alpha\beta}-\lambda^o_{\alpha\beta}\right)+3\,P^{oi}_{\alpha\beta}\left(\lambda^i_{\beta\alpha}-\lambda^o_{\beta\alpha}\right)-2\,P^{oi}_{\alpha\alpha}\left(\lambda^i_{\gamma\gamma}-\lambda^o_{\gamma\gamma}\right)\right]$$
$$+\frac{2\,S^I}{h\Delta}\left[3\,P^{oi}_{\alpha\beta;\beta}\left(m^i_\alpha-m^o_\alpha\right)+3\,P^{oi}_{\alpha\beta;\alpha}\left(m^i_\alpha-m^o_\alpha\right)-2\,P^{oi}_{\alpha\alpha;\gamma}\left(m^i_\gamma-m^o_\gamma\right)\right]$$
$$+\frac{2\,S^{II}}{h^2\Delta^2}\left[3\,P^{oi}_{\alpha\beta}\left(m^i_\alpha-m^o_\alpha\right)\left(m^i_\beta-m^o_\beta\right)+3\,P^{oi}_{\alpha\beta}\left(m^i_\beta-m^o_\beta\right)\left(m^i_\alpha-m^o_\alpha\right)-2\,P^{oi}_{\alpha\alpha}\left(m^i_\gamma-m^o_\gamma\right)\left(m^i_\gamma-m^o_\gamma\right)\right]\Bigg\} \qquad (120)$$

It should be noted that although this treatment was intended to deal only with non-degenerate ground states that cannot possess a magnetic moment, we have included its contribution to the dichroism in the derivation. This was done in anticipation of the coming treatment of degenerate ground states, where we shall retain all the terms of equation (120) but shall sum over the degenerate states of the ground level as well as over all excited states.

The zeroth derivative terms in equation (120) represent the mixing in of excited states into the ground state and the states i. The first derivative term involving the difference in magnetic susceptibilities of the ground and

excited states represents the effect of a shift of the center frequency due to the presence of the magnetic field. The other first derivative term represents a combination of mixing in of excited states and a shift of the center frequency. Finally, the second derivative contribution represents the first order shift of ν_{oi} of the excited states squared.

In the work of Badoz and coworkers,[124-126] a very sharp absorption line of aqueous $EuCl_3$ was investigated and a second derivative lineshape was observed. This term dominated their spectrum since the width of that absorption is so narrow and the second derivative term depends inversely on the bandwidth squared.

2. Extension To Degenerate Ground States

Under the application of a magnetic field, a degenerate ground state will split into various components. The occupation of these states will be described by a Boltzman-type distribution. The probability that a given state j is occupied by a molecule having orientation Ω is:

$$\rho(j,\Omega) = \frac{e^{-E_j(\Omega)/kT}}{\sum_k \int_\Omega e^{-E_k(\Omega)/kT} d\Omega} \tag{121}$$

where $d\Omega$ is an element of the Eulerian angle system describing the orientation. It is important to note that:

$$\int d\Omega = 8\pi^2 \tag{122}$$

In the preceeding section, an expression was developed for the energy of the i^{th} state, which was:

$$E_i(\Omega) = E_i^o - m_{i\gamma}H_\gamma - \tfrac{1}{2}\gamma_{i\gamma\delta}H_\gamma H_\delta \tag{123}$$

Previously, equation (116) described the dichroism resulting from a non-degenerate ground state, but if the ground state is now taken to be degenerate, then the equation for the dichroism' becomes:

$$\epsilon_\parallel - \epsilon_\perp = \frac{8\pi^2 \rho \nu}{h\,c} \sum_i \sum_k \int_\Omega \rho(k,\Omega)\, P^{ki}_{\alpha\beta}\, S^{ki} \cdot (\lambda^{\parallel}_\alpha \lambda^{\parallel}_\beta - \lambda^{\perp}_\alpha \lambda^{\perp}_\beta)\, d\Omega \tag{124}$$

In equation (124), one sums k over the states of the ground level and i over all the excited states responsible for the absorption. It is also necessary to integrate over the entire range of orientational elements, and this integration has the effect of averaging over all molecular orientations.

We will now replace the product of the probability function times the extinction tensor times the waveform by the appropriate second derivative, and introduce the magnetic field symmetry as described by equation (117). In doing so, we shall omit the terms arising from the second derivative of the probability function since we have been dealing with spherically-symmetric molecules only. The result is:

$$\epsilon_{\parallel} - \epsilon_{\perp} = \frac{8\pi^2 \rho \nu}{2!\, h\, c} \sum_i \sum_k \int_{\Omega} \left[\left(\frac{\partial \rho}{\partial H_\gamma} \right)_{H=0} \left(\frac{\partial (P^{ki}_{\alpha\beta} S^{ki})}{\partial H_\delta} \right)_{H=0} + \left(\frac{\partial \rho}{\partial H_\delta} \right)_{H=0} \left(\frac{\partial (P^{ki}_{\alpha\beta} S^{ki})}{\partial H_\gamma} \right)_{H=0} \right] \cdot (\lambda'_\alpha \lambda''_\beta \lambda''_\gamma \lambda''_\delta - \lambda'_\alpha \lambda'_\beta \lambda''_\gamma \lambda''_\delta)\, d\Omega \tag{125}$$

It is only necessary to evaluate the derivative of the probability function, since the values of the other derivatives were obtained in equation (114). To obtain this derivative, one substitutes equation (123) into equation (121) and differentiates with respect to the field. The result is:

$$\left(\frac{\partial \mathcal{P}(k,\Omega)}{\partial H_\gamma}\right)_{H=0} = \frac{m_{k\gamma}\, e^{-E_k^o/kT}}{kT\ 8\pi^2 \sum_k e^{-E_k^o/kT}} - \frac{e^{-E_k^o/kT} \sum_k \int_\Omega m_{k\gamma}\, e^{-E_k^o/kT}\, d\Omega}{kT \left[8\pi^2 \sum_k e^{-E_k^o/kT}\right]^2} \tag{126}$$

The second term in equation (126) vanishes when one sums over the magnetic moments of the ground state, so equation (126) shall be written as:

$$\left(\frac{\partial \mathcal{P}(k,\Omega)}{\partial H_\gamma}\right)_{H=0} = \frac{m_{k\gamma}}{8\pi^2\ kT\ d} \tag{127}$$

In equation (127), d is the degeneracy of the ground level:

$$d = \sum_k^d e^{-E_k^o/kT} \quad , \tag{128}$$

whose energy origin, E_k^o, equals zero. Substituting equation (127) into (125) we obtain:

$$\epsilon_{\parallel} - \epsilon_{\perp} = \frac{8\pi^2 \rho \nu}{2!\ h\ c} \sum_i \sum_k \int_\Omega \left\{ \frac{m_{k\gamma}}{4\pi\, kT\ d} \left[P^{ki}_{\alpha\beta} S^I \frac{(m_{i\delta} - m_{k\delta})}{h\Delta} + P^{ki}_{\alpha\beta;\delta} S \right] + \frac{m_{k\delta}}{4\pi\, kT\ d} \left[P^{ki}_{\alpha\beta} S^I \frac{(m_{i\gamma} - m_{k\gamma})}{h\Delta} + P^{ki}_{\alpha\beta;\gamma} S \right] \right\} \cdot (\lambda''_\alpha \lambda''_\beta \lambda''_\gamma \lambda''_\delta - \lambda^{\perp}_\alpha \lambda^{\perp}_\beta \lambda''_\gamma \lambda''_\delta)\, d\Omega \tag{129}$$

We will now carry out the same averaging of unit vectors that was described in the previous section. The result is:

$$\epsilon_{\parallel} - \epsilon_{\perp} = \frac{4\pi^2 \rho \nu H^2}{30\ kT\ h\ c\ d} \sum_i \sum_k \Bigg[P^{ki}_{\alpha\beta}\, S^I\, m_{k\gamma} \frac{(m_{i\delta} - m_{k\delta})}{h\Delta} + P^{ki}_{\alpha\beta;\delta}\, m_{k\gamma} S + P^{ki}_{\alpha\beta;\gamma}\, m_{k\delta}\, S + P^{ki}_{\alpha\beta}\, S^I\, m_{k\delta} \frac{(m_{i\gamma} - m_{k\gamma})}{h\Delta} \Bigg] \cdot \left[3(\delta_{\alpha\gamma}\delta_{\beta\delta} + \delta_{\alpha\delta}\delta_{\beta\gamma}) - 2\delta_{\alpha\beta}\delta_{\gamma\delta} \right] \tag{130}$$

After contraction, one obtains the additional dichroism expected for a molecule with a degenerate ground state:

$$\epsilon_{\parallel} - \epsilon_{\perp} = \frac{4\pi^2 \rho \nu H^2}{30\ kT\ h\ c\ d} \sum_i \sum_k 2S \Big[3\,(P^{ki}_{\alpha\beta;\beta} + P^{ki}_{\beta\alpha;\beta})\, m_{k\alpha} - 2\, P^{ki}_{\alpha\alpha;\gamma}\, m_{k\gamma} \Big] + \frac{2\, S^I}{h\Delta} \Big[3\,(P^{ki}_{\alpha\beta} + P^{ki}_{\beta\alpha})\, m_{k\alpha}\,(m_{i\beta} - m_{k\beta}) - 2\, P^{ki}_{\alpha\alpha}\, m_{k\gamma}\,(m_{i\gamma} - m_{k\gamma}) \Big] \tag{131}$$

The dichroism terms of equation (131) are to be added to those of equation (120) for molecules with degenerate ground states. Since the second derivative of the probab-

ility function was omitted from equation (125), no pure orientational effects have yet been introduced into these derivations. The terms of equation (131) represent a combination of orientational and distortional contributions to the induced dichroism, and thus are applicable to spherical molecules. A very important consequence of equation (131) is the temperature dependence of these new terms; all the contributions predicted for a spherical molecule having a non-degenerate ground state were found to be temperature independent. This observation parallels the occurrence of temperature dependent MCD bands for molecules possessing degenerate ground states,[120] but while the MCD bands only present a zeroth derivative lineshape the MLD bands predict both zeroth and first derivative lineshapes.

3. Description of the Optical System

Although a full discussion of the experimental details will be given shortly, a brief explanation of the nature of the optical system is necessary for the purposes of this section. Monochromatic light is polarized by a polaroid sheet and then is modulated by the action of a Pockels cell. At this point, the direction of the polarization vector of the incident light is varying sinusoidally between two orthogonal directions. The light then passes through a sample cell which possess linear dichroism and possibly linear birefringence, and finally reaches the detector.

A very elegant technique for the mathematical description of optical systems has been developed by Jones[129] and will be used here to describe the changes induced in the light as it passes through the various components of the MLD experiment. In this technique, a series of matrices may be written which describe the effect of each component on the light passing through. An example of the use of these Jones matrices is provided by the work of Disch and Sverdlik,[130] who considered the effect of linear dichroism

---

129) R. C. Jones, J. Opt. Sci. Am. 38, 671 (1948).

130) R. L. Disch and D. I. Sverdlik, Anal. Chem. 41, 82 (1969).

on circular dichroism spectra as measured by the method of Grosjean and Legrand.[131]

We shall commence analysis of the optical system by considering the light immediately after it has passed through the polarizer. If the light is polarized at 45° with respect to the laboratory vertical axis (this direction is considered the y axis and the direction of propagation of the light beam is the z axis), then the matrix which describes its form is given by:

$$\vec{E}_o = \frac{E_o \, e^{i\omega' t}}{\sqrt{2}} \begin{bmatrix} 1 \\ 1 \end{bmatrix} \qquad (132)$$

In equation (132) E_o is the amplitude of the light vector, and ω' is the angular frequency of the monochromatic light. The upper component of the matrix refers to the x component of the light and the lower component refers to the y component. The matrix describing the action of the Pockels modulator on the state of polarization of the light is:[129]

$$\vec{M}_m = \begin{bmatrix} e^{i\phi/2} & 0 \\ 0 & e^{i\phi/2} \end{bmatrix} \qquad (133)$$

where ϕ is the time-dependent retardation of the Pockels cell and is given by:

---

131) M. Grosjean and M. Legrand, Comp. Rend. Acad. Sci. (Paris) 251, 2150 (1960).

$$\phi = \phi_o \sin(\omega t) \tag{134}$$

In equation (134), ϕ_o is the peak value of the linear relative retardation of the Pockels modulator and ω is the modulation frequency. Finally, the matrix which describes a sample cell exhibiting both linear dichroism and linear birefringence:[130]

$$\vec{M}_s = e^{-kz} \begin{bmatrix} \cosh(Qz) + \cos(2\chi)\sinh(Qz) & \sin(2\chi)\sinh(Qz) \\ \sin(2\chi)\sinh(Qz) & \cosh(Qz) - \cos(2\chi)\sinh(Qz) \end{bmatrix} \tag{135}$$

where k is a mean amplitude absorption coefficent, χ is the angle measured postively counterclockwise facing the oncoming beam between the laboratory-fixed x axis and the principal x axis of the optical system, and Q is given by:

$$Q = p + ig \tag{136}$$

In equation (136), g is the linear birefringence and is defined as:

$$g = \frac{\pi}{\lambda}(n_y - n_x) \tag{137}$$

The linear dichroism, p, is defined as:

$$p = \tfrac{1}{2}(k_y - k_x) \tag{138}$$

where now the amplitude absorption coefficents are defined along the principal axes of the optical system. The linear dichroism may also be related to the differences in intensity absorption coefficents by:

$$p = \tfrac{1}{4}(\epsilon_y - \epsilon_x) \tag{139}$$

The light reaching the detector is given by:

$$\vec{E} = \vec{M}_s \cdot \vec{M}_m \cdot \vec{E}_o \tag{140}$$

Carrying out the necessary dot products yields the vector:

$$\vec{E} = \frac{E_o\, e^{i\omega t - kz}}{\sqrt{2}} \begin{bmatrix} e^{i\phi/2}\cosh(Qz) + e^{i\phi/2}\cos(2\chi)\sinh(Qz) \\ \quad + e^{-i\phi/2}\sin(2\chi)\sinh(Qz) \\ e^{-i\phi/2}\cosh(Qz) - e^{-i\phi/2}\cos(2\chi)\sinh(Qz) \\ \quad + e^{i\phi/2}\sin(2\chi)\sinh(Qz) \end{bmatrix} \tag{141}$$

Equation (141) is a description of the electric vector of the light reaching the detector. The intensity of this light is found by taking the dot product of the electric vector with its complex conjugate:

$$I = E^* \cdot E \tag{142}$$

Carrying out the dot product of equation (142) using equation (141) yields the expression:

$$I = E_o^2 \, e^{-2kz} \left[\cosh(2pz) + \sin(2\chi) \sinh(2pz) \cdot \cos(\phi) \right] \qquad (143)$$

It is to be noted that the contribution of the linear birefringence has **cancelled** in the taking of the dot product.

By carrying out the dot product of equation (142) on the initial light vector given in equation (132), one may obtain the intensity of the polarized light reaching the detector in the absence of absorption as:

$$I_o = E_o^2 \qquad (144)$$

so that we can express equation (143) as:

$$\frac{I}{I_o} = e^{-2kz} \left[\cosh(2pz) + \sin(2\chi) \sinh(2pz) \cdot \cos(\phi) \right] \qquad (145)$$

Since we know the expression for the retardation of the Pockels cell from equation (134), equation (145) becomes:

$$\frac{I}{I_o} = e^{-2kz} \left[\cosh(2pz) + \sin(2\chi) \sinh(2pz) \cdot \cos(\phi_o \sin(\omega t)) \right] \qquad (146)$$

In equation (146), we observe an expression calling for the cosine of a sine function. This factor is given by:[132]

$$\cos(\phi_o \sin(\omega t)) = 2 \sum_{n \text{ even}} J_n(\phi_o) \sin(n\omega t) \qquad (147)$$

---

132) M. Abramowitz and I. A. Stegun, "Handbook of Mathematical Functions", Dover Publications, New York, 1965.

A consequence of equation (147) is that the fundamental frequency of the signal due to the linear dichroism will occur at twice the modulation frequency of the Pockels modulator, and we shall return to this point in the description of the experimental details. The easiest method to relate this signal to the linear dichroism is to divide it by a voltage proportional to the mean light intensity, as is done in the method of Grosjean and Legrand.[131] This ratio may be shown to be proportional to tanh(2pz),[130] which approximately equals 2pz for very small dichroisms. Thus, the ratio of the rectified signal occurring at twice the modulation frequency of the Pockels modulator to the mean DC output of the detector is directly proportional to the linear dichroism.

C. Experimental Details

The apparatus used to measure magnetic linear dichroism is illustrated in block form in Figure 14. Initially, a He-Ne laser was used as the light source, but this was replaced by a Beckman model DU monochromator in order to record MLD at various wavelengths. The light coming out of the monochromator passes through a pair of collimating lenses, is polarized by a sheet of polaroid, and then is modulated by the Pockels cell. After leaving the Pockels cell, the direction of the polarization of the light varies sinusoidally between directions that are parallel and perpendicular to the magnetic field. The light then passes through the sample cell, and if any dichroism is present then one component polarized either perpendicular or parallel to the applied field is preferentially extinguished.

Light leaving the sample cell falls on the detector (N-Lee Products, spectral response S-20) and the dichroism is observed as an AC ripple superimposed on a large DC background. Any longitudinal component of the magnetic field which would cause a rotation of the polarized light is suppressed by the action of the cell compensator, whose operation was described in the previous section. Due to the low light intensity of the source (a 60 W tungsten-iodine lamp) an average spectral bandpass of 10 nm was used, and this large value reduced the resolution of MLD

Figure 14 - Apparatus Block Diagram

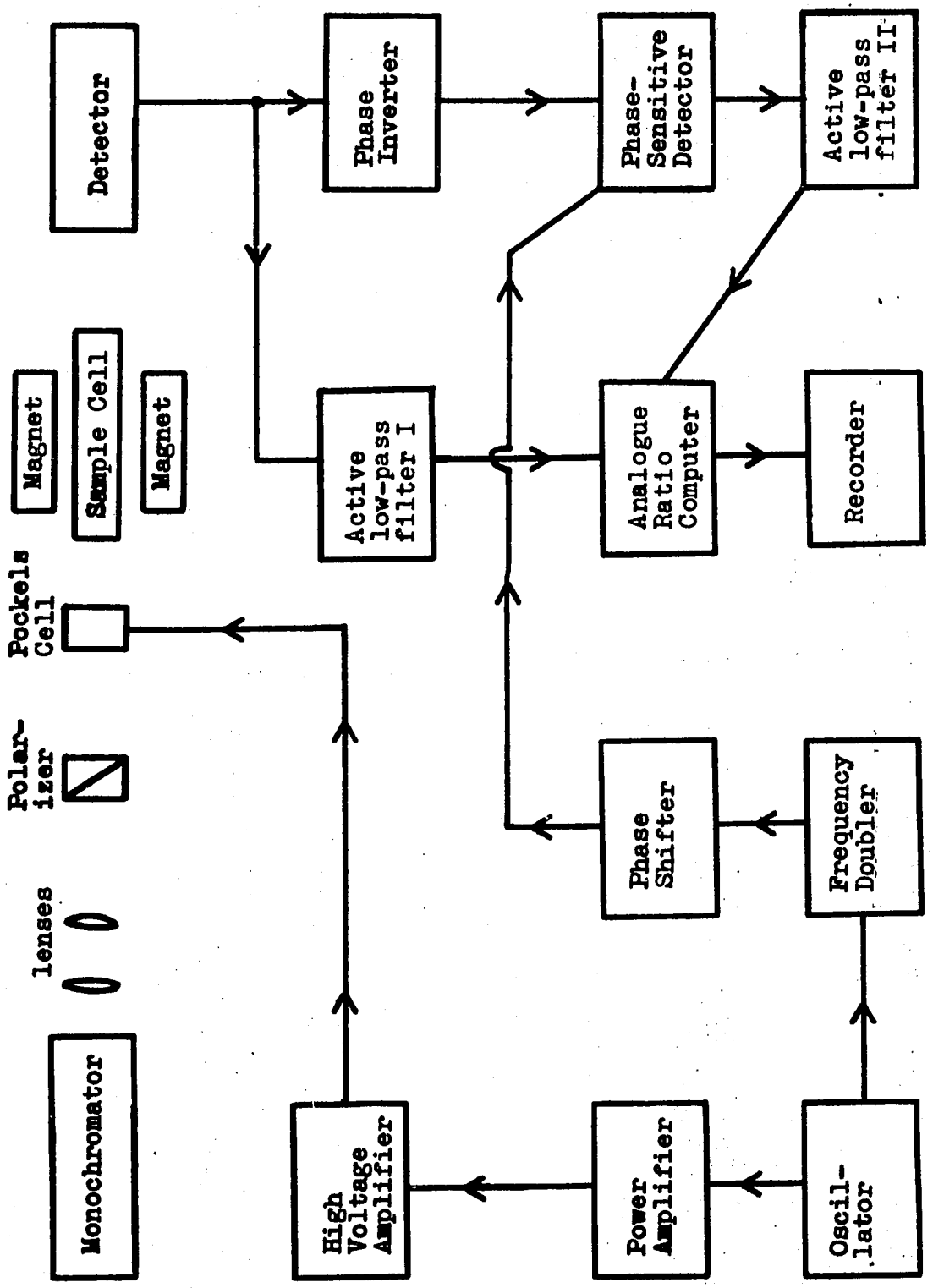

features.

The high voltage necessary to run the Pockels modulator (Lasermetrics, Inc., model EOM-401A) was obtained by taking the output from a waveform generator, passing it through a power amplifier, and then passing this output into a high voltage transformer. The voltage applied to the Pockels cell was measured on an electrostatic voltmeter, which yields a true rms measurement of the voltage. The purity of this modulating signal was observed by monitoring the waveform on an oscilloscope, and the input for this was obtained by connecting a 2400:1 voltage divider across the secondary of the high voltage transformer and feeding the output into the oscilloscope. It is essential to know the voltage applied to the Pockels cell, since it determines the induced retardation and this quantity enters into the equations for the observed dichroism. The Pockels cell is normally operated at half-wave peak retardation voltage.

The AC component of the output from the detector passes to a phase inverter and then is amplified by a pair of operational amplifiers (Philbrick-Nexus model QFT-5). These amplified signals are fed directly into a phase-sensitive detector, and the output from this stage is smoothed by an active low-pass filter and passed into an analogue ratio computer (Philbrick-Nexus model 4452). The DC component is separately smoothed and passed to the ratio computer as the denominator. A backoff voltage is provided

at the filter which is used to null out any dark voltage from the detector. The output of this ratio computer is proportional to the amplitude of the AC signal divided by the DC background voltage and is measured on a conventional recorder. Schematic diagrams for these components are shown in Figures 15 and 16.

The switching signal for the phase-sensitive detector is at twice the modulation frequency of the Pockels cell, since the theoretical analysis of the previous section shows that the fundamental frequency expected for the dichroism would occur at this value. It is derived from the waveform generator that drives the Pockels cell and is passed through a frequency doubler and a phase shifter to the phase sensitive detector. The schematic diagram for these components is found in Figure 17.

The cell used for these measurements is a polarimeter cell with a pathlength of 67 cm. It is wound with number 24 magnet wire in the same fashion as the Cotton-Mouton cell already described, but this cell is not thermostatted. This particular cell is used since its inner diameter is 0.7 cm and a considerable fraction of the light emitted by the monochromator can thus pass through the sample. No temperature-related phenemena were noticed if the magnet was turned on for very short periods. The temperature of all MLD measurements was $30 \pm 1\ ^{o}C$, as measured by a

Figure 15 - Phase Inverter and Phase-Sensitive Detector

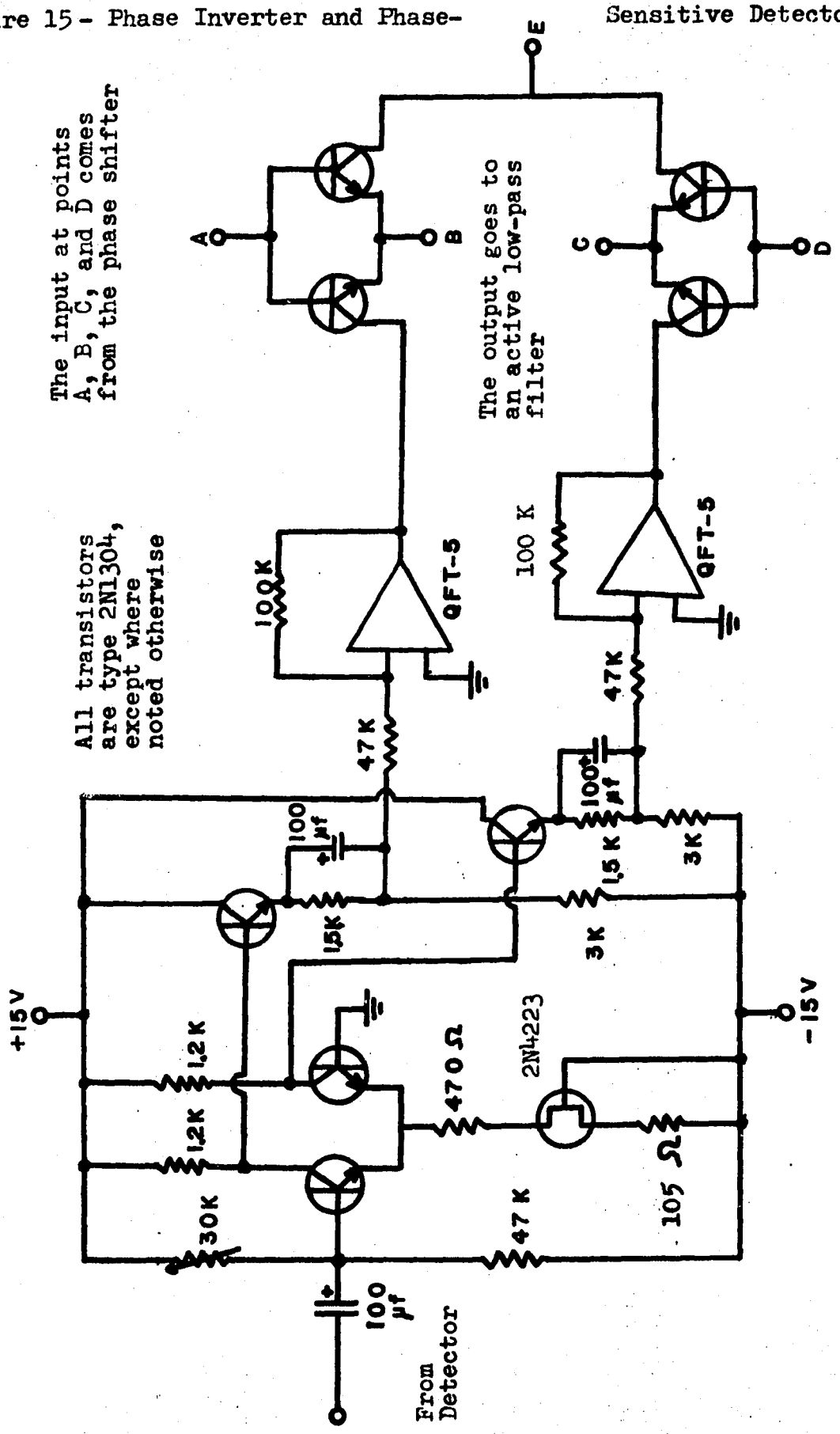

Figure 16 - Details of the active low-pass filters

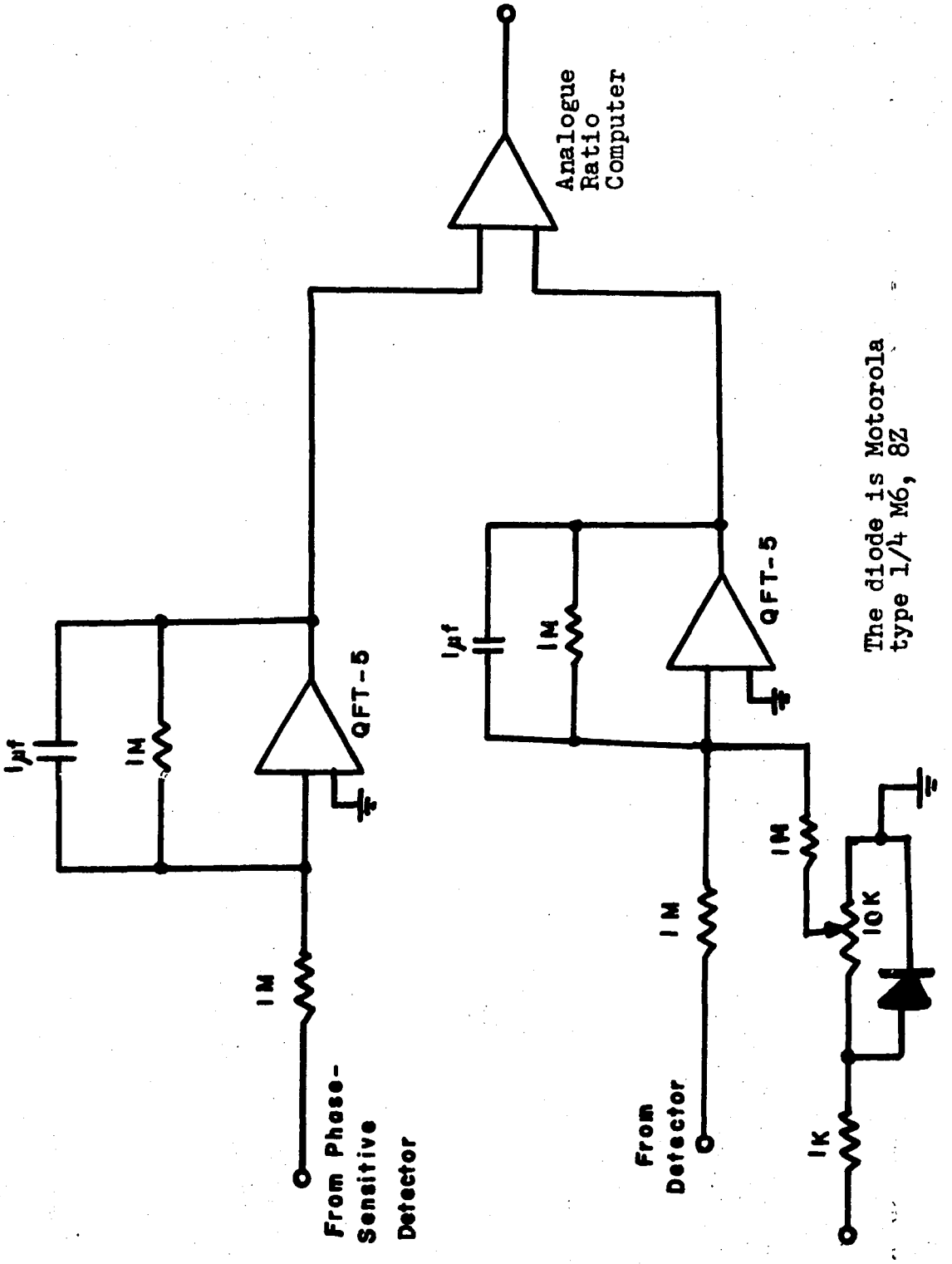

Figure 17 - Frequency Doubler and Phase Shifter

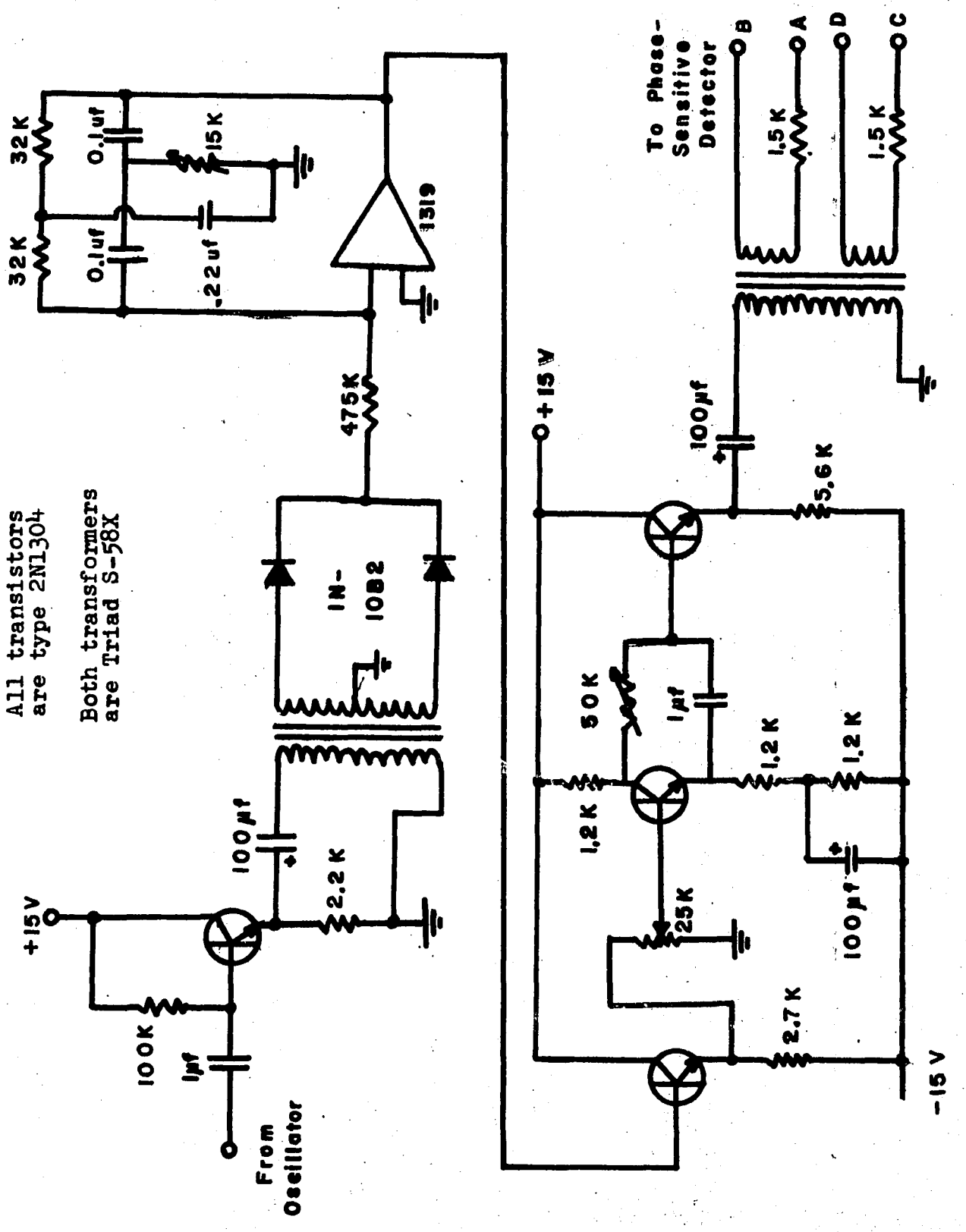

thermocouple in contact with the cell. The cell windows were made of zero stress-optical glass.

In actual practice, three determinations of the MLD constant were made at each wavelength and an average value reported. This empirical constant was defined as:

$$D = \frac{R \; a_{DC}}{\int H^2 \, dl \; a_{AC} \; C \sqrt{2} \sum_{n \text{ even}} \frac{a_n}{2} \; J_n(\phi_o)} \qquad (148)$$

where R is the ratio measured by the analogue ratio computer, a_{DC} is the gain of the active filter that smoothes the mean DC output of the detector, a_{AC} is the total rms gain of all stages between the detector and the ratio computer, C is the molar concentration of the solution used, ϕ_o is the peak value of the linear relative retardation induced by the Pockels cell, J_n is the n^{th} Bessel function having the argument ϕ_o, and a_n is the gain of the detector at the n^{th} harmonic relative to its gain at zero frequency.[133] Examination of the quantities $a_n J_n(\phi_o)$ showed that only the term with $n = 2$ was of significance for this particular detector.

The dichroism constant varies with wavelength and drops to zero outside of absorption bands. The observed

---

133) These relative gain measurements were performed by Dr. D. I. Sverdlik.

precision of the constants was quite good, and it is estimated that the major source of error lay in the lack of precise temperature control over the sample cell. The solvent used in all cases was absolute ethanol, since this solvent has a low refractive index and a fairly low coefficent of thermal expansion, and therefore not excessively given to schlieren due to slight variations in sample temperature. Absorption spectra were measured on a Cary 14 recording spectrophotometer.

D. MLD Spectra of some Transition Metal Acetylacetonates

1. $Co(acac)_3$

The MLD and absorption spectra of $Co(acac)_3$ are illustrated in two figures; Figure 18 showing the 400 to 550 nm spectral region and Figure 19 showing the 550 to 675 nm region. MLD values at each wavelength are collected in Table XXVIII. The absorption spectrum has been reported by various workers[98,134] and a polarized crystal investigation has also been published.[135] The absorption rises continuously from 500 to 400 nm with a slight bump near 400 nm, but no well-resolved features are observed in this area. The only well-resolved feature found in the visible spectrum is a d-d band centered near 595 nm.

The most interesting feature of the MLD spectra is the splitting of the d-d band observed at 595 nm. In octahedral symmetry two d-d transitions are expected for a low-spin d^6 ion like Co(III),[136] and this one corresponds to the $^1A_1 \longrightarrow {}^1T_1$ transition. Since the true molecular symmetry is D_3, a splitting of the T_1 state to yield an $A_2 + E$ combination is expected, and both transitions from

---

134) I. Hanazaki, F. Hanazaki, and S. Nagakura, J. Chem. Phys. 50, 265 (1969).

135) T. S. Piper, J. Chem. Phys. 35, 1240 (1961).

136) Y. Tanabe and S. Sugano, J. Phys. Soc. Jap. 9, 753, 766 (1954).

Figure 18. MLD and Absorption Spectra of $Co(acac)_3$

400 - 550 nm region

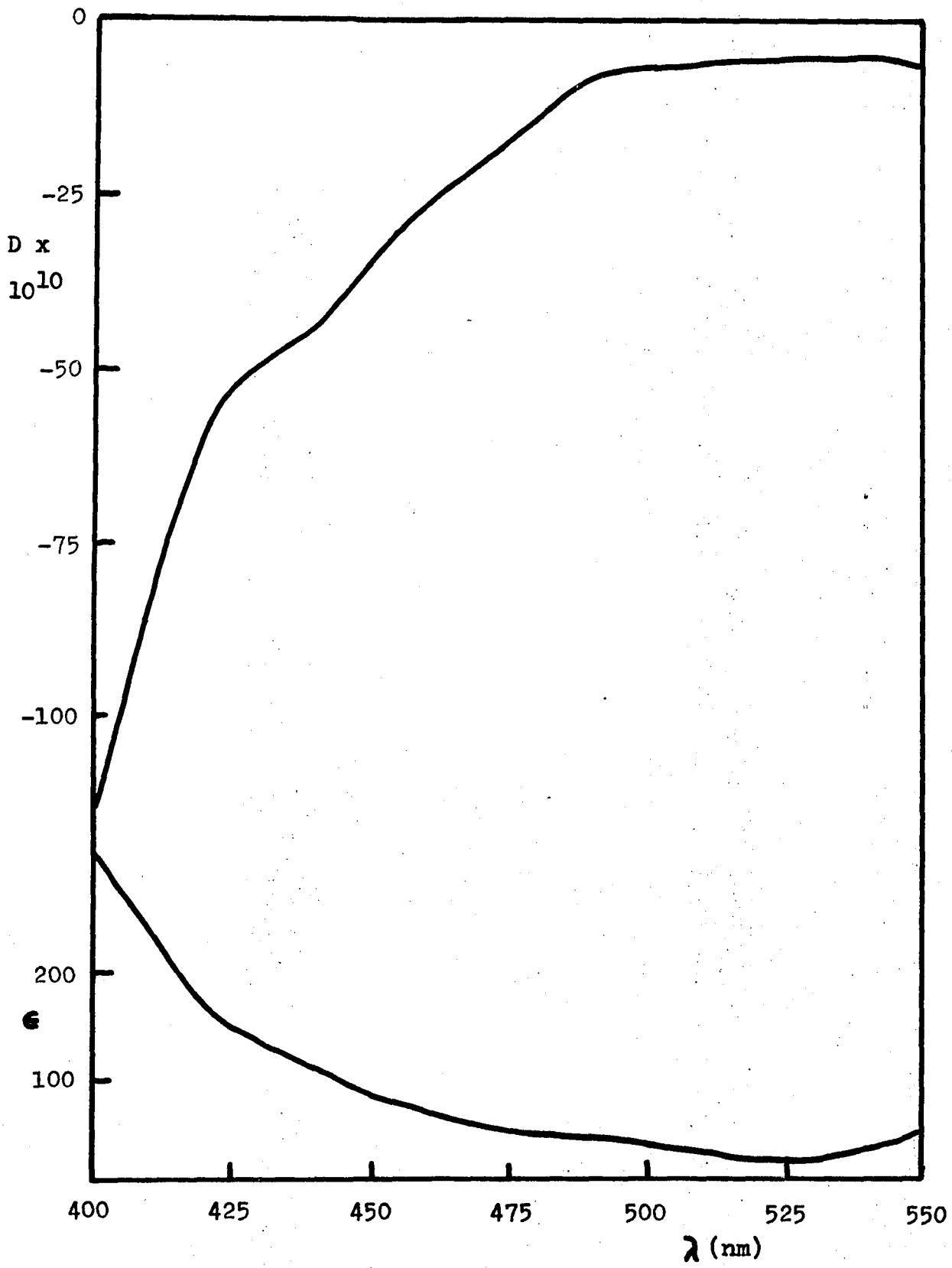

Figure 19. MLD and Absorption Spectra of $Co(acac)_3$

550 - 675 nm region

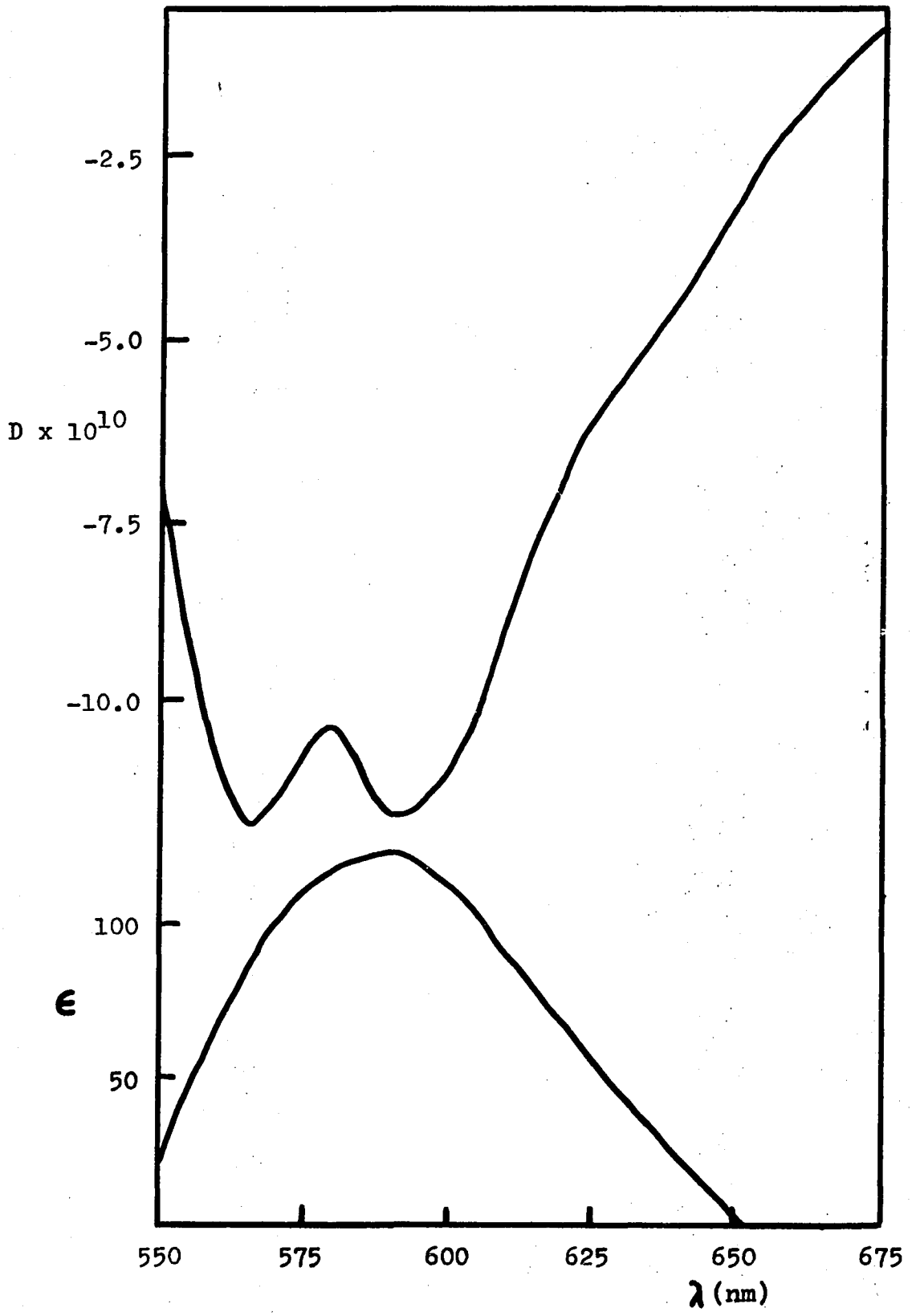

Table XXVIII - MLD Constants for $Co(acac)_3$

λ	$D \cdot 10^{10}$	λ	$D \cdot 10^{10}$
400	-115.2	550	-7.2
412	-77.4	562	-11.3
425	-52.0	575	-10.7
437	-45.9	587	-11.3
450	-33.6	600	-11.0
462	-25.0	612	-8.3
475	-17.9	625	-6.1
487	-7.8	637	-4.8
500	-7.3	650	-3.1
512	-6.7	662	-1.7
525	-6.2	675	-0.8
537	-5.8		

the A_1 ground state are group theoretically allowed. The trigonal splitting between these states is not observed in the visible , nor is it seen in the MCD spectrum,[137] but it has been determined to be about 800 cm^{-1} (0.10 ev) in the single crystal work of Piper.[135] This value agrees well with the observed MLD splitting of 750 cm^{-1} (0.09 ev). It appears that both MLD peaks are of a zeroth derivative lineshape, indicating that all observed features are derived from the leading terms of equation (120). Unfortunately, wehave not been able to assign symmetry labels to the MLD peaks due to their similarity, but we shall adopt the assignments of Piper and assign the longer wavelength peak to the A_2 component and the shorter wavelength peak to the E component.

The shoulder observed near 400 nm in the absorption spectrum has been assigned to the other d-d transition, $^1A_1 \longrightarrow {}^1T_2$, in octahedral symmetry. Since this state splits into an A_1 + E pair when the D_3 symmetry is taken into account, two transitions are possible. However, only the $^1A_1 \longrightarrow {}^1E$ transition is observed, since the $^1A_1 \longrightarrow {}^1A_1$ transition is forbidden in this point group. A definite shoulder was observed in the MLD spectrum (Figure 18) at 435 nm and this feature is abscribed to this second d-d transition. It is unfortunate that this band is reduced

---

137) H. Kato and J. Gohda, Bull. Chem. Soc. Jap. 46, 636 (1973).

to a shoulder by the nearby overlapping transitions because the lineshape is thus unable to be determined. The fact that the MLD feature lies at quite a distance (about 2000 cm^{-1}) from the absorption maximum indicates that the MLD feature might be part of a first derivative lineshape, half of which is obscured by nearby bands.

2. $Cr(acac)_3$

The MLD spectrum of $Cr(acac)_3$ is shown in Figures 20 and 21, and the MLD values are found in Table XXIX. The absorption of this chelate is well documented,[98,138-140] and the single crystal spectrum has also been obtained.[141] The visible absorption spectrum resembles that of $Co(acac)_3$ somewhat, and similar spectroscopic assignments have been made. A well-resolved d-d band is observed at 560 nm, and a shoulder is found near 410 nm. This shoulder was originally thought to be d-d in origin,[98] but is now believed to be due to either a $n \longrightarrow \pi^*$ or a $\pi \longrightarrow \pi^*$ local excit-

---

138) I. Hanazaki, F. Hanazaki, and S. Nagakura, J. Chem. Phys. 50, 276 (1969).

139) A. M. Fatta and R. L. Lintvedt, Inorg. Chem. 10, 478 (1971).

140) K. DeArmond and L. S. Forster, Spectrochim. Acta 19, 1393 (1963).

141) T. S. Piper and R. L. Carlin, J. Chem. Phys. 36, 3330 (1962).

Figure 20. MLD and Absorption Spectra of $Cr(acac)_3$

400 - 550 nm region

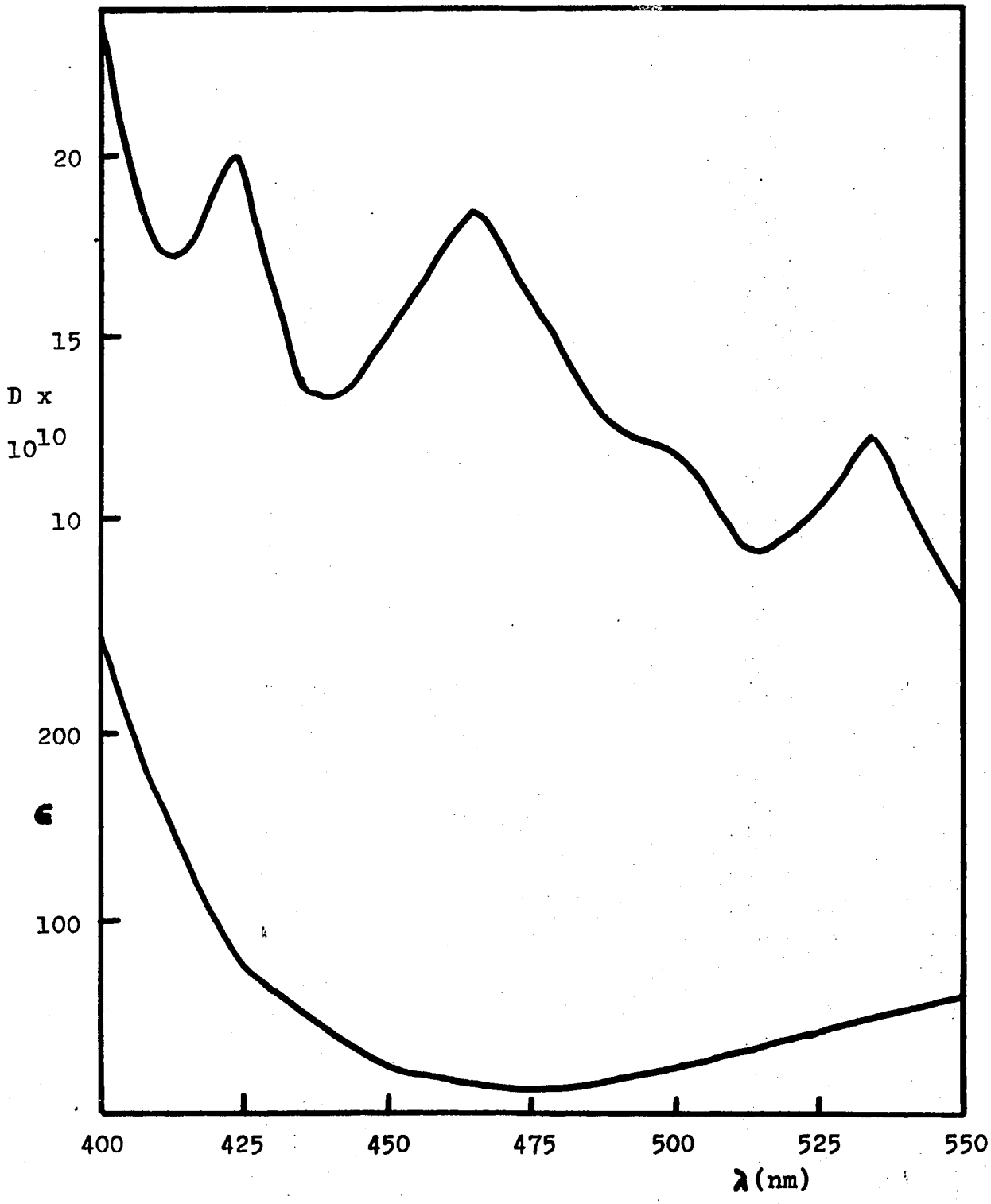

Figure 21. MLD and Absorption Spectra of $Cr(acac)_3$

550 - 675 nm region

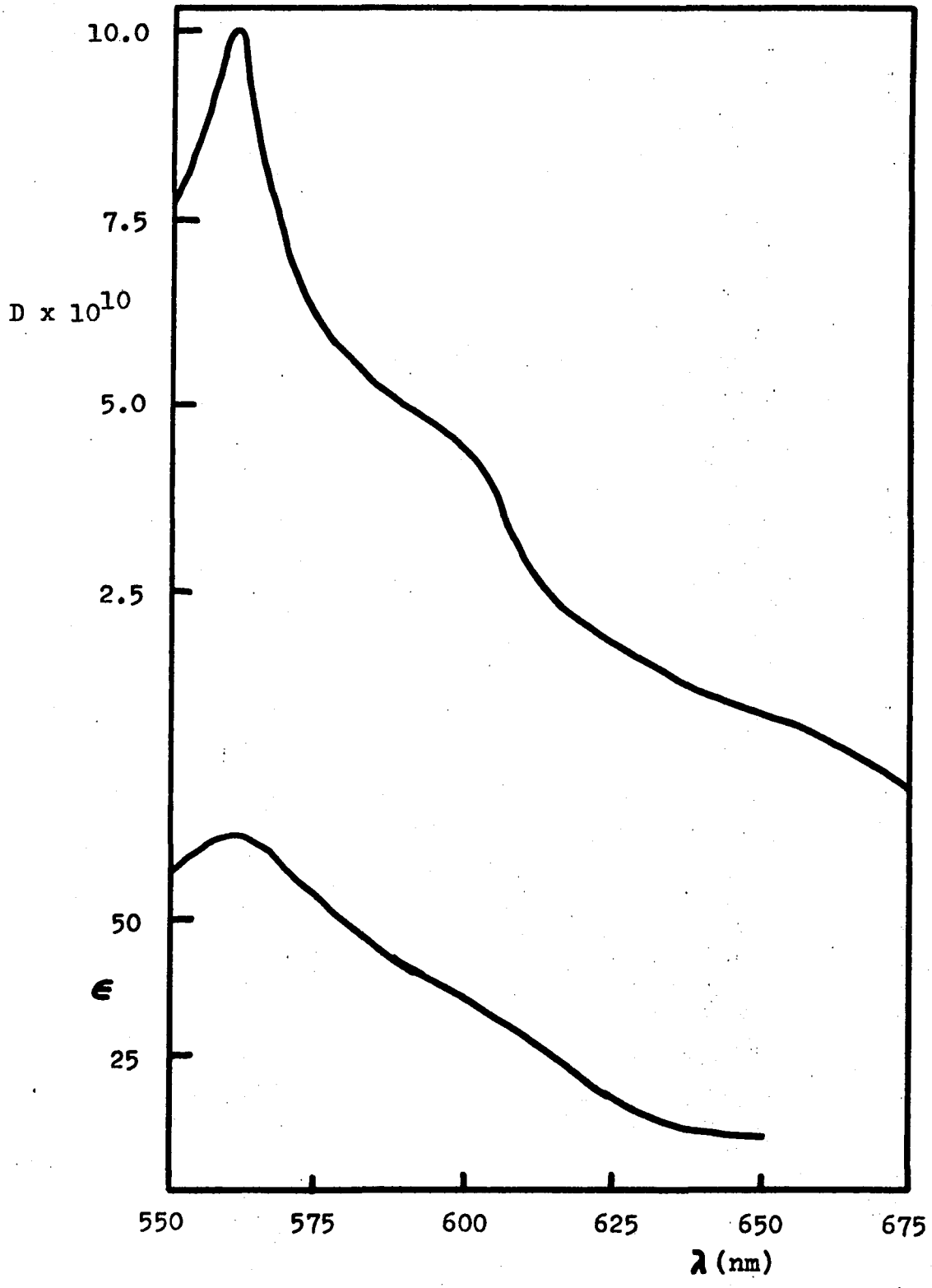

Table XXIX - MLD Constants for $Cr(acac)_3$

λ	$D \cdot 10^{10}$	λ	$D \cdot 10^{10}$
400	24.0	550	7.6
412	17.2	562	9.8
425	19.4	575	6.1
437	13.3	587	5.1
450	15.2	600	4.5
462	17.8	612	2.6
475	16.1	625	1.9
487	12.6	637	1.3
500	11.9	650	1.0
512	9.5	662	0.5
525	10.0	675	0.0
537	11.5		

ation transition,[138] and has been shown to contain both A_2 and E components.[141]

Some very interesting features are shown in the d-d band centered about 560 nm in the absorption spectrum. The MLD results show maxima for this band at 535 and 560 nm, with a pronounced shoulder observed at 600 nm. In octahedral symmetry, this band has been assigned to the $^4A_2 \longrightarrow {}^4T_2$ transition. The excited state splits into $^4A_1$ and ^4E components when the molecular symmetry is lowered to D_3, and electronic transitions to both of these states are allowed from the Cr(III) ground state. Piper and Carlin[141] found peaks at 543 and 568 nm, and assigned these to the ^4E and $^4A_1$ components, respectively. The near equality of our maxima with the absorption maxima indicates that only zeroth derivative terms have been observed. The trigonal splitting of 800 cm^{-1} (0.10 ev) found by Piper and Carlin agrees excellently with our value of 830 cm^{-1} (0.10 ev).

The origin of the MLD shoulder at 600 nm is very interesting and appears to be due to a spin-forbidden band. There are three such transitions in $Cr(acac)_3$, with the transition $^4A_2 \longrightarrow {}^2E$, $^2T_1$ (octahedral symmetry) occuring near 780 nm and $^4A_2 \longrightarrow {}^2T_2$ believed to be obscured by the d-d band at 560 nm. In most Cr(III) complexes, the $^2T_2$ state is obscured, but in some compounds it has been

identified at longer wavelengths than the spin-allowed band.[142] This observation would tend to confirm the assignment of the 600 nm MLD shoulder to a $^4A_2 \longrightarrow {}^2A_1$, ^2E transition. This band has never been observed before in $Cr(acac)_3$.

Assignment of the two MLD peaks at 420 and 465 nm is more difficult. The absorption maximum at 410 nm has been assigned to the local excitation peaks already mentioned,[138] but no further assignments have been made. Furthermore, these authors state that the second d-d band is probably covered by the 410 nm band, so presumably this $^4A_2 \longrightarrow {}^4E$ transition (transition to the other trigonal component, $^4A_2$, is forbidden) ought to appear in the MLD spectrum as well. DeArmond and Forster[140] have assigned the 410 nm band as $\pi \longrightarrow \pi^*$ and have eliminated the possibility of $n \longrightarrow \pi^*$, so it seems reasonable to assign the 420 nm MLD peak as part of the $\pi \longrightarrow \pi^*$ transition. It is possible that the 465 nm peak is due to the other component of this ligand transition, or it might be due to the allowed component of the d-d transition. No definite assignment is possible at this time.

3. $Fe(acac)_3$

The MLD and absorption spectra of $Fe(acac)_3$ are

---

142) A. B. P. Lever, "Inorganic Electronic Spectroscopy", American Elsevier, New York, 1968.

Figure 22. MLD and Absorption Spectra of $Fe(acac)_3$

400 - 550 nm region

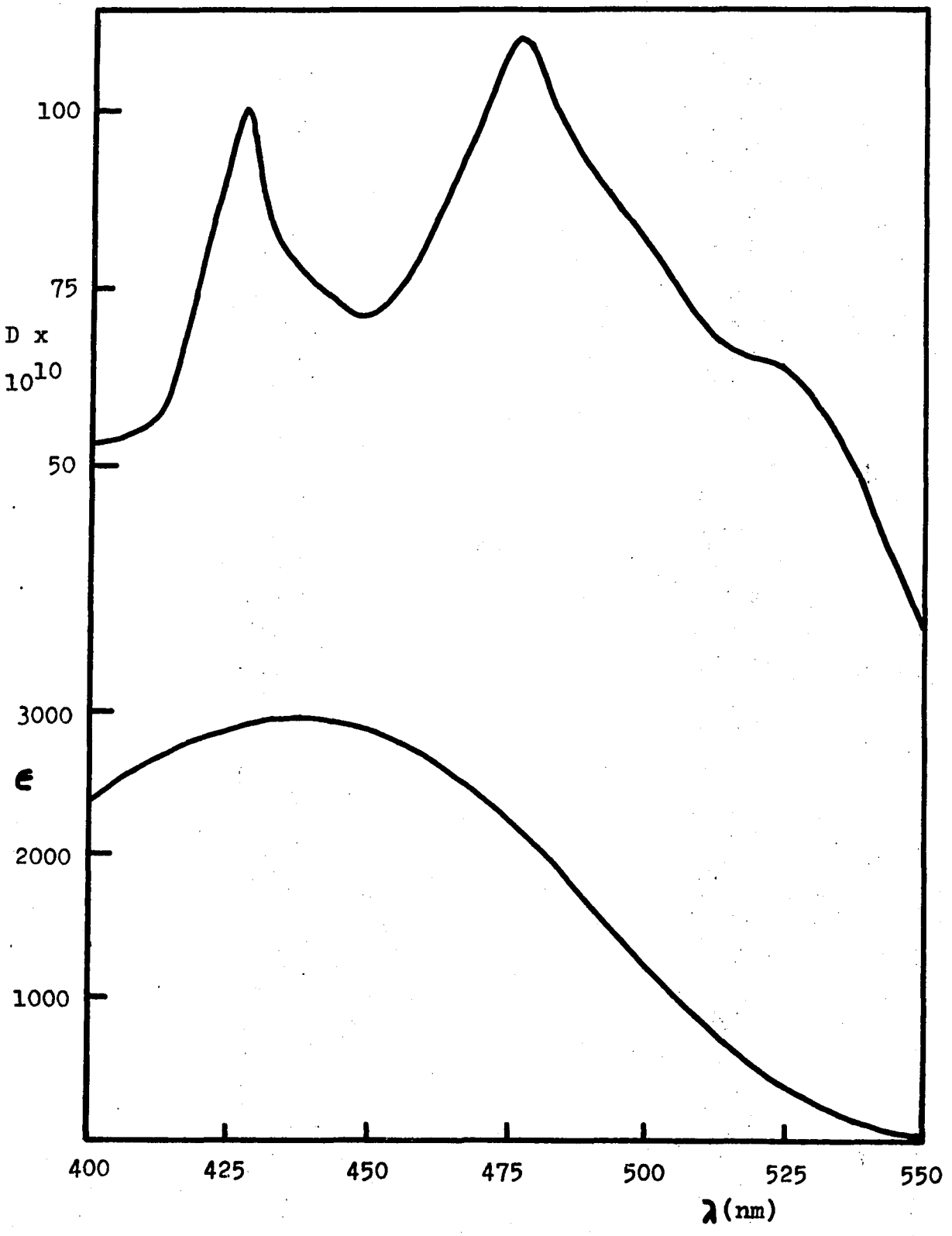

Figure 23. MLD and Absorption Spectra of $Fe(acac)_3$

550 - 700 nm region

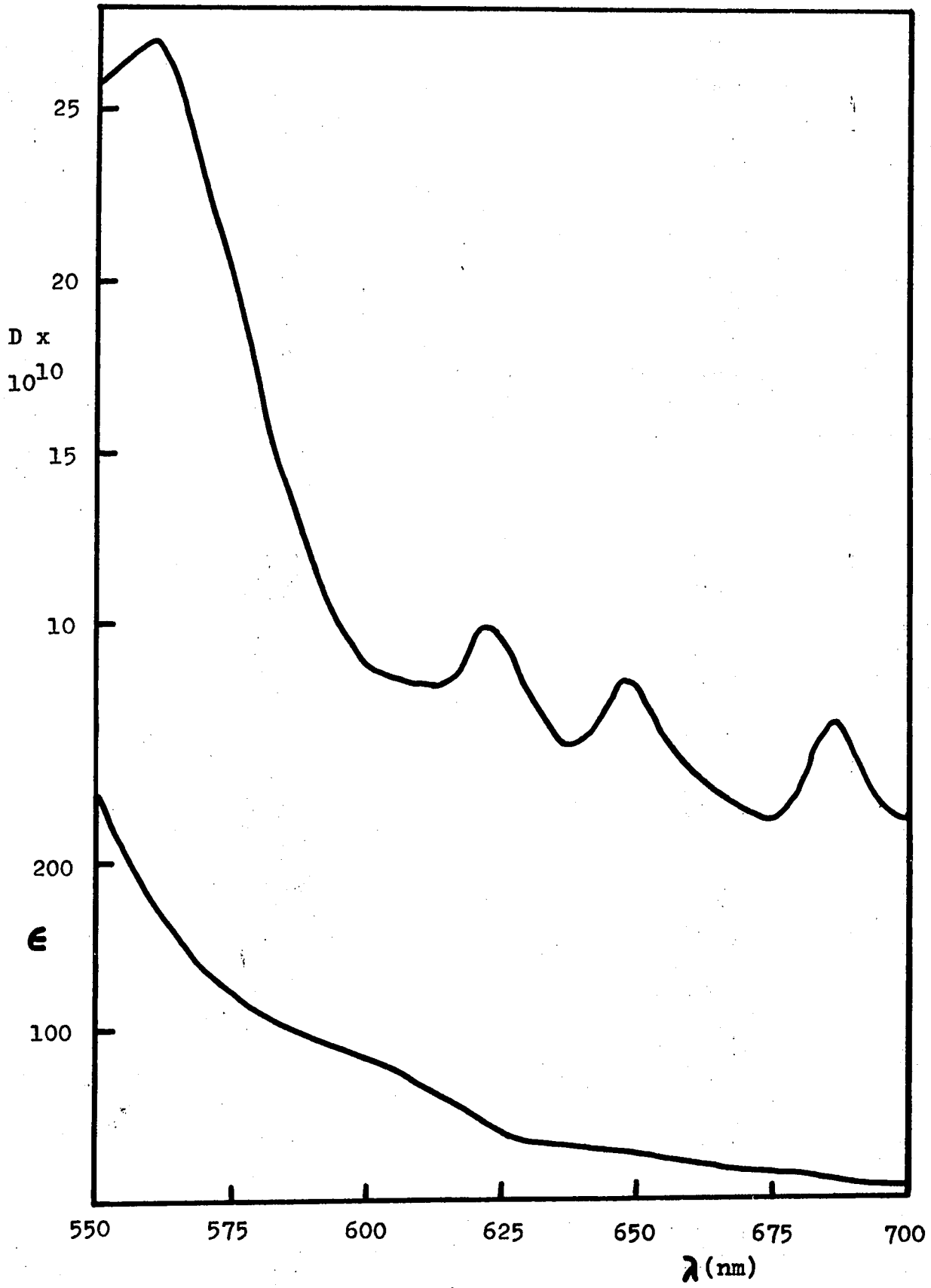

Table XXX - MLD Constants for $Fe(acac)_3$

λ	$D \cdot 10^{10}$	λ	$D \cdot 10^{10}$
400	53.8	562	26.8
412	55.8	575	20.2
425	94.2	587	12.9
437	77.7	600	8.8
450	70.9	612	8.2
462	83.4	625	9.6
475	109.2	637	6.6
487	95.3	650	8.2
500	81.7	662	5.6
512	68.4	675	4.4
525	64.4	687	7.2
537	50.6	700	4.5
550	25.8		

shown in Figures 22 and 23, and the actual dichroism values are collected in Table XXX. The absorption spectra are fairly well understood,[98,138,143] a report of the single crystal spectrum has been published,[144] and the MCD of $Fe(acac)_3$ has also been reported.[137] The absorption spectrum in the region studied consists of a broad, intense band centered at 430 nm. This band has been attributed to a ligand-to-metal charge transfer absorption, but two other local excitations are believed to lie buried under the charge transfer peak.[138] A weak band has been observed[98] at 725 nm which has been assigned to a spin-forbidden transition. All d-d transitions are spin-forbidden for this high-spin Fe(III) compound, but no assignments have been made for the possible bands. Examination of the Tanabe-Sugano diagram for this d^5 ion[136] shows that there are at least four possible sextet-to-quartet transitions (assuming octahedral symmetry) that might occur in the spectral range studied, and thus even more states would be expected in D_3 symmetry.

The MLD spectrum of $Fe(acac)_3$ shows two very strong maxima at 430 and 480 nm, a fairly strong shoulder near 530 nm, one moderately intense maximum at 560 nm, and three weak bands at 620, 645, and 685 nm. Hanazaki et al[138]

---

143) A. M. Fatta and R. L. Lintvedt, Inorg. Chem. 9, 491 (1970); ibid. 11, 88 (1972).

144) T. S. Piper and R. L. Carlin, Inorg. Chem. 2, 260 (1963).

assigned the 430 nm band in the absorption spectrum to a ligand-to-metal charge transfer (of e symmetry only), so we shall assign the MLD feature at 430 nm to the same transition. These authors also presented calculations which indicated that a pair of ligand-localized excitations (of A_2 and E symmetry) ought to occur near 580 nm, and that these bands are much less intense than the charge transfer absorption. Therefore, the moderate MLD band at 560 nm is assigned to this local excitation.

Since some evidence has been presented[144] that indicates the transition $^6A_1 \longrightarrow {}^4A_1, {}^4E$ ought to lie near 550 nm, the shoulder observed at 530 nm in the MLD spectrum is assigned to these spin-forbidden components. The weak features found at 620, 645, and 685 nm are also assigned to spin-forbidden transitions, as indicated by their low intensity. It is expected that the transition $^6A_1 \longrightarrow {}^4A_1, {}^4E$ (not the same transition as mentioned above) should lie in this region, although the exact location of these transitions has not been exactly determined.

The origin of the very intense MLD band at 480 nm is very puzzling. No spectral evidence has been presented to date which indicates that any transition ought to lie in this region. Its intensity precludes its assignment as being due to any spin-forbidden transition (unless a massive intensity-borrowing mechanism is operative in the MLD but

not found in the absorption spectrum) and would indicate that it must be due to either a local excitation (such as a $\pi \longrightarrow \pi^*$ transition) that has not yet been characterized or another charge transfer absorption. No charge transfer bands other than the afore-mentioned transition have been proposed, and it is believed that the visible absorption contains only one component. It is possible that this supposition is incorrect and the visible absorption actually contains two well-separated components. It is not yet possible to answer this question in a rigorous manner, but it is clear that the 480 nm MLD band must be due to a process of this sort.

E. Summary

Due to the large spectral linewidth used in the determination of the MLD spectra (normal Cary 14 linewidths are on the order of 0.1 nm and we used a width of 10 nm), no real evaluation of the MLD lineshapes was possible and consequently less information than theoretically available was obtained. It was observed that the MLD of $Co(acac)_3$ was negative in sign at all wavelengths, and the MLD of $Cr(acac)_3$ and $Fe(acac)_3$ were uniformly positive. As a result, no separation into zeroth, first, and second derivative contributions was possible in any of the MLD bands. This unfortunate result limited the application of the MLD technique to that of a spectroscopic probe, rather than that of a quantitative technique.

In spite of these experimental difficulties, much new information was obtained regarding the electronic spectra of the compounds studied. In several cases, new bands were uncovered in the MLD spectra which were not clear in the absorption spectrum, and considerably better resolution of overlapping bands was also found. The MLD technique was shown to be of greater value than the MCD method is providing spectral information not available in the absorption spectrum, since the MLD spectra showed more detail and better resolution than the MCD spectra of the

same compounds. Currently, the spectral bandwidth is being reduced by replacing the photodetector by a photomultiplier tube, so even better resolution is expected.

We conclude, then, that the spectroscopic technique of magnetic linear dichroism will be of great value in future investigations of the electronic structure of molecules. Its potential has only been hinted at in these first few studies, but continued work should demonstrate the usefulness of this method.